Sequestration of Landfill Gas Emissions using Basic Oxygen Furnace Slag

BY

ARCHANA GOPAKUMAR
B.Tech, College of Engineering Trivandrum (India), 2015

THESIS

Submitted as partial fulfilment of the requirements for the degree of
Master of Science in Civil Engineering
in the Graduate College of the
University of Illinois at Chicago, 2018

Chicago, Illinois

Defense Committee:

Krishna R Reddy, Chair and Advisor

Mohsen Issa, Civil and Materials Engineering

Amid Khodadoust, Civil and Materials Engineering

Dennis G Grubb, Phoenix Services LLC

ACKOWLEDGEMENTS

I would like to express my sincere gratitude to my advisor, Dr. Krishna Reddy, for providing me the opportunity to work under his guidance. His guidance and encouragements were vital to the successful completion of my thesis. I would like to thank Dr. Dennis G Grubb from Phoenix Services LLC for taking his time to share his knowledge and providing invaluable recommendations without which this work would not have been possible.

I would also like to thank my other committee members, Prof. Amid Khodadoust and Prof. Mohsen Issa for their support and suggestions for the improvement of this work. Many thanks to my friends from lab who have been a constant source of support and help throughout the two years which formed most crucial contributions to this work and my own individual development. In addition, I would also like to acknowledge the Electron Microscopy Service (Research Resources Center, UIC) for their contributions to this research, College of Engineering machine shop and technical staff of the Civil and Materials Engineering Department for their timely assistance and thoughtful suggestions.

Finally, I would like to express my profound gratitude to my mother and father, Sathi and Gopakumar, my brother and his wife, Harishankar and Lakshmi along with my other dearest friends for their unfailing support, immense love and encouragements throughout the years without which this accomplishment would never have been possible.

CONTRIBUTIONS OF AUTHORS

Chapter 1 is an introduction to the research problem statement, goals and objectives of this research. Chapter 2 is a review on prior CO_2 sequestration technologies and mechanisms involved, the iron and steel slag characteristics, and thereafter the utilization of steel slag in CO_2 sequestration and various other environmental applications. This chapter was written based on the collection and review of various relevant literatures as cited. My advisor, Dr. Krishna Reddy and fellow students Girish Kumar and Jyoti K C contributed to the review and editing of the content. Chapter 3 presents the study on effect of moisture and humid gas inflow to CO_2 sequestration by Basic Oxygen Furnace (BOF) Slag based on the batch and column experiments conducted by myself with the assistance of fellow student, Raksha Kishore Rai. Chapter 4 presents the study of BOF slag particle size on CO_2 sequestration based on the batch and column experiments conducted primarily by Raksha Kishore Rai. The result analysis and conclusions were drawn by me based on data from the valuable batch and column experiments conducted by her. My academic advisor, Dr. Krishna Reddy (UIC), industrial advisor, Dr Dennis G Grubb (Phoenix Services LLC), and fellow students, Girish Kumar and Jyoti KC reviewed, edited and provided valuable feedback on the contents of chapters 4 and 5. Chapter 5 provides the overall conclusions and recommendations based on the complete research.

TABLE OF CONTENTS

LIST OF TABLES

LIST OF FIGURES

CHAPTER 1 - INTRODUCTION

1.1 BACKGROUND

Fugitive methane (CH_4) and carbon dioxide (CO_2) emissions from organic waste decomposition at municipal solid waste (MSW) landfills, commonly known as landfill gas (LFG), constitute one of the major anthropogenic sources of greenhouse gas (GHG) emissions to the atmosphere (US EPA). In recent years, biocovers involving the addition of organic-rich amendments to landfill cover soils have promoted microbial oxidation of CH_4 to CO_2, thereby reducing CH_4 emissions from landfill. Biochar, a solid by-product obtained by organic mass pyrolysis, with favorable characteristics (internal porosity, stable organic C content) for enhanced microbial oxidation have shown significant potential for mitigating the CH_4 emissions from MSW landfills with biochar-amended covers (Reddy et al. 2014; Yargicoglu and Reddy, 2017). Although the CH_4 emissions are mitigated, there is still a considerable amount of CO_2 that is emitted into the atmosphere as a result of microbial oxidation of CH_4 in landfill covers as well as the CO_2 that prevails from MSW decomposition. The current study focuses on ways to mitigate both CH_4 and CO_2 emissions from MSW landfills by altering the matrix of biochar amended biocover with industrial by-products like steel slag that have CO_2 sequestration capacity.

1.2 PROBLEM STATEMENT

Complementing the CH_4 oxidizing biocover with CO_2 sequestration is considered to have the ability to result in a “zero-emission” landfill. Accordingly, carbon capture and storage (CCS) techniques using alkaline industrial by-products such as basic oxygen furnace (BOF) slag adds

an important dimension to potentially sustainable solutions to the challenge of landfill gas emission.

Until now, studies were conducted to analyze the CO_2 sequestration potential of BOF slag with respect to optimization of on-site CO_2 capture from industrial flue gas at elevated temperatures and pressures (Huijgen et al. 2005; Su et al. 2016) in stirred slurry states. Such conditions are unlikely at landfill sites that remain static and unsaturated under normal atmospheric conditions. Accordingly, CO_2 removal potential of BOF slag in biocover near standard temperature and pressure (STP) conditions not previously considered in the CO_2 sequestration literature needs to be explored.

1.3 RESEARCH GOALS AND OBJECTIVES

BOF slag, obtained from a steel making mill in Indiana Harbor was studied to analyze CO_2 removal capacity and carbonation mechanisms at static, unsaturated conditions and normal atmospheric temperature and pressure pertinent to landfill covers. Carbonation behavior in BOF slag would be studied by means of batch and column experiments. The main research objective was to deduct the capacity of BOF slag to capture CO_2 from a synthetic LFG mixture and learn the mechanisms involved in carbonation which could act as the baseline while delineating design recommendations for the biocover amended with BOF slag. To this end, the main two parameters effecting CO_2 sequestration by BOF slag: moisture and particle size, were also studied as part of this thesis work.

With this chapter serving as the introduction, following discussions are pursued in the upcoming chapters:

Chapter 2: A review on previous studies dealing with CO_2 sequestration by steel slag is discussed first, followed by the use of steel slag in environmental remediation applications along with the mechanisms involved. The challenges and opportunities to increase the beneficial applications of steel slag in environmental engineering are also discussed.

Chapter 3: Effects of moisture content and humid gas flow conditions on CO_2 sequestration capacity of BOF slag is discussed based on batch and column experiments as well as scanning electron microscopy results. Further, BOF slag carbonation consisting of two-stage mechanism is explained.

Chapter 4: Effect of BOF slag particle size on CO_2 sequestration is studied based on batch and column experiments on three BOF slag fractions of different sizes.

Chapter 5: Overall summary and conclusions of this study.

1.4 CITED REFERENCES

Huijgen, W. J., Witkamp, G. J., & Comans, R. N. (2005). "Mineral CO_2 sequestration by steel slag carbonation." *Environ. Sci. Technol.*, 39(24), 9676-9682.

Reddy, K.R., Yargicoglu, E.N., Yue, D., & Yaghoubi, P. (2014). "Enhanced microbial methane oxidation in landfill cover soil amended with biochar." *J. Geotech. Geoenviron. Eng.*, ASCE, 140(9).

Su, T. H., Yang, H. J., Shau, Y. H., Takazawa, E., & Lee, Y. C. (2016). "CO_2 sequestration utilizing basic-oxygen furnace slag: Controlling factors, reaction mechanisms and V–Cr concerns." *J. Environ. Sci.*, 41, 99-111.

US Environmental Protection Agency (US EPA). "Landfill Methane Outreach Program (LMOP)." <https://www.epa.gov/lmop/benefits-landfill-gas-energy-projects> (June 4, 2018).

Yargicoglu, E. N., & Reddy, K. R. (2017). "Effects of biochar and wood pellets amendments added to landfill cover soil on microbial methane oxidation: A laboratory column study." *J. Environ. Manag.*, 193, 19-31.

CHAPTER 2 - APPLICATIONS OF IRON AND STEEL SLAGS FOR CARBON SEQUESTRATION AND ENVIRONMENTAL REMEDIATION: A REVIEW

ABSTRACT: One of the major concerns faced by the iron and steel industry, other than the abundant emission of carbon dioxide into the atmosphere, is the huge quantity of slag that is generated during the manufacturing of iron and steel. A comprehensive understanding of the iron and steel slag properties has diverted them away from stockpiling or disposal in landfills to useful materials in engineering applications. The similarity of these slags to natural minerals used in geologic carbon dioxide sequestration has made them sustainable alternative for industrial-scale carbon capture and storage. Further, they possess properties that promote remediation of soil and groundwater contaminated with heavy metals and other toxic chemicals. This paper reviews the iron and steel slag characteristics suitable for engineering applications, describes several engineering application examples, and discusses challenges and opportunities to develop practical applications using iron and steel slags.

2.1 INTRODUCTION

Carbon dioxide (CO_2) is considered the most common and abundant greenhouse gas (GHG) in the atmosphere that gets generated as a result of various natural and industrial processes (**Figures 2-1 and 2-2**).

Power plants and manufacturing plants are the major sources with about 2 tons of CO_2 emission per ton of steel produced accounting steel industry to about 3-4% of the global CO_2 emissions (Yu and Wang 2011). With anthropogenic activities and related GHG emissions

projected to increase in the foreseeable future, the scientific society has turned towards exploring environmentally sound and sustainable techniques to curb GHGs.

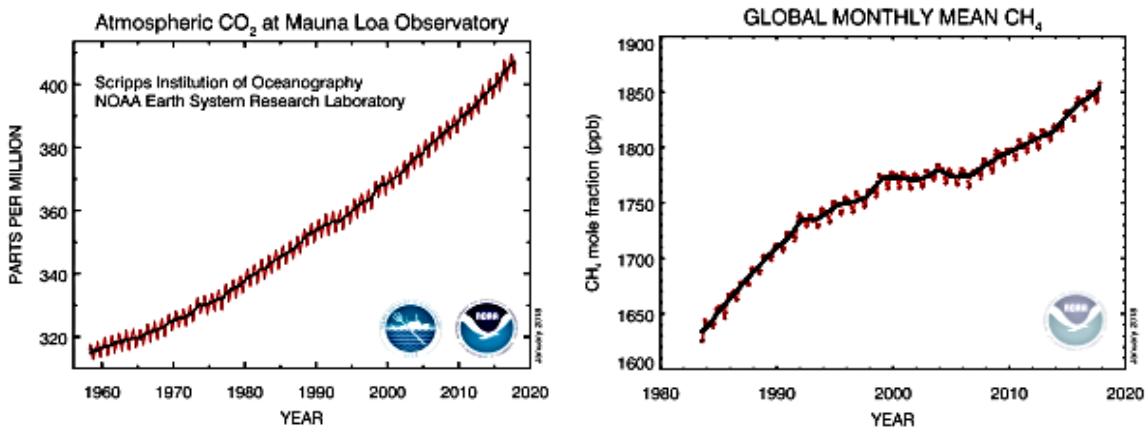

(a) (b)

Figure 2-1: (a) CO_2 and (b) CH_4 atmospheric data from Mauno Lao (Source: https://www.esrl.noaa.gov/gmd/ccgg/trends/full.html)

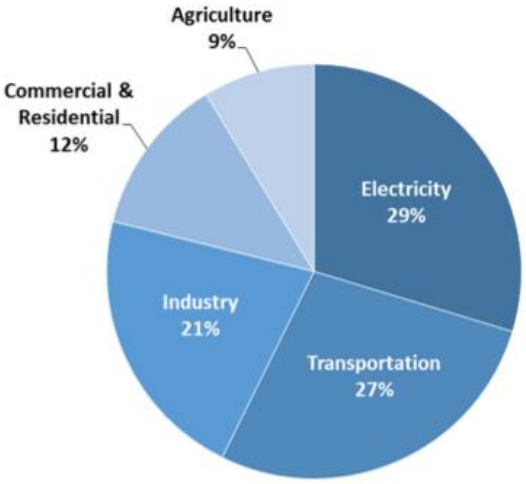

Figure 2-2: Total US greenhouse gas emissions by economic sector in 2015 (Source: US Environmental Protection Agency (2017). Inventory of U.S. Greenhouse Gas Emissions and Sinks: 1990-2015)

Iron and steel manufacturing industry aims at capturing CO_2 from its flue gas with carbon-trapping technologies (eg: amine scrubbing, electrostatic precipitator) and recycling their waste products within the plant itself to limit excess handling and transportation of waste to disposal

facilities. The industry has been successful in recycling scrap metals by utilization in refinement and conversion (of iron to steel) processes within the industry. The iron and steel slags produced abundantly from iron and steel-making are diverted to construction and transportation industry where they are used as replacement materials. Use of iron slag has been found to enhance the strength and microstructure of the slag-cement blend making it widely desirable as a replacement material in the cement and construction industry. However, steel slag from the steel producing furnaces have different composition and morphology than the iron or blast furnace slag which makes it less suitable for construction use. The coarser steel slags are partially used in asphaltic mixtures and aggregate replacement, while applications of steel slag fines are limited resulting in large stockpiles of steel slag fines in the iron and steel mills posing major concerns such as environmental and aesthetic land degradation.

A major breakthrough in the use of steel slag came about due to its compositional similarity to natural minerals like olivine that are capable of fixing CO_2 in the form of stable carbonates in geologic sequestration technology. Naturally occurring silicate minerals that contain divalent metal cations dissolve and release the cations to form stable carbonates such as calcite and magnesite, but over a long geologic time. Similarly, the steel slags with calcium-magnesium (Ca-Mg) silicate minerals, free-lime (CaO) and portlandite ($Ca(OH)_2$) contents, alkaline pH and lower chemical stability is considered highly suitable mineral source for CO_2 sequestration. The iron and steel industry is exploring methods to utilize CO_2 sequestration capacity of steel slag in a technologically viable manner to control its high CO_2 emissions due to mineral feedstock availability at the point of CO_2 emission and technical simplicity of the reaction. Beneficial use of more steel slag would also result in reduction of its landfilling. Better understanding of properties of steel slag has also led to its use in several environmental

engineering applications including contaminated site remediation, acid mine drainage remediation, stormwater and wastewater treatment, and even as soil modifier in agriculture. The chemical composition and alkaline pH (pH ~ 12) of steel slag are the major driving factors for increasing its utilization in environmental engineering applications.

This study reviews the previous studies dealing with CO_2 sequestration by steel slag first. Then, it describes the use of steel slag in environmental remediation applications. The main mechanisms for CO_2 sequestration or environmental remediation are discussed. The challenges and opportunities to increase the beneficial applications of steel slag in environmental engineering are discussed.

2.2 CARBON DIOXIDE MITIGATION STRATEGIES

The concern of rise in GHG emissions and especially CO_2 emission from power plants due to increased energy demand by population inflation led to consideration of five major strategies to reduce CO_2 in atmosphere (Chiang and Pan 2017): (1) reducing amount of CO_2 producing sources; (2) use of the emitted CO_2 in concrete curing or plastic manufacture from biomass; (3) capturing and storing CO_2; (4) switching to less carbon intensive fuels; and (5) increasing renewable energy usage. Other mitigation and adaptation strategies include imposing emissions trade system (ETS) and carbon taxes that put pricing on carbon and force the industries to switch to less carbon intensive processes. The first two strategies that calls for reduction and utilization of CO_2 are aimed at switching to less energy and carbon intensive methods that also includes the fourth strategy. Increased use of renewable energy sources would result in a shift from usage of coal for power generation to wind and solar power. Even though the renewable energy usage has increased over the past years, it still faces limitations due to limited sunlight exposure, wind

speed and unavailability of favorable conditions all year round. Also, the power generation in large industries such as iron and steel industries would still require coal power to meet its huge and continuous energy requirements. Hence, the capturing and storing of CO_2 is considered as one of the most efficient and easily adaptable CO_2 mitigation strategies, as discussed in the following sections.

2.2.1 Carbon Capture and Storage (CCS)

Carbon capture and storage (CCS) technologies have been developing in multiple dimensions in an effort to reduce our ecological footprint (Huijgen et al. 2005). A projection reported by the IEA indicated that CCS could contribute to 14% reduction in the anthropogenic CO_2 emissions by 2050 (Pan et al. 2016). Typically, the CO_2 from industrial flue gas is captured in high purity form by adopting low energy processes like adsorption and desorption in a cost-effective manner. CO_2 separation from flue gas is the most expensive and complex step of such CO_2 capturing techniques because of its low concentration (below 20%) in flue gases (Yu and Wang 2011), which necessitates a simple and low-cost method for CO_2 capture in industries. The captured CO_2 is then stored away in geologic or saline formations in the form of carbonates commonly known as carbon sequestration. In geological carbon sequestration (GCS), the captured CO_2 is injected thousands of feet deep beneath the earth's surface under high pressure using deep injection wells into rock formations capable of long term storage. It is one of the safest and stable CCS method (US EPA). The rock formations are selected such that they possess certain characteristics: exhausted coal and oil reserves, basalt formations, saline aquifers, and those that contain minerals chemically reactive with CO_2. The CO_2 injection method was previously used for enhanced oil recovery, but not completely optimized for CO_2 storage. The

carbonates being more stable (or lesser energy state) than CO_2, the GCS is thermodynamically stable and occurs naturally as in the weathering of rocks over geologic periods. However, CO_2 injection under geologic sequestration involves technical and economic issues including potentially larger volumes of CO_2 and larger scale projects. US EPA (UIC) regulates the injection wells for CGS under 'Class VI-wells used for geologic sequestration of CO_2' such that the CO_2 injection does not affect underground drinking water sources. This method is expensive, energy intensive, and not optimized with the presently available technology and knowledge.

2.2.2 Mineral Carbon Sequestration

Mineral carbon sequestration, where minerals having high affinity towards CO_2 are utilized for carbon sequestration, has been extensively studied as it can alleviate the economic burden as well as contribute to sustainable CCS methods. The chemistry behind mineral carbon sequestration is to mimic natural weathering (Kasina et al. 2015). In weathering, rock minerals, especially calcium (Ca) and magnesium (Mg) silicates containing divalent metal cations (Ca, Mg, Fe) in the form of oxides react with CO_2 to form stable carbonates (Kasina et al. 2015). It is also known as silicate weathering and the reaction takes place over long geologic time periods. Olivine (Mg_2SiO_4 - Fe_2SiO_4), larnite (Ca_2SiO_4), and pyroxene are minerals that are highly susceptible to carbonation in rocks.

In mineral carbonation, the metal oxides leach out of the minerals and react with CO_2 to form their respective thermodynamically stable carbonates with release of energy as shown in **Equation 1**. The energy released in this exothermic reaction depends on the metal (M).

$$MO + CO_2 \rightarrow MCO_3 + Heat \qquad (1)$$

Thermodynamically, the formation of carbonates is favorable at low temperatures and the reaction kinetics could be enhanced by increased temperature (Kasina et al. 2015). The formation of chemically stable carbonates upon carbonation, makes mineral carbonation an attractive alternative as the mineralized CO_2 rarely gets released back to environment. It can thus ensure stable storage of CO_2. Mineral carbonation is advantageous as raw materials other than rocks containing the reactive Mg and Ca minerals that are abundantly available could be used efficiently for the purposes of carbon sequestration (Goldberg et al. 2001).

Mineral carbonation has been tested ex-situ (above ground carbonation in a chemical processing plant) on minerals mined from earth's surface after pre-treatment (grinding) both directly and indirectly. Direct carbonation of minerals involves a single step reaction of CO_2 with the reactive compounds to form carbonates. Indirect carbonation includes two steps where the reactive compounds are first extracted from the mineral (lixiviation of feedstock) using acids or bases followed by the reaction of lixiviate material with CO_2. The choice of extraction conditions and extraction solutions are very important in indirect carbonation. Ca and Mg extraction are more feasible under acidic conditions as it favors metal extraction (Kunzler et al. 2011). Direct carbonation is hence better as it requires less raw materials, involves lesser number of steps and would eventually result in lesser wastage of materials. However, economical and environmental development is required to utilize direct carbonation in industrial applications by recognizing and optimizing efficient feedstock, reaction conditions and kinetics.

The direct carbonation can take place in two ways: (i) gas-solid carbonation (liquid to solid ratio (L/S) <0.2) and (ii) aqueous carbonation (L/S > 5). The direct gas-solid carbonation has slower reaction kinetics and larger energy requirement due to the unavailability of moist media that helps in better reactants interaction. Hence, accelerated carbonation under aqueous

condition is preferred in industrial applications. The aqueous carbonation can be described as given in **Equation 2:**

$$(Ca,Mg)_xSi_yO_{x+2y+z}H_{2z}(s) + xCO_2(g) \rightarrow x(Ca,Mg)CO_3(s) + ySiO_2(s) + zH_2O(l) \quad (2)$$

which is explained by following reaction steps (Chiang and Pan 2017):

- Leaching of reactive metal ions (Ca^{2+}, Mg^{2+}) from the solid matrix.
- Dissolution of CO_2 into liquid phase, thus forming carbonate/bicarbonate ions (**Equation 3)**; and
- Nucleation and precipitation of carbonates (**Equation 4).**

$$CO_2(g) + H_2O(l) \rightarrow H_2CO_3^*(aq) \rightarrow H_2CO_3(aq) + HCO_3^-(aq) + CO_3^{2-}(aq) \quad (3)$$

$$(Ca,Mg)^{2+}(aq) + CO_3^{2-}(aq) \rightarrow (Ca,Mg)CO_3(s) \quad (4)$$

The dissolution of CO_2 in aqueous phase can form both carbonate (CO_3^{2-}) and bicarbonate (HCO_3^-) ions. Accelerated carbonation is more favored under alkaline conditions due to higher activity of CO_3^{2-} ions in the solution because CO_3^{2-} formation dominates at high pH (~12), while carbonic acid formation is favored at pH in the range of 4-5.6 and HCO_3^- at ~8 pH. The CO_3^{2-} ions potentially have four pathways upon reaction with alkaline minerals including direct conversion inside solid particle, crystallization on surface, precipitation in bulk solution, and adsorption on surface of the particle.

The dissolution and precipitation of carbonates are kinetically balanced based on leaching of cations from mineral feedstock. The affinity of oxides to carbonation decreases from basic oxides (CaO, MgO) → amphoteric oxides (Al_2O_3, Cr_2O_3, iron oxides etc) → acidic oxides (SiO_2) and thermodynamically, both alkaline earth metals (eg: Ca, Mg) and alkaline metals (Na, K) are reactive with CO_3^{2-} ions to form their carbonates. However, the alkaline metal carbonates are water soluble which makes it unsuitable for permanent CO_2 sequestration. In addition, Ca^{2+} ions

are more mobile than Mg^{2+} ions, making Ca^{2+} ions more reactive when in contact with CO_2 although minerals containing Mg^{2+} ions are more abundant in nature (Chiang and Pan 2017). Hence, alkaline materials with more Ca^{2+} ions content that is easily available without resource depletion can be considered the most desirable feedstock for CO_2 sequestration.

2.2.3 Alkaline Wastes Carbon Sequestration

The use of natural minerals can induce environmental impacts as it requires large scale mining and associated energy use. Hence, alkaline industrial wastes (AW) containing Ca-Mg silicates, free lime (CaO) and Portlandite ($Ca(OH)_2$) form an alternative feedstock for carbon sequestration. The use of several AW has been studied by researchers for their CO_2 sequestration capacity as shown in **Table 2-1**.

Table 2-1: Alkaline industrial wastes studied for carbon sequestration capacity (Source: Chiang and Pan 2017)

Waste Group	Example
Iron and steel slag	Blast furnace (BF) slag Basic oxygen furnace (BOF) slag Electric arc furnace oxidizing (EAFO) slag Electric arc furnace reducing (EAFR) slag Argon oxygen decarburization (AOD) slag Ladle furnace (LF) slag
Air pollution control (APC) residues	Cyclone dust Cloth-bag dust Municipal solid waste incinerator (MSWI) fly ash Coal fly ash
Bottom ash (from furnace and incinerator)	MSWI bottom ash Boiler ash Coal slag Oil shale ash
Cement wastes	Cement kiln dust (CKD) Cement bypass dust (CBD) Construction and demolition waste

	Cement/concrete waste Blended hydraulic slag cement (BHC)
Mining and mineral processing wastes	Asbestos tailings Copper tailings Red mud
Paper mill wastes	Lime kiln residues Green liquor dreg Paper sludge

Advantages of using AW are as follows (Chiang and Pan 2017):

- High availability of mineral feedstock at low cost, offering higher opportunity for CO_2 sequestration at lower economic burden.
- Carbonates obtained as end products are stable under ambient conditions and their formation is favored more at high pH which is the common characteristic of the AW.
- Carbonated AW can be reused as construction materials due to higher strength as carbonation reduces the amount of free-lime (CaO) in AW decreasing the impacts of hydration expansion.
- Carbonation fixes the amount of leachable heavy metal in AW and makes it non-hazardous to environment.
- Energy consumption in treating AW or from natural mineral carbon sequestration is reduced due to higher reactivity of AW
- Environmental impact and energy dependency is notably reduced by avoiding mining for rock minerals.
- Cost-effective and energy-efficient method for industries as the feedstock mineral is near CO_2 emission point source, minimizing transportation.
- Beneficial use of industrial waste and divertion from excess stockpiling and landfilling.

Though mineral carbonation with AW is a viable technology, it needs to be optimized for its full potential. AW may have to be pretreated such as grinding and thermal activation for increasing the reactivity to achieve carbonation in a short span of time (i.e, within few hours). Besides, the selection of AW must be optimized based on the reactivity of minerals in AW and immediate need for its handling within the parent industry. Such an approach can lead to sustainable carbon sequestration method that is less expensive, not energy intensive, and contributes to the beneficial use of AW by diverting it away from landfill disposal.

2.3 IRON AND STEEL SLAG CO_2 SEQUESTRATION

Among the available AW feedstock, the iron and steel slags have higher carbonation capacity relative to materials such as fly ash and paper mill wastes due to the presence of more Ca oxide content (Chiang and Pan 2017). Iron and steel industry accounted for almost 22% of industrial energy-use and about 7% of total CO_2 emissions globally in 2011 (Pan et al. 2016; Chiang and Pan, 2017). The slag from iron and steel industry is generated upon treating the iron ore with flux containing limestone to produce pig iron (called iron-making) and further upon the treatment of pig iron with scrap metal, limestone and dolomite to produce low carbon steel (called steel-making). According to U.S. Geological Survey (USGS), every year almost 15-20 million ton of iron/ferrous slag and about 10-15 million ton of steel slag is produced. These large quantities of slag are often stockpiled in huge heaps posing land degradation, air pollution from slag dust and affecting aesthetics. A part of the iron and steel slag is utilized in civil and construction industry such as cement production and road building while the concern of stockpiling and landfilling of iron and steel slag is still critical as its production continues with increasing demand for iron and steel products with no reciprocal increase of its utilization elsewhere and not all the slag has been

identified with its potential recycling opportunities. The slag is characterized by highly alkaline nature and significant levels of metal ions, especially Ca.

2.3.1 Types of Slags

The chemical composition of iron and steel slags, primarily as Ca-Mg silicates, is similar to natural sand, gravel, or stones. The slag composition largely varies depending on its source and particle sizes (Chiang and Pan, 2017). Depending on the stage at which the slag is collected, it can be classified broadly into: (1) *Iron/ferrous slag* collected upon completion of iron-making process; and (2) *Steel slag* formed as by-product of steel-making resulting in differences with respect to their mineralogy, reactivity, morphology and hence applications. Further, the iron and steel slags are also classified based on the technology used in production of the iron and steel (**Figure 2-3,** Yildrim and Prezzi 2011):

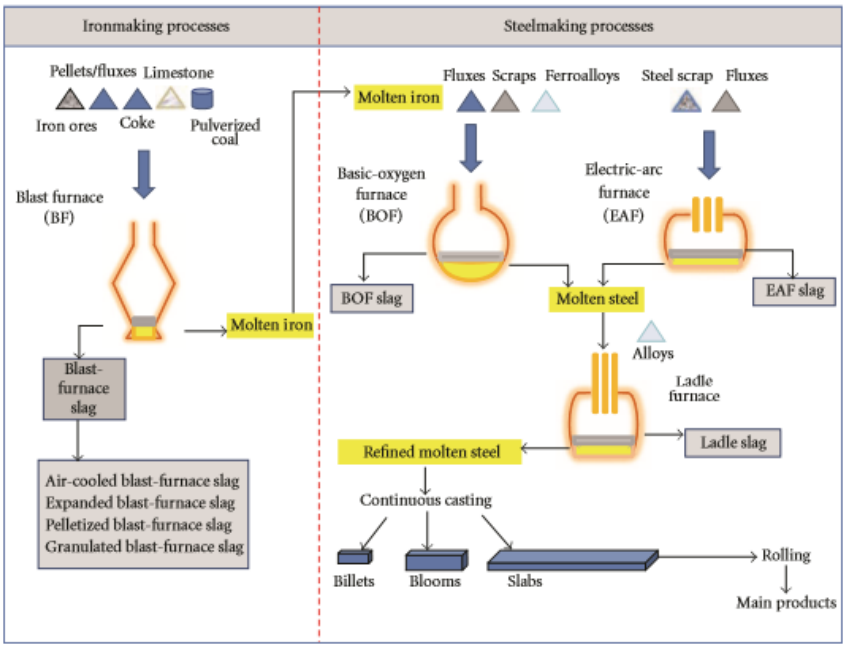

Figure 2-3: Iron and steel slag production
(Source: Yildirim and Prezzi, 2011)

- *Blast Furnace (BF) Slag*: It is a co-product from conversion of iron ore to pig iron (iron-making) in a blast furnace that is either air-cooled or quenched (also known as granulated). Its specific gravity is about 2-2.9 while its field density may vary from 1.2 to 1.3 g/cm^3 (Chesner et al. 1998; Das et al. 2007). BF slag consists of inorganic compounds that consist of SiO_2 (30-36%), CaO (32-45%), Al_2O_3 (10-16%), MgO (6-9%) and Fe_2O_3 (0.2-1.5%). BF slag is also characterized by their amorphous crystalline structure, whitish color and low iron content (Chiang and Pan 2017).
- *Basic Oxygen Furnace (BOF) slag*: It is formed as the co-product during conversion of pig iron from blast furnace to steel (steel-making) within BOF which are charged with 80-90% of the molten pig iron, 10-20% scrap metals and fluxing agents like lime and dolomite (to remove impurities) in presence of 99% pure oxygen blown at supersonic speed. The oxygen blowing makes sure carbon and other materials with affinity to oxygen is removed from the process, which is essential to produce low-carbon steel (Chiang and Pan 2017). The scrap metal helps in maintaining temperature within the furnace around 1600°C (Yildrim and Prezzi 2011). The impurities combined with the burnt fluxing agent forms the BOF slag. The chemical reactions within the furnace is responsible for the BOF slag mineralogy. It may vary slightly from one source to another depending on final composition of steel, but typically it consists of CaO (>35%), SiO_2 (7-18%), MgO (0.4-14%), Al_2O_3 (0.5-4%) and iron oxides (as high as 38%). The iron oxide is that percentage of iron which could not be recovered in the steel making process (Yildrim and Prezzi 2011). The high iron oxide content results in higher specific gravity for BOF slag in the range of 3.45-3.7.
- *Electric Arc Furnace (EAF) slag*: Steel slag obtained from steel-making within an EAF where an electric arc is used for charging the scrap metal, molten iron and fluxing agent

rather than gaseous fuel (Yildrim and Prezzi 2011). Also, the composition of steel scrap could be more than that of pig iron, essentially making the EAF process a steel scrap recycling process. Typically, EAF slag composition include FeO, CaO, SiO_2, Al_2O_3, and MgO contents in the 10–40%, 22–60%, 6–34%, 3–14%, and 3–13%, respectively (Yildrim and Prezzi 2011), but could vary depending on the type of scrap metal used. EAF slag is characterized as a denser, stronger, non-porous material unlike other forms of slag. Electric arc furnace slag can be classified into two types: oxidized EAFS (low CaO content), and reduced EAFS (high CaO content).

- *Ladle Furnace (LF) slag*: High quality steel-making slag where the pig iron is converted into high quality steel by passing through several LF converters to undergo refining such as desulphurization.

2.3.2 Characteristics of Slags

Among the different iron and steel slags, BF slag is most widely used in civil and construction industry. The high Ca content and low quantity of iron oxide makes BF slag suitable to be used in slag-cement blends. Air-cooled BF slag is used in road construction as a substitute for stones, aggregates and chips, while the granulated BF slag is used as a cement component which can substitute about 50% of the clinkers in cement manufacture (Chiang and Pan 2017). The BF slag-substituted cement is found to have higher strength, denser microstructure and higher durability compared to Portland cement concrete (Shi 2004). The lower content of iron in BF slag makes it suitable for use in numerous construction projects along with its other properties including low heat of hydration, resistance to acid, and limited alkali-silica reaction (Chiang and Pan 2017).

While almost 100% of the BF slag gets utilized in the USA, steel slags are not completely utilized. Steel slags are heavier than normal aggregate and are very hard, stable, and abrasion resistant owing to the high iron content. The mineralogical composition of steel slags are more complex than other types of residue such as ashes. They are a consolidated mix of many compounds (such as Ca, Mg, Fe, Si, Al) in different phases. The CaO and SiO_2 content dictates its use in cement industry (for hydraulic and pozzolanic properties) and in CO_2 fixation, while the Fe_2O_3 content contributes to hardness and grindability (Chiang and Pan 2017). Though BOF slag is utilized in road construction along with asphalt due to the lipophilic nature of CaO to reduce stripping and enhance water resistance, it cannot be used as cement-blend as its high iron content retards hydration (Chiang and Pan 2017; Shi 2004). Further, the hardness of steel slags leads to requirement of increased grinding energy. Steel slag also exhibits expansive tendency due to the presence of free-lime unless properly aged with water. These properties of steel slags limits its use in construction industry to asphalt paving, fill material, railroad ballast, and for snow and ice control.

Although a typical range for composition of common oxides in steel slag is available (Shi 2004; Yildrim and Prezzi 2011), these oxides concentration and other minor compounds are highly variable and change from batch to batch within the steel slag obtained from same plant depending on raw materials, type of steel, and furnace conditions (Shi 2004). Further, the studies by Zhang et al. (2011) inferred that the composition of BOF slag is highly variable within a sample obtained from the same source depending on particle size. It was found that the calcium oxide and silicate content increases and the iron content decreases with decrease in particle size. For instance, in the fraction with D_{50} = 1.43 μm, the amounts of SiO_2 and CaO increased by 28.9% and 13.4%, respectively, while the Fe_2O_3 content decreased by 69.7% compared to the

fraction with D_{50} = 60.24 μm (Zhang et al. 2011). The mineralogy of BOF slag differs with various particle size, hence providing opportunities for optimized utilization.

Steel slag is generally represented as CaO-MgO-SiO_2-FeO quaternary system (Shi 2004) as it consists of minerals such as larnite, portlandite, srebrodolskite, and merwinite in varying proportions. These minerals when found in steel slag are not as stable as they are in geologic formations because of their high reactivity (Chiang and Pan 2017). The addition of limestone (CaO) and dolomite ($CaMg(CO_3)_2$) results in large proportions of CaO and MgO in steel slag along with silicates and ferrites in their reactive charged phase. The iron and steel slags are highly alkaline (pH > 11) due to the presence of these basic (CaO, MgO) and amphoteric oxides (Al_2O_3, iron oxides), making it favorable to undergo accelerated carbonation as discussed earlier.

2.3.3 Benefits of Slag Carbonation

The concern of stockpiled steel slag, especially BOF slag and its suitability as a carbon sequestration material (due to alkalinity and Ca content) in accelerated carbonation has led to many studies that explore its carbonation capacity (Baciocchi et al. 2011; Sarperi et al. 2014; Kasina et al. 2015). As the demand of iron and steel processing will only keep increasing, there is a need to devise an efficient and low-cost method to reduce the GHG emissions, especially CO_2 emissions from steel plants in order for the industry to move towards environmental sustainability. One of the best ways to achieve this aim is to utilize the readily available steel slag feedstock at the steel mills that possess high carbonation capacity to capture CO_2 emissions from its flue gas. (Yu and Wang 2011).

Although the Ca and Mg oxide contents are comparable in BOF and BF slag, it has been found that the BF slags are comparatively resistant to carbonation. Kasina at al. (2015) reported

the carbonate content increased from 0.8 wt% to 13.4 wt% upon carbonation of steel making slags or BOF slag and from 0.4 wt% to only 2.2 wt% with BF slag. BOF slag has been reported to have a carbonation capacity of 93.5%, corresponding to CO_2 fixing of 290 kg/ton slag (Chang et al. 2012) and 0.264 kg/kg slag (Tu et al. 2015). Another study by Sarperi et al. (2014) reported a removal capacity of 63g CO_2 per 1 kg of BOF slag at an optimal L/S in the range 0.05-0.2. Hence, BOF slag is deemed as a suitable AW for CCS by accelerated carbonation. The use of steel slag for CCS at steel mills have several advantages that include:

- Cost reduction by avoiding the need to set up a new carbon capture facility with the conventional methods like water or amine scrubbing, membrane filtration or cryogenic distillation (Sarperi et al. 2014).
- Cut short on the transportation and fresh raw materials requirement.
- Utilization of stockpiled steel slag on-site for beneficial CCS purpose which in turn improves the steel slag properties such as compressive strength, soundness etc.
- Improved properties of carbonated steel slag allow its use as aggregates.
- Improvement of steel slag leaching properties (Boone at al. 2013).
- Comparatively easier, inexpensive and technologically viable mechanism with reduced energy consumption.

2.3.4 CO_2 Sequestration Mechanisms

The carbon sequestration mechanism by steel slag is essentially the same as the general carbonation mechanism discussed earlier. Nevertheless, carbonation with steel slag faces some challenges wherein optimization of carbonation reaction is required. Several studies have been reported to understand the carbon sequestration mechanism by steel slag (**Table 2-2**). Huijgen et

al. (2005) reported that the degree of carbonation with steel slag can be determined using its total calcium content (Ca_{total}), the molar masses of Ca (MW_{Ca}) and CO_2 (MW_{CO_2}), and the initial mass of carbonate present in the system as given by **Equation 5** (Huijgen et al. 2005):

$$\xi_{Ca}(\%) = \frac{\frac{CO_2(wt\%)}{100-CO_2(wt\%)} \times \frac{MW_{Ca}(kg/mol)}{MW_{CO_2}(kg/mol)}}{Ca_{total}(kg/kg)} \quad (5)$$

Table 2-2: Selected previous studies on carbonation mechanisms

References	**Slags studied**	**Carbonation mechanism**
Huijgen et al. (2005)	Linz Donawitz steel slag	Similar to natural weathering in which Ca and Mg minerals are converted into Ca or Mg carbonates: $(Ca,Mg)SiO_3(s) + CO_2(g) \rightarrow (Ca,Mg)CO_3(s) + SiO_2(s)$ Three major phases of Ca in the fresh steel slag was identified as $Ca(OH)_2$; Ca-(Fe)-silicates and Ca-Fe-O. The first two phases were reported as the ones reacive with CO_2. Particle size, temperature and CO_2 pressure were listed as most affective process variables in carbonation. The limiting reaction step in carbonation was concluded as the diffusion of Ca toward the surface of slag particle.
Huijen and Comans (2006)	Linz Donawitz steel slag	Effect of carbonation on leaching and its implications for reaction mechanism is discussed by dividing the minerals into 4 categories: (1) Elements involved in cabonation (Ca and Si), (2) potential alkaline earth metals susceptible to carbonation (Mg, Sr and Ba), (3) elements that provide reactive hydroxide surfaces (Al, Fe and Mn); and (4) potentially harmful oxyanions and heavy metals.
Deiner et al. (2010)	EAF and LF slag	Studied long-term stability of steel slags within landfill cover based on the acid neutralization capacity and leaching of 3 and 10 months old slag that was exposed to various CO_2 pressure. "Carbonation at high CO_2 concentration reduced pH by almost two units and ANC 8.3 about 50%. ANC 4.5

		increased, indicating buffering, possibly by the new carbonates formed.” Ba leaching decreased for the 10 months sample in higher humidity levels compared to lower independent of CO_2 content. Increased V leaching was linked to the dissolution of Ca-vanadate or to hydration of free lime that increases pH causing lower dissolution of V containing Ca-silicates. Leaching from aged steel slags was generally low and concluded to be influenced by the ageing time, CO_2 in the atmophere and temperature.
Yilmaz et al. (2013)	BOF slag	Evolution of hydraulic properties of BOF slag upon carbonaion was studied assuming that carbonation occurred mainly through the dissolution of portlandite and precipitation of calcite as ~20 µm coating that clogs throats and the smallest pores. Predicted a decrease in the pore radius by formation of 2- o 4- cm thick crust. Mineral alterations were favored by contact with water by being a part of the weathering and carrier of CO_2. Modelling indicated the dependency of hydraulic properties on mineral deposition. Both uniform and linear coating triggered decrease in hydraulic conductivity while effect of linear coating had stronger effects. However, the uniform coating model decreased capilarity while linear coating increased capilarity and hence requires better understanding of mineral deposition in pores to accurately determine the mechanism.
Kasina et al. (2015)	BF and Steel-making (SM) slag	Based on the dissolution of divalent cations (Ca, Mg, Fe) from minerals in the presence of CO_2 $MO + CO_2 \rightarrow MCO_3 + heat$ SM slag more efficient compared to BF, due to the presence of dicalcium silicate minerals in the former that is highly soluble in pH > 10. The melilite minerals in BF slag do not undergo dissolution in the pH range. In SM slag, the calcite formation was found on rims, slag edges as well as it infilled the pores, while in BF carbonation, a singly calcite crstal rim was formed, with most common form being gypsum.

		Portlandite and lime phase that was common in SM slags were absent in BF slags. Dissolution of larnite does not lead to release of SiO_2 as as the concentration level was still below sauration. It instead forms a calcium depleted silicate rim. The silicate rims and calcite rims are believed to prohibit the progress of carbonation.

It is assumed that carbonation in steel slag occurs only upon Ca carbonation and initial carbonate content in steel slag is negligible as well as no significant mass loss occurs due to leaching. These assumptions are made in order to explain the complex nature of leaching of several compounds in the steel slag in a simpler and comprehensive way with respect to the most reactive and easily leachable Ca content. According to Huijgen et al. (2005), three Ca species were found to exist in steel slag as $Ca(OH)_2$, Ca-Fe-silicates and Ca-Fe-O, out of which $Ca(OH)_2$ has higher carbonation rate compared to Ca-Fe-silicates. It was found that $Ca(OH)_2$ was completely converted into calcite ($CaCO_3$) upon carbonation. The study was also successful in distinguishing the carbonation into three different stages, correlating Ca responsible for each stage which are referred to as fraction I, fraction II and fraction III. Based on the solubility products of the identified Ca species and the pH drop of steel slag upon carbonation, Ca fraction I (pH dip from 11.1 to 9.6) was deduced to consist mainly of $Ca(OH)_2$ and Ca silicates (similar to CSH) that are relatively easily leachable. Fraction II was assumed to consist of Ca silicates that are more difficult to dissolve, owing to the slight decrease in pH after 9.6. The rest, Ca fraction III, consists of Ca that is virtually insoluble or physically not available for leaching within a particular particle size or reaction time. Fraction III was assumed to identify the Ca-Fe-O phase in steel slag. The fraction I was responsible for the first stage of carbonation, which was significantly rapid and occurs in just over 2 min in the reactor. Stage I leads to 40% carbonation, where in fraction I and 36% of fraction II were responsible, while only an extra 13% (or 39% of

fraction II) reacted when the reaction time was increased to 30 min. This shows a trend of carbonation reaction which is initially rapid due to the availability of easily leachable Ca species, followed by a gradual decline in the reaction rate. Stolaroff et al. (2005) studied the carbonation mechanism in steel slag with respect to Ca leaching. Their study reports a shift of Ca leaching kinetics from rapid to much slower rate, similar to the carbonation rate trend. It signifies that the Ca leachability plays a significant role in the kinetics of carbonation. Huijgen et al. (2005) also applied this trend to conclude that $CaCO_3$ precipitation is not a rate determining step in steel slag carbonation.

2.3.5 Parameters Affecting Slag Carbonation Potential

Carbonation of steel slag, being dependent on the mineralogy, pH, kinetics and reaction temperature, should be studied for the parameters that can alter the reaction extend to maximize the carbonation capacity of steel slags. Huijgen et al. (2005) and other researchers also studied the various parameters that affected the carbonation capacity of steel slag including:

- *Reaction time*: As discussed above, the reaction time of 30 min resulted only in the rapid reaction of fractions I and II, while the fraction III reaction could not be established. Hence, a longer reaction time was assumed suitable for carbonation in which several more ions like in fraction III could also contribute eventually. Ca ions itself from within more closely held minerals, Mg ions which are less mobile could potentially contribute to CO_2 capture if it is exposed to the gas-liquid atmosphere for longer period. However, the reaction kinetics are usually the most rapid during the initial 60 min and then it gradually declines to continue at lower kinetics (Tu et al. 2015).

- *Particle size*: A reduction in particle size from <2mm to <38ɥm was observed to have a significant effect in increasing the carbonation capacity from 24 to 74% (Huijgen et al. 2005). This is also in conjunction with the observations of Zhang et al. (2011), wherein a higher CaO and SiO_2 content and lower iron oxide content was observed with decreasing particle size. Correlating the two studies, it is possible to conclude that the higher carbonation capacity of smaller particle sized steel slag could be due to the increase in availability of CaO and SiO_2. The decrease in availability of iron oxides with reduction in particle size could also increase the affinity of particles towards moisture (Chiang and Pan 2017), leading to higher moisture availability for accelerated carbonation. It could also be attributed to the increase in specific surface area. Further, Capobianco et al. (2014), in his studies on use of steel slag in revitalization of brownfields also observed that grain size had a great influence on CO_2 sequestration, wherein the smaller sized particles performed better. Another study on Ca leaching from various steel slag particle sizes was conducted by According to Lekakh et al. (2008), approximately 33% of the calcium leached from the 45 – 75 µm fraction in the first hour, while less than 5% of the Ca leached from the 2300 – 3300 µm fraction after 24 hours depicting that smaller particle size could also result in faster reaction kinetics. As Ca leaching is one of the limiting reaction-step in steel slag carbonation, the smaller particle sizes with greater surface area are deemed better for the purpose.
- *Temperature*: It was discussed that the carbonation reaction is exothermic and hence, could easily proceed under lower temperature conditions. The two important steps within the carbonation, namely, leaching of Ca and dissolution of CO_2 forms the determining factors for optimum temperature. The Ca leaching proceeds faster at higher temperatures while the solubility of CO_2 in liquid phase decreases with an increase in temperature. Hence,

temperature range for optimum carbonation was determined by Huijgen et al. (2005) as 25-175°C. Tu et al. (2015) also discussed the contrary effects of high temperature on Ca leaching and CO_2 dissolution and arrived at an optimum temperature of 60°C for carbonation by stainless steel slag because the carbonation degree increased from 20°C to 60°C, while it decreased from 60°C to 80°C in their study. The reported optimum temperatures are well within the ambient conditions in our environment, thus decreasing the need for high energy requirement in terms for maintaining high reaction temperatures.

- *CO_2 pressure and stirring rate*: A CO_2 pressure and stirring rate above 9 bar and 500 rpm, respectively, was found to have negligible effect on carbonation below the optimum temperature range. Hence, these parameters were not considered as rate determining step. However, stirring rate could aid in increasing the carbonation degree as stirring could strip-off the carbonates formed on the slag surface exposing more reactive surfaces.
- *Liquid to Solid ratio (L/S)*: Generally applicable L/S ratio could not be established based on the published studies (Sarperi et al. 2014; Su et al. 2016; Ukwattage et al. 2017), while a 2 kg/kg was generally considered to be the optimum L/S for reactor mixing by Huijgen et al. 2005 and observed that a slight decrease in moisture resulted in increase in carbonation due to increased ionic strength and consequent increase in solubility of Ca.

The above parameters were studied to arrive at conclusions on rate-determining steps in steel slag carbonation and developing the three basic steps of carbonation as discussed earlier. According to Huijgen et al. (2005), the Ca leaching was concluded as the rate-determining step in steel slag carbonation. This step was further subdivided into 2 steps: (1) Diffusion of Ca toward the surface of particle; and (2) Dissolution of Ca from surface into the solution. As the effect of stirring rate on carbonation was found negligible, step (2) given above was determined

to be very fast and independent, and hence, step (1) was ultimately concluded to be the most critical step in determining the rate of carbonation. The previously discussed study about higher Ca leaching and better carbonation capacity with smaller particle sizes is hence, presumed to be because of the importance of step (2) in the process. In a smaller particle, the pathway of Ca for leaching from slag matrix is extremely cut-short making the reaction faster. Moreover, it also provides more surface area for the slag-water-CO_2 interaction.

In spite of the necessity to optimize the carbonation of steel slag for industrial scale application, the slag-water-gas reaction essentially takes place naturally without any monitoring commitments at a reasonable rate. Several Northeastern Ohio pavement construction projects use steel slag as base and sub-base aggregates. The highway department requires that the steel slag be cured or aged for at least 6 months prior to its use. The clogging of drains and creation of water retention in pavements in the Ohio region leading to premature failure of pavements caused a concern in transportation department that lead to a detailed study of different types of steel slag by Gupta et al. (1994). This study aimed to investigate the free lime content in the steel slag stockpiles at different depths up to 10 m. It was observed that the CaO content in BOF was less at the top of the pile exposed to the environment after 6 months of aging when compared to that at 10 m depth. The carbonation degree decreases with depth as it does not come in contact with CO_2-charged pore water. Hence, the observations from this study is self-explanatory in understanding that a substantial level of carbonation leading to $CaCO_3$ precipitation is possible in a steel slag pile left exposed to the atmosphere.

2.3.6 Effects of Carbonation on Slag Properties

Studies by Pan et al. (2016) and reports by Chiang and Pan (2017) have analyzed changes in physical, chemical, mineralogical and leaching properties of steel slag after carbonation. **Table 2-3** summarizes some of the changes observed in steel slag after carbonation as evaluated by Pan et al. (2016).

Table 2-3: Changes observed in steel slag upon carbonation
(Source: Pan et al. 2016)

Process	Type	Categories	Description
Direct	**Physical**	Density	Reduce: 3.56 → 2.47-3.27 g/cm^3
		Particle size	Become coarser due to agglomeration
		BET surface area	Surface area increases
		Porosity	Decreases due to calcite filling up pores
		Microstructure	Regular morphology obtained upon continuous coating of product on the surface
	Chemical	Mineralogy	Formation of $CaCO_3$, $Ca_5(SiO_4)_2CO_3$ Consumption of $Ca(OH)_2$
		Free CaO and $Ca(OH)_2$	Partial to complete elimination depending on type of slag and particle size
		Heavy metal leaching	Leaching of metals like Cr reduced by several orders of magnitude
Indirect	**Physical**	Particle size	Spherical agglomerates of 10-20ɥm
		Particle shape	Cubic crystals of calcite formed at 40-80°C Needle-like structured aragonite formed at 90°C
	Chemical	Mineralogy	Calcite at low temperatures while aragonite formed at high temperatures

The most common methods of analyzing the change in morphology and mineralogy of steel slag upon carbonation is using Scanning Electron Microscopy and X-Ray Energy Dispersive Spectrometer (SEM-XEDS) imaging and analysis, Thermogravimetric Analysis (TGA) and quantitative X-ray Diffraction (XRD) methods. Carbonation of steel slag can be observed in SEM by the formation of distinctive structures (polymorphs) that represent calcium carbonate, namely calcite, aragonite and vaterite (**Figure 2-4**).

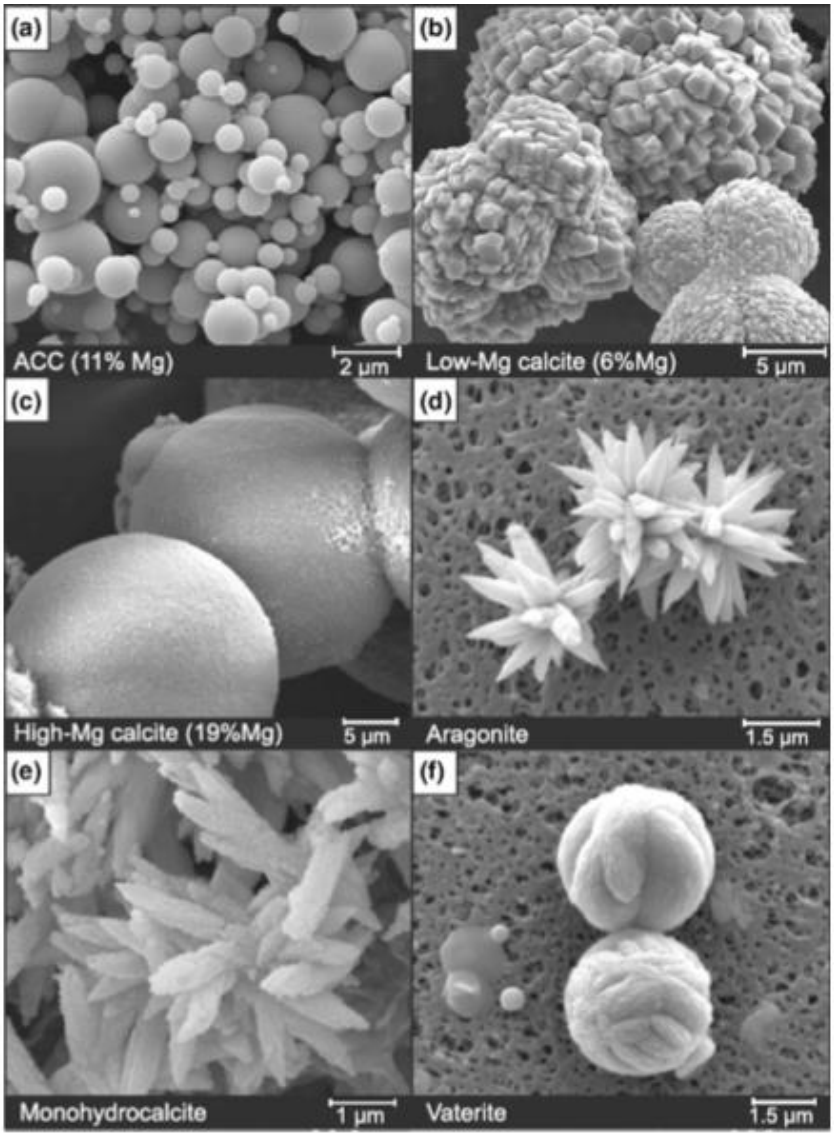

Figure 2-4: Calcium carbonate polymorphs (Source: Chiang and Pan 2017)

Rhombohedral, prismatic, or scalenohedral crystal types are common to calcite formations, while aragonite is typically found as needle-like crystals with high aspect ratio. In nature, hexagonally shaped calcite crystals or orthorhombic aragonites are the most common calcium carbonate formations. The formation mechanism of the polymorphs depends on the crystallography of the original calcium silicate hydrate (Chiang and Pan, 2017). The change in mineralogy with carbonation is best understood by the quantitative XRD. XRD is the most commonly used rapid analytical method based on dual nature of X-rays to analyze the mineralogical changes in non-carbonated and carbonated steel slag, helping in determination of the mechanisms and minerals involved in carbonation. TGA is particularly useful for analyzing the carbonation degree depending on weight loss in temperature steps ramping from ~400-1000°C. The weight loss is attributed to moisture loss and chemical decomposition of compounds into gaseous forms. The individual compounds can hence be characterized as the thermal decomposition temperature varies among compounds (Chiang and Pan 2017).

Studies show that with carbonation, CaO, $Ca(OH)_2$ and Ca-silicates diminish from the steel slag. Also, a simultaneous decrease in Mg content and increase in SiO_2 content have also been reported with carbonation (Kasina et al. 2015). The oxides and Ca ions from minerals leach into solution to react with dissolved CO_2 to form the carbonates. Hence, carbonated steel slag also show an increase in the carbonate content upon analysis. From SEM analysis, often an inner rim of Ca exhausted silicate rim coated by carbonates have been found which forms due to the Ca ion leaching from Larnite in the steel slag to the surface to form calcium carbonates. With the formation of carbonates on slag surface, a change in pore structure and hydraulic permeability was also observed (Yilmaz et al. 2013; Wu et al. 2015). The porosity decreased, number of fine pores increased, and large pores decreased (Wu et al. 2015). It leads to decrease in hydraulic

permeability and increase in capillarity (Yilmaz et al. 2013). One of the relevant observations in terms of environmental application of steel slag is the reduction of leachability of most of the heavy and toxic metals with carbonation. It was observed by Huijgen and Commans **(**2006) as well as van Zomeren et al. (2011) that while a notable reduction in leaching of Ba, Sr, Ca and other heavy metals were observed, the leaching of vanadium (V) increased substantially. However, studies have led to the conclusion that leaching of heavy metals from steel slag before and after carbonation poses low environmental impact.

A white crusty formation is usually found to be formed on the slag surface as carbonation extends. This is attributed to the carbonate formation that sticks to each other and holds together the slag particles to form a cemented concrete block type material with compressive strength and elasticity comparable to concrete (Takahashi and Yabuta 2002). Such change in morphology and strength properties of steel slag upgrades it to be utilized in the construction industry as explained later.

2.4 ENVIRONMENTAL APPLICATIONS OF IRON AND STEEL SLAG

The steel slag has been used in a variety of construction applications which has tremendously helped in reducing the amount of steel slag that otherwise would have required stock piling at the site or landfilling. Landfilling, though effective in reducing the stock piling, consumes a large volume of useful space otherwise available for the commercial and household wastes. The application of steel slag in cement, pavement construction and other applications, faces certain limitations due to the volume expansion property of steel slag owing to the presence of free-CaO. Hence, there has been several studies that aimed at studying it’s utility in other fields as well as

modifying slag suitably. Other than the construction field, the utility of steel slag has most widely been studied for environmental applications.

In the case of environmental applications, the properties of steel slag like pH, carbon sequestration properties and mineralogy are given more importance rather than the strength, soundness, and hardness. Recent studies have shown utilization of iron and steel slag in devicing efficient, easy and comparatively inexpensive methods in various environmental applications. **Table 2-4** summarizes selected studies showing various environmental applications of steel slag.

Table 2-4: Previous Studies on Steel Slag Applications

References	**Slag used**	**Applications**
Baker et al. (1998)	BOF slag	Phosphorous removal by adsorption and precipitation in the form of calcium phosphate
Smith (2003)	Steel slag	Reactive barriers to remove Cr (VI) and TCE from wastewater
Ochola & Moo Young (2004)	Modified steel slag	Reduction of Cr(VI) to Cr(III) in water
Wang et al. (2006)	Steel slag	Fe fertilizer for agricultural land
Xian et al. (2006)	Steel slag	10-20 g/kg addition resulted in increased corn yield
Bowden et al. (2009)	BOF slag	Phosphorous and phosphate removal along with pathogen removal from waste and storm water
Hermann et al. (2010)	EAD and LD slag	Barrier material in sanitary landfill cover construction
Grubb et al. (2011)	BOF slag fines	As^{3+} and As^{5+} immobilization in reactive barriers
Grubb & Wazne (2011)	BOF slag fines	Heavy and toxic metal immobilization
Tsai et al. (2011)	BOF slag	Iron-mineral supplement in Fenton-like oxidation for enhanced TCE removal
Sarperi et al. (2014)	BOF slag	Raw biogas up-gradation to natural gas composition for vehicle fuel
Sheridan (2014)	BOF & Stainless steel slag	Acid mine drainage remediation by replacing alkaline minerals with steel slag with better results from BOF slag

Ning et al. (2016)	Steel slag	Fe and Si fertilizer and modification of acidic soil for paddy cultivation

The most widely advocated environmental applications of steel slag include phosphate removal from wastewater, storm water treatment, reduction of hexavalent chromium, CO_2 sequestration, sand capping, and remediation of acid mine drainage. More details on these various beneficial applications are presented in the next section.

2.4.1 Wastewater and Stormwater Treatment

The commercial and industrial wastewater affects the environment in which it is discharged based on the watershed, in-stream quality, heavy metal usage in industries etc. It is important that the wastewater is treated properly before discharging it to natural environment and the concentration of various contaminants be within permissible limits. The disposal of untreated wastewater and stromwater with excess fertilizers and detergents adds to the nutrients in the wastewater that causes eutrophication.

Phosphate (inorganic anion) presence in wastewater could be a major environmental issue affecting various regions. The higher amount of phosphates (>0.005 - 0.05 mg/L) is generated through activities related to agriculture, industrialization, and urbanization. The current phosphate removal methods such as chemical precipitation are highly expensive and less-efficient and cause a 40% increase in sludge volume. Studies on permeable reactive mixtures using BOF slag have observed that the slag could remove phosphorous/phosphate and reduce pathogens in water to very low concentrations (Bowden et al. 2009; Lu et al. 2008). According to the study by Bowden et al. (2009), the clast size of the BOF slag played a significant role in increasing the P removal capacity of the reactive mixture. The column tests on P removal by slag

exhibited high initial removal (52-74%) attributed to the chemisorption by the initially flushed Ca from BOF, that gradually reduced to more stable removal level (24%) due to the limited Ca availability, attaining a maximum effective P removal of 8.39 mg/g. Most of the phosphate removal capacity was attained within the initial 30 min which implies the rapid nature of reaction (Lu et al. 2008; Bowden et al. 2009). Lu et al. (2008) found that the phosphate adsorption on BF and steel slag followed the Freundlich isotherm with different k and 1/n constants for each slag. Calcite formed on the slag surface is known to provide sorption sites for the nucleation and precipitation of calcium phosphates (Freeman and Rowell 1981), thus prolonging the continuous successful operation of the treatment system (Bowden et al. 2009).

The high permeability and alkaline pH (~10-12) of slag act as favorable properties contributing to water purification processes. A 10 year long column experiment by Baker et al. (1998) revealed a continuous redution of phosphorous from 3 mg/L to 0.05 mg/L. The most recent application include the passing of wastewater from septic tank though a permeable reactive barrier containing BOF slag (Smyth et al. 2004). A wastewater treatment plant for the township of Waiuku obtained an 80% reduction of phosphate content with iron slag. In other such projects in Canada and Massachussets, a reduction of BOD and E.coli content was also observed in addition to the phosphate removal (IMS, T.C.). Lu et al. (2008) concluded in his studies that both BF and steel slag were highly efficient in removal of phosphate from aqueous solutions. In the study, the reversibility of the phosphate-slag reaction was also explored and it was found that the reaction is not completely reversible with the slag-phophate bond being very strong allowing only 9-43% phosphate desorption within the pH range of 3-7.

Another major industrial contaminant which is considered a priority pollutant is the hexavalent chromium (Cr (VI)) which is relased from processes such as tanning, wood

preservation, and metal plating. It is carcinogenic to living cells even at small levels as it is highly soluble over a large pH range and easily penetrates cell membranes, while trivalent chromium (Cr(III)) is non-toxic and essential for glucose metabolism (Ochola and Moo-Young 2004). Hence, the most commonly adopted method to control Cr (VI) is its reduction to Cr(III) at pH~2.0 and subsequent precipitation in the form of hydroxides at elevated pH~9.0-10.0 using lime (Mohan and Pittman 2006). Several studies have explored the reduction of Cr(VI) to Cr(III) and the adsoprtion of Cr(VI) by iron and steel slags (Srivastava et al. 1997; Ochola and Moo-Young 2004). Studies by Ochola and Moo-Young (2004) showed that modified steel slag used in their tests reduced Cr(VI) through redox mechanisms. The modified steel slag, due to the presence of iron based compounds suitable for adsorption of Cr(VI) was studied for Cr(VI) removal by adsorption as well as reduction. Simultaneous measurements of the redox potential during tests established that redox reactions were primarily responsible for the reduction of Cr(VI) to Cr(III) from water passed through steel slag. Furthermore, they postulated that the mechanism responsible for the reduction occurred via a one electron transfer process within an inner sphere complex that occurs between steel slag and chromium. The process is repeated until the stable form of Cr(III) is attained and due to the high pH of the solution, it is precipitated in the form of hydroxides. It was also observed that the removal of Cr(VI) by adsoprtion was also possible in spite of presence of competing anions like orthophosphates in water.

2.4.2 Soil, Sediment and Groundwater Remediation

The use of steel slag has been explored extensively in the revitalization of superfund sites, brownfields, and other contaminated sites. Environmental remediation is to be incorporated at such sites to prevent the leaching of heavy metals into groundwater and its contamination. Use of

steel slag is particularly advantageous as it is avalable as the byproduct of industrial activity making it an economic and sustainable method to the achieve the remediation goals. Steel slags that contain Fe(0) is also geochemically active with the capacity to immobilize several cationic and oxyanionic heavy metals from aqueous, soil and soil-like media by oxidation, precipitation, adsorption and complexation.

Chlorinated solvents like trichloroethylene (TCE) is a major contaminant group commonly found at hazarduous waste disposal and spill sites (Tsai et al. 2011). It is used as cleaning agents in industries and released into the groundwater upon mishandling, improper storage and disposal of spent solvent. TCE removal to non-hazardous levels is difficult with normal water purification methods like coagulation and sedimentation. The USEPA has listed air-stripping, air-stripping with carbon adsorption, soil venting, and bioremediation as few promising remediation technologies for removal of TCE (Russell et al. 1992). Chemical oxidation like Fenton-oxidation (a solution of hydrogen peroxide with ferrous iron as catalyst) mechanism has also been found to remove TCE effectively. The chemical oxidation method for TCE removal was found to be enhanced upon using BOF slag as the supplement source of iron minerals in Fenton oxidation and persulphate oxidation processes (Tsai et al. 2011) which can be converted to a design for permeable reactive barrier system for groundwater remediation.

The use of steel slag is deemed as a sustainable option as it will reduce the consumption of iron oxides in the form of geothite and hematite (Mohammed et al. 2016). Smith (2003) investigated the use of a permeable reactive barrier that solely consists of steel slag with a median diameter of about one-eighth of an inch to one inch, and prefereably between one-quarter to three-eighths of an inch, in order to remove groundwater contaminants. The method involves placing an underground barrier of porous steel slag bed in the flow path of contaminated

groundwater allowing its purification as it passes through the barrier, with contemplation of replacing spent slag with fresh slag or of building an adjacent wall as required. The Fe(0) reactive barriers that are usually used to serve the purpose and their high cost served as the background of this invention. According to the study, it was found to be effective in removing TCE and Cr(VI) from groundwater.

The heavy metal laden soils and soil-like materials from quarry, dredged material and outdoor firing ranges (Scott 2001; Lee et al. 2002; Ahmad et al. 2012) are known to affect the groundwater as the heavy meals leach underground. Grubb and Wazne (2011) showed successful immobilization of heavy and toxic metals like As(III), As(V), Cd, Cu, Pb, P, Ni, W, Se(IV), Se(VI) and Zn by blending slag fines (BOF slag and BF slag fines) with soil to form a stabilized media. Moon et al. (2015) also conducted studies on stabilization of As, Pb, and Cu using waste oyser shells and steel slag that act as a supply of both Ca and Fe. The soil-slag blends are proposed to be used as firing range backstop berm into which bullets and projectiles are directly fired, filter medium or even in conjunction with geosynthetics (Grubb and Wazne 2011; Moon et al. 2015).

In a study conducted to analyze promotion of dredged material (DM) recycling in Maryland for geotechnical fill and trenches etc, the ability of steel slag fines-DM (SSF-DM) blends to immobilize 100 mg/kg arsenite (As^{3+}) and arsenate (As^{5+}) that were usually found in their DM was investigated. The SSF materials performed extremely well by immobilizing approximately 7900 mg/kg As^{3+} and 8800 mg/kg As^{5+}, resulting in TCLP and SPLP concentrations <0:010 mg/L in three out of four samples (Grubb et al. 2011). Capobianco et al. (2014) even advanced the use of alkaline soil-like media in brownfields such as the steel slag-

soil blends at steel industry sites as a media for in-situ CO_2 sequestration of CO_2 released as a consequesnce of soil and groundwater remediation treatment techniques employed.

2.4.3 Sediment Capping and Marine Improvement

Sand-capping is a marine environment improvement method. The sludge layers in the sea bed that produce hydrogen sulphide (H_2S) upon decomposition causes blue tide, reduction of dissolved oxygen in marine water and increase the chances of red tide. Sand capping reduces the elution of nutrient salts that cause eutrophication and H_2S from the organic sediment layers in the sea bed. However, sand capping uses sand borrowed from other regions which has detrimental effects on land resources. To reduce the land degradation, alternative materials like slag have been tested for its suitability as capping material for marine sludge layer (Takahashi and Yabuta 2002). Slag sand that consisted of BF slag was chosen to study its feasibility in H_2S suppression, increasing silicate availability and promotion of marine organism culture in marine environment by analyzing test plots of sea bed with traditional sand-capping and an area with slag sand-capping. The analysis showed an increase in the marine diversity in region with slag sand-capping, H_2S elimination, and reduction of blue tides. In particular, the slag acted as a silicate supply to the sea bed environment, leading to rise in the silicate concentration to ~0.28 ppm that is necessary for diatoms. Hence, the proliferation of diatoms and its competition with the red-tide causing dinoflagellates also lead to the prevention of red tides. More species such as shrimp, goby fish, and clamworm were also found in the slag sand-capped area due to the modification of the sea bed grain size. The BF slag sand-capping was tested in the field on Naka-umi Sea Purification and Sand-capping Project in west Japan. The H_2S-slag reaction mechanism and the

H_2S removal capacity by slag have been studied (Kim et al. 2012; Sarperi et al. 2014). Sarperi et al. (2014) found that BOF slag has a capacity of removing 140 g_{H_2S}/kg.

Another marine application of the slag was in the construction of artificial reefs using carbonated slag blocks called marine blocks (Takahashi and Yabuta 2002). One cubic meter marine blocks were constructed in airtight molds packed with steel slag and water that was solidified by injecting CO_2 at a designated pressure through it. The carbonation started from bottom, slowly moved up and finished upon reaching the top of the mold. The calcium carbonate formed on the slag surface was found to firmly join to each other and lead to much lower alkalinity compared to traditional concrete blocks when placed in marine water. The slag blocks attained a compressive strength of 19 MPa and density of 2.4 g/m^2, similar to that of concrete block. The utilization of steel slag in making marine blocks was considered as a method of CO_2 sequestration to attain one-tenth of the Japan's Iron and Steel making industry's CO_2 reduction target.

The slag marine blocks were experimented for marine plants cultivation as its surface majorly consisted of calcium carbonate, the same substance that comprises coral reefs and seashells (Takahshi and Yabuta 2002). The porosity and roughness of slag block (328 μm) was also in the range of that required for the growth of sargassum (100-300 μm) and such marine plants. It was found that mean number of plants on the slag blocks were higher than that on granite and cement concrete blocks which were simultaneously tested at all times during the experiments.

2.4.4 Acid Mine Drainage Remediation

Acid mine drainage (AMD) is the acidic outflow from the abandoned metal mines that are abundant in sulfide minerals and metals such as Fe, Ni, Cu, and Pb. It is formed upon the interaction between exposed sulfur containing minerals (pyrite) with groundwater and air. It has been a major cause of concern in regions where mining industry contributes the largest to its economic growth. Many regions in South Africa face a continuous string of problems associated with effects of AMD on their environment. The ferric iron that gets converted into ferrous hydroxide at pH below 3.5 coats streams with orange color sludge causing the characteristic yellow boy condition at the AMD sites that can pollute water, smother plants and destroy stream ecosystem. The contamination of soil and water due to AMD can pose long-term detrimental risk to human health as well as corrosion of building and infrastructure.

General practices to combat the AMD include active and passive measures. In the active method, neutralizing materials like limestone and dolomite with an alkaline pH are carefully dispersed in the AMD to control the pH. This method requires high maintenance cost, expertise and constant monitoring (Sheridan 2014). It can also cause environmental and economic issues as the limestone has to be mined. The passive methods include the constructed wetlands. Both active and passive methods have their own limitations and hence, minimization and control of mining has been referred to as the best practice to avoid AMD. The use of industrial by-products has been considered an economically and environmentally effective alternative to remediate acid mine drainage, with studies recommending use of steel slag to replace limestone (Ziemkiewicz and Skousen 1999; Leite et al. 2013; Sheridan 2014).

Use of steel slag as a leaching bed to alter the pH of the acid mine drainage was recommended in the study by Ziemkiewicz and Skousen (1999). The leaching bed was suggested

to be built upstream to the acidic refuse at the cleaner non-acidic site of the stream so that the fresh water leaches through the bed to become alkaline before it interacts with the acid mine refuse to raise the pH up to neutral levels. Sheridan (2014) studied the use of BOF slag and stainless steel slag in place of alkaline chemicals in the active method to treat AMD. Steel slag was selected as a substitute material due to its high alkalinity and easy availability from the waste of steel plants. The removal of iron and sulfate from AMD by slag owes to the acid neutralizing capacity and formation of gypsum, respectively as shown by the following chemical reactions 6-9 (Sheridan 2014):

$$CaO + H_2O \rightarrow Ca(OH)_2 \quad (6)$$

$$Ca(OH)_2 \rightarrow Ca^{2+} + OH^- \quad (7)$$

$$Fe^{m+} + mOH^- \rightarrow Fe(OH)_m \quad (8)$$

$$Ca^{2+} + SO_4^{2-} + 2H_2O \rightarrow CaSO_4.H_2O \quad (9)$$

In the study by Sheridan (2014), stainless steel slag (SSS) and BOF were analysed to assess the suitability of each slag for AMD remediation. The study was conducted on two artificially prepared AMD with different iron and sulfur concentration typical of a natural AMD: Solutions A and B. The solution A (600 mg/l Fe, 4800 mg/l SO_4^{2-}) represented low-strength AMD at a pH of 2.5 and Solution B (1000 mg/l Fe, 5000 mg/l SO_4^{2-}) represented high-strength AMD at pH of 2.25. It was then treated with slag at concentrations 20, 40, 60, 80, 100, 120, and 140 mg/l of artificial AMD and pH measured after 4 hrs. The pH change due to SSS and BOF was recorded as 2.5-6.0 and 2.5-12.1, respectively. The slag concentration required for AMD treatment was optmized as 100 mg/l as pH change further from 100 mg/l was small compared to that from 20-100 mg/l. Though most batch reaction was completed within 30 min indicating a rapid process, it was also observed that an increase in contact time increased the pH of AMD for the same

concentration of slag. The BOF slag was concluded as a better replacement as remediating agent for AMD due to its higher alkalinity owing to the larger concentration of free CaO and lesser SiO_2 compared to SSS. The higher porportion of silica in SSS decreases the free CaO content in the slag as it gets locked up in the amorphous mineral matrix. The BOF slag reduced the soluble Fe concentration by 99% and sulfate concentration by 75% in solution A, while the SSS slag reduced Fe by 64% and sulfate by 40%.

As an example for field application of steel slag in AMD treatment, the poor quality of water in the 33.6 acres Huff Run Watershed area due to years of unregulated surface and deep mining was cleaned up under the Ohio Department of Natural Resources (ODNR) by installing passive treatment system using steel slag (Hamilton et al. 2007). The reclamation project included establishing positive drainage and installing passive AMD treatment systems including alkaline ponds using steel slag and open limestone channels. Steel slag was utilized to supersaturate the relatively clean water and then interact with effluent AMD waters to neutralize the low pH such that recommended by Ziemkiewicz and Skousen (1999). An increase in pH from 3 to 6, acidity decrease from 209 mg/l to 17 mg/l and alkalinity increase from 0 to 20 mg/l was observed upon post construction monitoring of the watershed. Decrease in the total content of Fe (34 mg/l to 14 mg/l), Mn (23 mg/l to 3 mg/l) and Al (8.7 mg/l to 0 mg/l) were also reported. Steel slag application above surface water in drainage channels, submerging and as pond additive to charge deep mine pools were proved to work well by boosting pH of discharge from 3 to 6. The system was designed to spread the alkaline $CaCO_3$ precipitate formed upon reaction of steel slag with water and CO_2 to surrounding impoundments and deep mine to ensure continuous treatment of watershed during low and high levels of precipitation. A combination of Fe precipitate ponds and wetlands were also recommended by Hamilton et al. (2007)

downstream of slag bead to allow adequate retention prior to streamflow in order to collect the metal precipitates.

2.4.5 Use as Fertilizer and Soil Modifier in Agriculture

Researchers have deliberated the use of steel slag in agriculture as fertilizer and soil modifier in order to sustain plant growth in difficult soils (Zhang et al. 2003; Gutierrez et al. 2010; Kimio 2015). Steel slag has been used as an effective, inepxensive Fe fertilizer to treat calcareous soils that are deficient in Fe (Xian et al. 2006). A pot experiment was conducted to analyse the effectivesness of steel slag as Fe fertiliser and soil improvement for corn growth. Steel slag is abundant in Fe, K, Mn and P alongwith Cd and Pb within the desirable limits. Hence, it has been studied as a potential source for plant nutrients in China. It's use has shown promising results in terms of higher yield in regions where plant iron chlorosis was a major problem. Steel slag has also been used for increasing rice yield in China due to the abundance of Si that is necessary for rice plant and as a fertilizer to modify acidic soil for paddy culture (Ning et al. 2016).

In the study by Gutierrez et al. (2010), steel slag was studied to reduce the As phytoextractability. Contaminated soil was prepared by mixing non-contaminated soil and mine tailings which was then blended with steel slag. This soil was used to cultivate radish and compared to another contaminated soil sample that was treated with $Ca(OH)_2$. It was found that the soil treated with steel slag effectively suppressed the As uptake and increased the yield compared to the soil treated with $Ca(OH)_2$.

In the pot experiments to study the corn yield by Xian et al. (2006), steel slag as-is and acidified slag were tested. At moderate application of steel slag as-is, an increase in the corn dry matter yield and Fe uptake was observed. An increase in steel slag as-is did not have any effect

on the yield probably due to the high alkaline pH. Hence, acidified slag was tested which again increased the yield and the available extractable Fe in the soil. An optimal addition of both steel slag as-is and acidified slag was recommended since an increased addition of either slag did not improve the soil. Slag was added to soil at 0, 10, 20 and 40 g/kg of soil. There was no significant increase in yield above 20g/kg. The acidified slag was added at 10 and 20 g/kg of soil at a pH 2.5. In steel slag as is, the yield in 10g/kg was not significantly higher than control, but 20g/kg resulted in higher yield. In the case of acidified slag, 10g/kg addition resulted in higher yield than 10g/kg steel slag as is.

2.4.6 Landfill Cover Material

The strict rules in Sweden and parts of Europe in terms of landfill cover permeability ($\leq$50 Lm^{-2} yr^{-1} for non-hazardous landfills) have led researchers to explore the use of alternative landfill cover materials (in liue of soils) such as steel slag that reduce the material cost in construction of much thicker covers (Andreas et al. 2005; Hermann et al. 2010; Andreas et al. 2014) and reduce the burden on natural resources. Andreas et al. (2005) conducted a preliminary study on EAF and LD slags that consisted of particle size distribution, mixing and compaction tests, and hydraulic conductivity. The use of slag was confirmed to be feasible in cover layers except vegetation layer with specific recommendations on mixing of EAF and LD slag to decelerate curing period, extend workability and a narrowed optimum water content range.

Herrmann et al. (2010) present laboratory and field test results on the EAF/LD slag mixture in sanitary landfill covers as a barrier material. The compaction density, compression strength and hydraulic permeability were analyzed in detail. It was found that the maximum density was achieved by the ~50% EAFS and ~50% LD slag at 10% moisture content when it

was compacted soon after adding water while the density decreased significantly when the mixture was compacted after 24 hours from adding water. Hence, it was recommended by Hermann et al. (2010) to minimize the time between the water addition and compaction. The hydraulic conductivity of the mixture was only 10^{-11} m/s when the mix was compacted as soon as the water was added to it, while the hydraulic conductivity significantly increased with increasing time between water addition and compaction. The optimized EAF/LD slag mix with 10^{-11} m/s hydraulic conductivity resulted in only ~27 $Lm^{-2}yr^{-1}$ leachate in 2 years during the field test meeting the Swedish threshold for hazardous landfills. The compressive strength of the EAF/LD slag mix was found to be comparable to that of concrete (~47.6 MPa) due to which the mix was thought safe against the compression stresses during settlement. However, further tests are needed to confirm its resistance to tensile and shear stresses. Andreas et al. (2014) also discusses about the same mixture that results in a landfill barrier that meet the Swedish regulations for hazardous landfills. The researchers pointed out the importance of understanding different kinds of slag as they exhibit variable characteristics which can alter the required slag to soil ratio as well as the need for considering appropriate landfill cover slope inclination while designing the cover to reduce percolation of rainwater into the landfill.

Diener et al. (2010) studied the long-term effects of carbonation of steel slag in a landfill cover. The leaching behavior and pH change were analyzed for 3 and 10 months aged slag from the cover. The release of heavy and toxic metals into groundwater from steel slag was assessed as below detection limits. Further, the pH of the 3-month old steel slag sample had decreased by 2 units upon carbonation, while not an appreciable further decrease was observed in the 10 months old sample. Diener et al. (2010) reported that carbonation of slag in cover upon its exposure to CO_2 produced by solid waste biodegradation depends on the operation procedure

adopted in the landfill, existing soil type and climatic conditions. The carbonation of slag in landfill cover layers is assumed to be dependent on availability of CaO present in the slag, temperature, CO_2 concentration, and humidity.

The concept of CO_2 sequestration applied in conjunction with the biochar-amended landfill biocover to mitigate both CH_4 and CO_2 emission from MSW landfills was explored by Reddy et al. (2014), Yargicoglu and Reddy (2017) and Reddy et al. (2018a). The BOF slag is capable of capturing and storing both the CO_2 produced directly from biodegradation of MSW as well as that formed upon the oxidation of methane by methanotrophs in the biochar-amended soil layer (Reddy at al. 2014; Yargicoglu and Reddy 2017; Reddy et al. 2018a, 2018b). The alkalinity and presence of heavy metals in BOF slag could be a major challenge in the implementation of the slag-based biocover due to the close contact between BOF slag and methanotrophic community in biocover. The ability of methanotrophs to survive in such high alkaline environment is to be studied in detail. Also, the design of a biocover profile that would not affect the methanotrophic methane oxidation in the presence of slag is of utmost importance. These aspects are being investigated in ongoing studies at the University of Illinois at Chicago (Reddy et al. 2018a).

Investigations on H_2S suppression by iron and steel slag (Kim et al. 2012; Montes-Moran et al. 2012; Sarperi et al. 2014; Ng et al. 2017) as described previously could also be an additional benefit of using iron and steel slag as a soil conditioner in landfill cover material to lower the levels of H_2S emission from landfill to olfactory threshold levels of 0.01-1.5 ppm (OSHA). The H_2S suppression mechanism by BF slag was studied in detail by Ng et al. (2017), especially with regards to landfill cover applications and H_2S-slag reaction mechanism in general. Column experiments were conducted on unamended loess soil and loess soil amended

with 30% ground granulated blast furnace slag (GGBS) at moisture contents 0%, 10% and 20%. The mean particle size (D_{50}) of the unamended and amended loess soil was 32 ɥm and 28 ɥm, respectively. Based on experimental results that consisted of elemental sulphur (S(0)), mineral sulphide, thiosulphate and acid volatile sulphide (AVS), mechanism of H_2S suppression was concluded to include both oxidation and acid-base reaction guided by the formation of AVS, S(0) and thiosulphate. The GGBS also exhibited the capacity to be reused for H_2S capture after regenerating it by air-ventilation, where AVS plays a major role. The AVS forms hydroxides upon ventilation and then reacts again with H_2S upon its reuse. The water content of 20% with the amended soil was found to be the most favorable composition for removal of H_2S as it increased dissolution of H_2S, suppresed formation of elemental sulphur and promoted formation of AVS, making the authors conclude higher moisture content would be better for H_2S reaction with GGBS. Ongoing studies at the University of Illinois at Chicago are aimed at developing biochar-slag-soil cover system to mitigate CH_4 and CO_2 as well as H_2S at landfills.

2.5 CHALLENGES AND OPPORTUNITIES

GHG emissions have been increasing due to industrialization and population explosion. The conventional methods for controlling these emissions along with the proposed CCS techniques that include geologic sequestration have proven to be uneconomical and energy-intensive, leading to the need for sustainable CCS technologies. The CCS aims at capturing the CO_2 emissions from industrial sources and storing in the form of stable carbonates so that it is not released back into the atmosphere. Feedstock with CaO and $Ca(OH)_2$ as primary compounds are required for this purpose. Hence, studies on several alkaline industrial wastes have been conducted that confirmed the iron and steel slag, especially BOF slag, as one of the best alternate

material. It is highly alkaline and possesses mineralogical similarity to natural minerals like olivine that is highly consumed for geologic carbon sequestration. The mechanism of carbonation essentially consists of three steps where the Ca ions leach out of the matrix, CO_2 forms carbonate ions in solution, and then the Ca ions and carbonate ions react and precipitate as carbonates. Further, alkalinity of the slag promotes the suitable pH (~11-12) for carbonate formation in solution.

Iron slag has been used profusely in the construction industry, although steel slags are only partially consumed as a construction material due to its higher iron and calcium oxide content. However, steel slag has been found to have a high potential for several environmental applications due to its unique chemical properties. It has been used in a wide range of projects including acid mine drainage remediation, phosphate removal, and sand capping in marine environment. It has also been used as a replacement for soil in landfill cover construction. The increasing knowledge of iron and steel slag properties as well as its proper utilization has lifted a major burden off the iron and steel-making industry by alleviating the stockpiling of slag. The usual concerns of heavy metal leaching and pH effects has been studied to be within the desirable limits for its usage in construction and environmental applications.

Steel slag has great potential for mitigation of LFG, which is one of the largest anthropogenic sources of GHGs. A previous study on biocovers for methane oxidation (Reddy et al. 2014) may be modified with steel slag to attain a zero-emission landfill. It is presumed that steel slag has the capacity to capture the CO_2 that arises directly from waste biodegradation as well as methane oxidation in biocover. A new study has been undertaken by the authors to assess steel slag carbonation capacity and effects of its high alkalinity on landfill microbial community

that promote biodegradation and methane oxidation. The project could have major positive environmental, social and economic impacts as it would serve the following advantages:

- Mitigate LFG emission that forms the third largest source of anthropogenic CH_4 as well as CO_2.
- Divert large quantities of steel slag from stockpiling and landfilling.
- Reduce the need to use natural soil in landfill cover construction and hence the associated quarrying and energy-use.
- Additional benefit of mitigating H_2S emissions thus reducing the stench characteristic of sanitary landfills.

Overall, the composition and reactions with oxides and minerals can be highly dependent on the slag type and environmental factors. Careful investigations using the available slag for a specific application should be undertaken. Fundamental understanding is essential to develop the practical and robust carbon sequestration or environmental remediation applications. Slags can offer many benefits in agriculture and landfill covers.

2.6 CITED REFERENCES

Ahmad, M., Lee, S. S., Yang, J. E., Ro, H. M., Lee, Y. H., & Ok, Y. S. (2012). “Effects of soil dilution and amendments (mussel shell, cow bone, and biochar) on Pb availability and phytotoxicity in military shooting range soil.” *Ecotoxicol. Environ. Saf.*, 79, 225-231.

Andreas, L., Herrmann, I., Lidstrom-Larrsson, M., and Lagerkvist, A. (2005). “Physical properties of steel slag to be reused in a landfill cover.” *Proc., Sardinia 10th Int. Waste*

Management and Landfill Symp., Environmental Sanitary Engineering Centre, Cagliari, Italy, 3-7.

Andreas, L., Diener, S., & Lagerkvist, A. (2014). "Steel slags in a landfill top cover–Experiences from a full-scale experiment." *Waste Manage.*, 34(3), 692-701.

Baciocchi, R., Costa, G., Di Bartolomeo, E., Polettini, A., & Pomi, R. (2011). "Wet versus slurry carbonation of EAF steel slag." *Greenh. Gases*, 1(4), 312-319.

Baker, M. J., Blowes, D. W., & Ptacek, C. J. (1998). "Laboratory development of permeable reactive mixtures for the removal of phosphorus from onsite wastewater disposal systems." *Environ. Sci. Technol.*, 32(15), 2308-2316.

Boone, M. A., Nielsen, P., De Kock, T., Boone, M. N., Quaghebeur, M., & Cnudde, V. (2013). "Monitoring of stainless-steel slag carbonation using X-ray computed microtomography." *Environ. Sci. Technol.*, 48(1), 674-680.

Bowden, L. I., Jarvis, A. P., Younger, P. L., and Johnson, K. L. (2009). "Phosphorus removal from waste waters using basic oxygen steel slag." *Environ. Sci. Technol.*, 43(7), 2476-2481.

Capobianco, O., Costa, G., Thuy, L., Magliocco, E., Hartog, N., and Baciocchi, R. (2014). "Carbonation of stainless steel slag in the context of in situ brownfield remediation." *Miner. Eng.*, 59, 91-1

Chang, E. E., Pan, S. Y., Chen, Y. H., Tan, C. S., and Chiang, P. C. (2012). "Accelerated carbonation of steelmaking slags in a high-gravity rotating packed bed." *J. Hazard. Mater.*, 227, 97-106.

Chesner, W. H., Collins, R. J., & MacKay, M. H. (1998). *User Guidelines for Waste and By-product Materials in Pavement Construction*, Federal Highway Administration (FHWA), FHWA-RD-97-148.

Chiang, P. C., & Pan, S. Y. (2017). *Carbon Dioxide Mineralization and Utilization*, Springer, Singapore.

Diener, S., Andreas, L., Herrmann, I., Ecke, H., and Lagerkvist, A. (2010). "Accelerated carbonation of steel slags in a landfill cover construction." *Waste Manage.*, 30(1), 132-139.

Freeman, J. S., & Rowell, D. L. (1981). "The adsorption and precipitation of phosphate onto calcite." *Eur. J. Soil Sci.*, 32(1), 75-84.

Goldberg, P., Chen, Z. Y., O'Connor, W., Walters, R., & Ziock, H. (2001). "CO_2 mineral sequestration studies in the US." National Energy Technology Laboratory (NETL), Pittsburgh, PA (United States).

Grubb, D. G., and Wazne, M. (2011). *Metal Immobilization Using Slag Fines*, U.S. Patent Application No. 12/874,079.

Grubb, D. G., Wazne, M., Jagupilla, S. C., & Malasavage, N. E. (2011). "Beneficial use of steel slag fines to immobilize arsenite and arsenate: slag characterization and metal thresholding studies." *J. Hazard. Toxic Radioact. Waste*, 15(3), 130-150.

Gupta, J. D., Kneller, W. A., Tamirisa, R., and Skrzypczak-Jankun, E. (1994). "Characterization of base and subbase iron and steel slag aggregates causing deposition of calcareous tufa in drains." *Transportation Research Record*, 1434.

Gutierrez, J., Hong, C. O., Lee, B. H., & Kim, P. J. (2010). “Effect of steel-making slag as a soil amendment on arsenic uptake by radish (Raphanus sativa L.) in an upland soil.” *Biol. Fertil. Soils*, 46(6), 617-623.

Hamilton, J., Gue, J., & Socotch, C. (2007). “The use of steel slag in passive treatment design for AMD discharge in the Huff Run watershed restoration.” *Proc., Amer. Soc. of Mining and Reclamation,* Gillette, WY, 272-282.

Herrmann, I., Andreas, L., Diener, S., and Lind, L. (2010). “Steel slag used in landfill cover liners: laboratory and field tests.” *Waste Manag. Res.*, 28(12), 1114-1121.

Huijgen, W. J., Witkamp, G. J., and Comans, R. N. (2005). “Mineral CO_2 sequestration by steel slag carbonation.” *Environ. Sci. Technol.*, 39(24), 9676-9682.

Huijgen, W. J., and Comans, R. N. (2006). “Carbonation of steel slag for CO_2 sequestration: leaching of products and reaction mechanisms.” *Environ. Sci. Technol.*, 40(8), 2790-2796.

Tube City IMS (IMS, T.C.). “Utilizing iron and steel slag in environmental applications-an overview.”

Kasina, M., Kowalski, P. R., and Michalik, M. (2015). “Mineral carbonation of metallurgical slags.” *Mineralogia*, 45(1-2), 27-45.

Kim, K., Asaoka, S., Yamamoto, T., Hayakawa, S., Takeda, K., Katayama, M., and Onoue, T. (2012). “Mechanisms of hydrogen sulfide removal with steel making slag.” *Environ. Sci. and Technol.*, 46(18), 10169-10174.

Kimio, I. T. O. (2015). “Steelmaking slag for fertilizer usage.” *Nippon Steel Sumitomo Metal Tech Rep*, 109, 130-136.

Kunzler, C., Alves, N., Pereira, E., Nienczewski, J., Ligabue, R., Einloft, S., & Dullius, J. (2011). "CO_2 storage with indirect carbonation using industrial waste." *Energy Procedia*, 4, 1010-1017.

Lee, I. S., Kim, O. K., Chang, Y. Y., Bae, B., Kim, H. H., & Baek, K. H. (2002). "Heavy metal concentrations and enzyme activities in soil from a contaminated Korean shooting range." *J. Biosci. Bioeng.*, 94(5), 406-411.

Leite, C. M. D. C., Cardoso, L. P., & Mello, J. W. V. D. (2013). "Use of steel slag to neutralize acid mine drainage (AMD) in sulfidic material from a uranium mine." *R. Bras. C. Solo*, 37(3), 804-811.

Lekakh, S. N., Rawlins, C. H., Robertson, D. G. C., Richards, V. L., & Peaslee, K. D. (2008). "Kinetics of aqueous leaching and carbonization of steelmaking slag." *Metall. Mater. Trans. B*, 39(1), 125-134.

Lu, S. G., Bai, S. Q., and Shan, H. D. (2008). "Mechanisms of phosphate removal from aqueous solution by blast furnace slag and steel furnace slag." *J. Zhejiang Univ. Sci. A*, 9(1), 125-132.

Mohammed, S. A. S., Sanaulla, P. F., Basha, M. B., Reddy, H. P., Alnuaim, A. M., and Moghal, A. A. B. "Potential of Soils Amended with a Nano Calcium Silicate Mixture for Lead Encapsulation in an Aqueous Medium." *Geo-Chicago 2016*, 467-476.

Mohan, D., and Pittman Jr, C. U. (2006). "Activated carbons and low cost adsorbents for remediation of tri-and hexavalent chromium from water." *J. Hazard. Mater.*, 137(2), 762-811.

Montes-Morán, M. A., Concheso, A., Canals-Batlle, C., Aguirre, N. V., Ania, C. O., Martín, M. J., and Masaguer, V. (2012). "Linz-Donawitz steel slag for the removal of hydrogen sulfide at room temperature." *Environ. Sci. Technol.*, 46(16), 8992-8997.

Moon, D. H., Wazne, M., Cheong, K. H., Chang, Y. Y., Baek, K., Ok, Y. S., & Park, J. H. (2015). "Stabilization of As-, Pb-, and Cu-contaminated soil using calcined oyster shells and steel slag." *Environ. Sci. Pollut. Res.*, 22(14), 11162-11169.

Ng, C. W. W., Ng, M., & Leung, A. K. (2017). "Removal of Hydrogen Sulfide Using Soil Amended with Ground Granulated Blast-Furnace Slag." *J. Environ. Eng.*, 143(7).

Ning, D., Liang, Y., Liu, Z., Xiao, J., and Duan, A. (2016). "Impacts of steel-slag-based silicate fertilizer on soil acidity and silicon availability and metals-immobilization in a paddy soil." *PloS One*, 11(12).

Ochola, C. E., and Moo-Young, H. K. (2004). "Establishing and elucidating reduction as the removal mechanism of Cr (VI) by reclaimed limestone residual RLR (modified steel slag)." *Environ. Sci. Technol.*, 38(22), 6161-6165.

Pan, S. Y., Adhikari, R., Chen, Y. H., Li, P., and Chiang, P. C. (2016). "Integrated and innovative steel slag utilization for iron reclamation, green material production and CO2 fixation via accelerated carbonation." *J. Clean. Prod.*, 137, 617-631.

Reddy, K. R., Yargicoglu, E. N., Yue, D., and Yaghoubi, P. (2014). "Enhanced microbial methane oxidation in landfill cover soil amended with biochar." *J. Geotech. Geoenviron. Eng.*, 140(9).

Russell, H. H., Matthews, J. E., and Guy, W. S. (1992). "TCE removal from contaminated soil and groundwater." *EPA Environ. Eng. Sourcebook.*

Sarperi, L., Surbrenat, A., Kerihuel, A., & Chazarenc, F. (2014). "The use of an industrial by-product as a sorbent to remove CO_2 and H_2S from biogas." *J. Environ. Chem. Eng.*, 2(2), 1207-1213.

Scott, R. I. (2001). "Lead contamination in soil at outdoor firing ranges." <https://www.princeton.edu/~rmizzo/firingrange.htm> (June 4, 2018).

Sheridan, C. (2014). "Remediation of acid mine drainage using metallurgical slags." *Miner. Eng.*, 64, 15-22.

Shi, C. (2004). "Steel slag—its production, processing, characteristics, and cementitious properties." *J. Mater. in Civil Eng.*, 16(3), 230-236.

Smith, J. S. (2003). *Method for Purifying Contaminated Groundwater using Steel Slag.* U.S. Patent No. 6,602,421.

Smyth, D. J. A., Blowes, D. W., Ptacek, C. J., Groza, L. E., Baker, M. J., & Crawford, W. (2004). "Phosphorus and pathogen removal from wastewater, storm water and groundwater using permeable reactive materials." *Canadian Water Network Meeting,* Ottawa, ON.

Srivastava, S. K., Gupta, V. K., & Mohan, D. (1997). "Removal of lead and chromium by activated slag—a blast-furnace waste." *J. Environ. Eng.*, 123(5), 461-468.

Stolaroff, J. K., Lowry, G. V., & Keith, D. W. (2005). "Using CaO-and MgO-rich industrial waste streams for carbon sequestration." *Energy Convers. Manag.*, 46(5), 687-699.

Su, T. H., Yang, H. J., Shau, Y. H., Takazawa, E., & Lee, Y. C. (2016). "CO2 sequestration utilizing basic-oxygen furnace slag: Controlling factors, reaction mechanisms and V–Cr concerns." *J. Environ. Sci.*, 41, 99-111.

Takahashi, T., & Yabuta, K. (2002). *New Application of Iron and Steelmaking Slag*, NKK Technical Report-Japanese Edition, 43-48.

Tsai, T. T., Kao, C. M., and Wang, J. Y. (2011). "Remediation of TCE-contaminated groundwater using acid/BOF slag enhanced chemical oxidation." *Chemosphere*, 83(5), 687-692.

Tu, M., Zhao, H., Lei, Z., Wang, L., Chen, D., Yu, H., & Qi, T. (2015). "Aqueous Carbonation of Steel Slag: A Kinetics Study." *ISIJ Int.*, 55(11), 2509-2514.

Ukwattage, N. L., Ranjith, P. G., & Li, X. (2017). "Steel-making slag for mineral sequestration of carbon dioxide by accelerated carbonation." *Measurement*, 97, 15-22.

United States Environmental Protection Agency (US EPA) Landfill Methane Outreach Program (LMOP). "Basic Information about Landfill Gas" <https://www.epa.gov/lmop/basic-information-about-landfill-gas> (June 4, 2018)

United States Department of Labor, Occupation Safety and Health Administration (OSHA). "Hydrogen Sulfide." <https://www.osha.gov/SLTC/hydrogensulfide/hazards.html> (June 4, 2018)

US EPA, Underground Injection Control (UIC). "Class VI- Wells used for Geologic Sequestration of CO_2." <https://www.epa.gov/uic/class-vi-wells-used-geologic-sequestration-co2> (June 4, 2018)

US EPA. "Carbon Dioxide Capture and Sequestration: Storage Safety and Security." <https://19january2017snapshot.epa.gov/climatechange/carbon-dioxide-capture-and-sequestration-storage-safety-and-security_.html> (June 4, 2018)

U.S. Geological Survey (USGS), Mineral Commodity Summaries. "Iron and Steel Slag." <https://minerals.usgs.gov/minerals/pubs/commodity/iron_and_steel_slag/> (June 4, 2018)

van Zomeren, A., Van der Laan, S. R., Kobesen, H. B., Huijgen, W. J., and Comans, R. N. (2011). "Changes in mineralogical and leaching properties of converter steel slag resulting from accelerated carbonation at low CO_2 pressure." *Waste Manage.*, 31(11), 2236-2244.

Wu, H. Z., Chang, J., & Wang, H. (2011). "Pore Structural Changes and Carbonated Depth of Carbonated Steel Slag." *Adv. Mater. Res.*, 306, 1122-1125.

Xian, W. A. N. G., and Qing-Sheng, C. A. I. (2006). "Steel Slag as an Iron Fertilizer for Corn Growth and Soil Improvement in a Pot Experiment." *Pedosphere*, 16(4), 519-524.

Yargicoglu, E. N., & Reddy, K. R. (2017). "Effects of biochar and wood pellets amendments added to landfill cover soil on microbial methane oxidation: A laboratory column study." *J. Environ. Manag.*, 193, 19-31.

Yildirim, I. Z., and Prezzi, M. (2011). "Chemical, mineralogical, and morphological properties of steel slag." *Adv. Civil Eng.*, 2011.

Yilmaz, D., Lassabatere, L., Deneele, D., Angulo-Jaramillo, R., & Legret, M. (2013). "Influence of carbonation on the microstructure and hydraulic properties of a basic oxygen furnace slag." *Vadose Zone J.*, 12(2).

Yu, J., & Wang, K. (2011). "Study on characteristics of steel slag for CO2 capture." *Energy Fuels*, 25(11), 5483-5492.

Zhang, Y. L., Liu, M. D., Wang, Y. J., & Du, L. D. (2003). "Effects of Slag Application on Si, Fe and Mn in Paddy Soil and Rice Plant." *Chinese J. Soil Sci.*, 4, 016.

Zhang, T., Yu, Q., Wei, J., Li, J., and Zhang, P. (2011). “Preparation of high performance blended cements and reclamation of iron concentrate from basic oxygen furnace steel slag.” *Resour. Conserv. Recycl.*, 56(1), 48-55.

Ziemkiewicz, P., & Skousen, J. (1999). “Steel Slag in Acid Mine Drainage Treatment and Control'.” *Proc., Annual National Meeting of the Society for Surface Mining and Reclamation*, 16, 651-656.

CHAPTER 3 - SEQUESTRATION OF LANDFILL GAS EMISSIONS USING BASIC OXYGEN FURNACE SLAG: EFFECTS OF MOISTURE CONTENT AND HUMID GAS FLOW CONDITIONS

ABSTRACT: Fugitive methane (CH_4) and carbon dioxide (CO_2) emissions from municipal solid waste (MSW) landfills constitute one of the major anthropogenic sources of greenhouse gas (GHG) emissions. In recent years, several researchers have focused on developing biocovers which are primarily aimed at reducing GHG emissions. Although some studies have been successful in reducing the CH_4 emissions, the continuous CO_2 emissions due to microbial CH_4 oxidation and MSW decomposition remain a major concern. In this regard, basic oxygen furnace (BOF) steel slag offers significant potential for CO_2 removal due to its unique characteristics such as high alkaline buffering capacity and calcium content. The addition of BOF slag to biocovers is thus proposed to substantially curb the landfill gas (LFG) emissions while also promoting beneficial use of BOF slag. This paper evaluates the CO_2 removal capacity of BOF slag in batch experiments against other landfill biocover materials such as cover soil and biochar. Also, column experiments using dry and humidified synthetic LFG gas showed considerable cumulative CO_2 removal by BOF slag. The CO_2 removal rate appeared to have a two-step mechanism: initial rapid CO_2 removal, followed by more gradual removal. The CO_2 removal capacity of BOF slag was found to be approximately 7 times greater than soil and biochar, on the order of 2,250 mg/g and 155 mg/g of CO_2 under humid and dry LFG conditions, respectively. Breakthrough curves from the column experiments showed complete CO_2 removal up to about 100 pore volumes (PV), beyond which the removal rate remained constant at 10-20% until no

more CO_2 was removed. Stoichiometric calculations at 100 PV suggest only 60% of the total residual lime/portlandite (11.4-11.7 wt%) was available at slag surface capable of instantaneous carbonation removing 42 mg/g CO_2, while the long-term carbonation depended on the leachability of the interstitial Ca in the presence of moisture. An appreciable CH_4 removal by BOF slag (750 mg/g and 40 mg/g under humid and dry conditions, respectively) was also observed.

3.1 INTRODUCTION

Biodegradation of the waste in landfills result in landfill gas emissions (LFG) which is approximately 50% methane (CH_4), 50% CO_2, trace amounts of hydrogen sulfide (H_2S) and other non-methanogenic organic compounds (US EPA; Spokas et al. 2006; Ng et al. 2017) In the U.S., LFG emissions are one of the major anthropogenic sources of GHG emissions (US EPA; Spokas et al. 2006). Currently, LFG emissions are addressed by active gas extraction systems, though it is recognized that they are not 100% efficient due to the limited radius of influence of each gas extraction well. In 2016, fugitive emissions of LFG into the atmosphere were estimated at ~86.6 million metric tons CO_2 equivalents per year (US EPA, 2016). Fugitive CH_4 emissions from landfills pose a major problem due to its global warming potential (GWP) of 28-36 over 100 years (US EPA, 2015) and emission rates ranging from -2.2 to 10,000 mg CH_4 m^{-2} d^{-1}, of which only 4-50% undergoes oxidation while passing through the landfill cover (Spokas et al. 2006).

Several studies address alternate cover systems (biocovers) that leverage the microbial CH_4 oxidation that occurs in the landfill cover soils by methanotrophs. Biocovers that incorporate biologically-amended soils enhance methanotrophic activity leading to higher CH_4

oxidation rates (Sadasivam and Reddy 2014). However, the organic materials commonly used as biocover amendments include dewatered sewage sludge, compost, and biosolids consisting of unstable/degradable organic carbon that eventually add to LFG emissions, exacerbating the situation. Alternatively, recent biocover studies investigating the use of biochar as an organic amendment showed enhanced methanotrophic activity and enhanced CH_4 oxidation (Yargicoglu and Reddy 2015, 2017). Biochar is a solid product derived from pyrolysis or gasification of organic matter. It contains more stable forms of organic carbon (compared to compost and biosolids), high internal porosity, water-holding capacity and specific surface area making it a good host media for CH_4 oxidizing bacteria and result in more desirable long-term landfill cover soil amendment (Yargicoglu and Reddy 2015, 2017).

Although, CH_4 emissions can be mitigated/controlled through the use of biochar-amended soils there are still uncontrolled emissions of CO_2 due to CH_4 oxidation and prevailing waste decomposition. Complementing the CH_4 oxidation with CO_2 sequestration in biocovers has the ability to result in a “zero-emission” landfill. Accordingly, carbon capture and storage (CCS) techniques using alkaline industrial by-products such as basic oxygen furnace (BOF) slag adds an important dimension to potentially sustainable solutions to this challenge. A review of the BOF slag and its CO_2 removal mechanisms have been discussed in detail in Reddy et al. (2018). The free-lime (CaO), portlandite [$Ca(OH)_2$] and oxide/silicate minerals containing divalent cations (Ca, Mg, Fe) in BOF slag can promote CO_2 conversion to stable carbonates.

Historically, studies have been conducted to analyze the CO_2 removal potential of BOF slag with context to on-site carbon capture at industries with CO_2 content in their flue-gas and optimization of reaction parameters (Huijgen et al. 2005; Su et al. 2016) and scrubbing of raw biogas to natural gas levels (Sarperi et al. 2014). However, the conditions under which BOF slag

carbonation was experimented in these studies cannot be related to its potential under landfill cover conditions. Huijgen et al. (2005) and Su et al. (2016) conducted experiments on BOF slag under stirred slurry conditions considered most conducive for accelerated carbonation whereas landfill cover soils mostly exist under unsaturated and static conditions. According to a Midwest US landfills temperature study completed by Yesiller and Hanson (2003), temperatures reach maximum of 23°C at the top of landfill cover soil during summer, whereas industrial carbon capture studies are considerably warmer on the order of 100°C (Huijgen et al. 2005;Su et al. 2016) with elevated pressures (~ 20 bar and 250 kg/cm^2). Sarperi et al. (2014) conducted carbonation experiments at conditions that were closest to landfill conditions with unsaturated BOF slag samples at 20°C wherein CO_2 sequestration potential of BOF slag was confirmed for normal atmospheric conditions with <6 mm particles. Accordingly, there is a need to conduct CO_2 removal and immobilization in biocover at or near standard temperature and pressure (STP) conditions not previously considered in the CO_2 sequestration literature.

To this end, batch experiments were conducted with BOF slag, biochar and cover soil with synthetic LFG to determine the CO_2 removal mechanisms and the carbonation kinetics at unsaturated moisture conditions and normal atmospheric temperature pertinent in landfill covers. Column experiments were also conducted to determine the breakthrough curve and analyze the CO_2 removal behavior of the BOF slag tested.

3.2 MATERIALS AND METHODS

3.2.1 Materials

The materials studied included BOF slag, soil and biochar. The crushed and screened BOF slag with a top size of 10 mm (3/8 inches) was obtained from Indiana Harbor East Steel Mill (supplied by the Phoenix Services, LLC). The soil was collected from Zion Landfill, IL from the intermediate cover placed over municipal solid waste. The BOF slag and cover soil were collected manually using shovels and collected in clean 5-gallon buckets. The buckets were immediately sealed with air tight lids to avoid moisture loss. The biochar used in the experiments was acquired from commercial vendors and it was produced by gasification of waste wood (pinewood) at 570°C as described by Yargicoglu et al. (2015).

The specific gravity of the three materials was determined in accordance to ASTM D854. ASTM D422 was followed to determine the grain size distribution of each media, while Atterberg limits of soil were determined as per ASTM D4318. Hydraulic conductivity and water holding capacity (WHC) were also determined for all media according to the ASTM D2434 and ASTM D2980, respectively. A flexible-wall permeameter was used to determine the hydraulic conductivity of the soil sieved through No. 4 sieve, compacted at 20% target moisture content using a Harvard miniature setup to a unit weight of 2.11 g/cm^3. A rigid wall permeameter was used to determine the hydraulic conductivity of BOF slag sample passing through sieve No. 4 and biochar sample as original gradation obtained, without any sieving.

Oven-dried (100-110°C for 24 hours) samples (~10 g) of BOF slag, soil and biochar were used to determine the loss-on-ignition (LOI) or organic content according to ASTM D2974. pH and oxidation-reduction potential (ORP) using an ORION Model 720A pH meter as per ASTM

D4972 and the electrical conductivity (EC) was measured using Corning 311 Conductivity meter.

The basic physical, chemical and geotechnical properties of BOF slag, soil and biochar used in this study are summarized in **Table 3-1**.

Table 3-1: Physical, chemical and geotechnical properties of experimentally tested BOF slag, cover soil and biochar.

Properties	ASTM Method	BOF Slag	Soil	Biochar
Specific Gravity	D854	3.04	2.65	0.65
Grain Size Distribution:	D422			
Gravel (%)		0	0	45
Sand (%)		90.5	7.2	54
Fines (%)		9.5	92.8	1
D_{50} (mm)		0.47	0.0068	4.3
C_c		0.55	-	0.82
C_u		11.92	-	2.42
Atterberg Limits:	D4318			
Liquid Limit (%)		Non-Plastic	35.0	Non-Plastic
Plastic Limit (%)		-	20.34	-
Plasticity Index (%)		-	14.66	-
USCS Classification	D2487	SP-SM	CL	SP
Water Holding Capacity (w/w)	D2980	40.5	45.9	51.6
Dry Density (g/cm^3)		1.32	2.11	1.15
Hydraulic Conductivity (cm/s)	D2434	4.2×10^{-4}	2.75×10^{-8}	2×10^{-4}
Loss of Ignition (%)	D2974	2.5	4.47	96.71
pH (1:1)	D4972	12.4	7.04	6.5
Electrical Conductivity (mS/cm)	D4972	6.68	0.4	0.8
Redox Potential (mV)	D4972	-317.9	-37.7	-6.3

The grain size distribution of each media is shown in **Figure 3-1**. The representative sample of BOF slag tested consisted of ~91% sand-sized particles and is classified as SP-SM according to Unified Soil Classification System (USCS) due non-plastic fines.

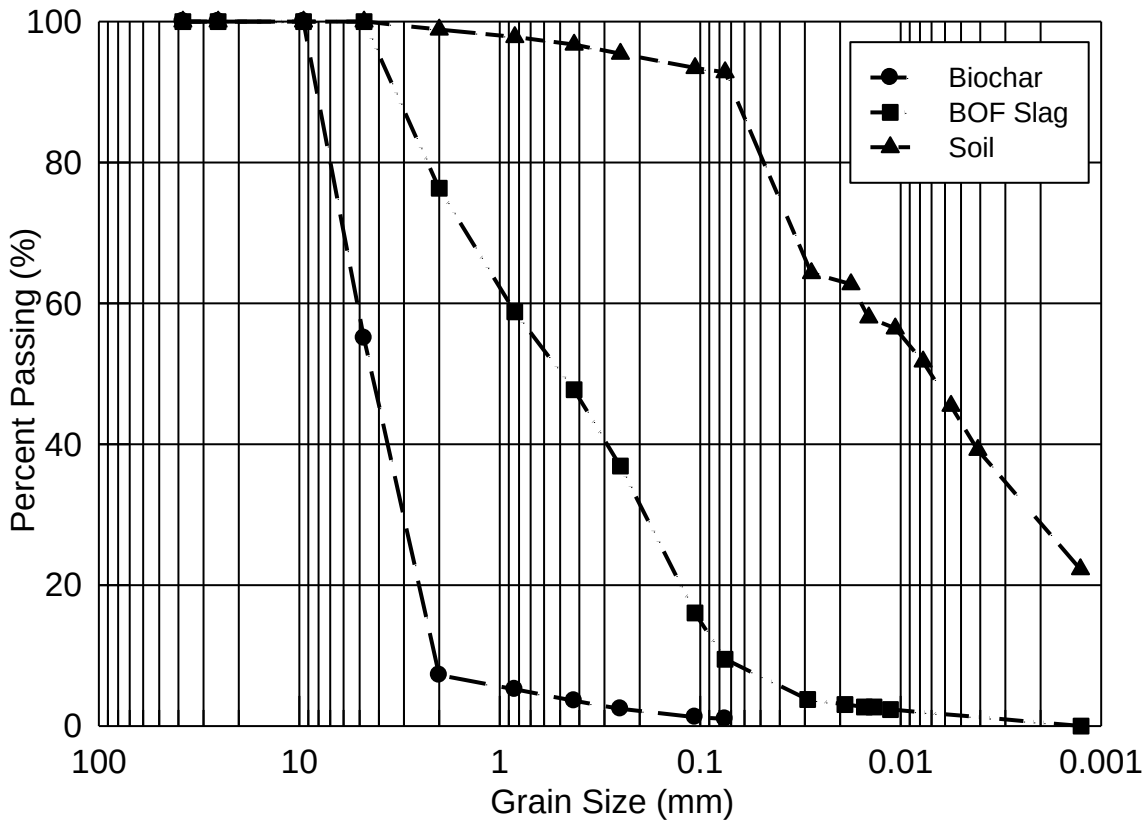

Figure 3-1: Grain size distribution of BOF slag, soil and biochar

The specific gravity of the BOF slag, soil and biochar were determined as 3.04, 2.65 and 0.65, respectively. The hydraulic conductivity of BOF slag and biochar were both on the order of ~10^{-4}cm/s, consistent with typical values for fine sands to loose silt (Holtz and Kovacs 1981). The soil was highly impermeable with a hydraulic conductivity in the order of 10^{-8} cm/s. The WHC of soil (45.9 w/w) and BOF slag (40.5 w/w) were comparable, whereas the water holding capacity of biochar was ~51.55 w/w. BOF slag was observed to be highly alkaline with pH ~12.4. The ORP of all three materials were negative, demonstrating higher reducing capacity.

The minerals present in BOF slag were determined by X-ray powder diffraction (XRD) and Rietveld quantification analysis. The sample preparation for XRD included grinding of a 3 g sample, which was then spiked with corundum (Al_2O_3) on a 90:10 weight basis in a mixer for 10 min. Standard spike intensity reference was used to determine the amorphous content. Step-scanned XRD data were collected by the Siemens D500 computer-automated diffractometer using Bragg-Brentano geometry. The reference databases for powder diffraction and crystal structure data were the International Center for Diffraction Data database (ICDD, 2001) and the Inorganic Crystal Structure Database (ICSD, 2010, v.2).

The total elemental content was determined as a result of combined XRF/acid digestion tests. The leaching tests for the BOF slag were conducted in order to evaluate the potential toxicity of the use of BOF slag from leaching of toxic metals. Both Toxicity Characteristic Leaching Procedure (TCLP, EPA 1311) and Synthetic Precipitation Leaching Procedure (SPLP, EPA 1312) leaching tests were conducted.

Scanning Electron Microscopy (SEM) imaging and analysis was conducted on crushed and air-dried samples of BOF slag before and after carbonation experiments. Images were captured using a JEOL JSM-6320F High Resolution Scanning Microscope operated at 2.5 kV. Further, the elemental composition was determined using an Oxford X-Ray Energy Dispersive Spectrometer (XEDS) fitted with a Hitachi S-3000N Variable Pressure Electron Microscope. The specimens were sputter coated with 20 nm Pt/Pd using Cressington HR208 sputter coater to minimize sample charging.

3.2.2 Batch Experiments

Batch experiments were conducted using BOF slag, soil and biochar. The materials were dried in oven at 100-110°C for 24 hours before they were used in the batch experiments. The batch experiments were conducted by taking 1g of dry sample in a 125 ml vial and adding 0%, 10%, 20%, 30% and 40% (w/w) water, under normal atmospheric conditions. Each vial was then purged completely with a synthetic LFG mix containing 50% CH_4 and 50% CO_2 by volume, closed with rubber septa, and secured tightly with a metal crimp cap. The tests were conducted in triplicate for each of the water contents evaluated. The samples were shaken vigorously before sampling the gas from their headspace. Gas samples were taken and analyzed using SRI 9300 GC equipped with a thermal conductivity detector (TCD) and CTR-1 column capable of simultaneous analysis of CO_2, CH_4, O_2 and N_2. For each replicate, 1 ml of gas sample was withdrawn from the vial, and 0.5ml was wasted before injection into the GC. This ensured the sample volume was within the acceptable limit for the GC and in equilibrium with the atmospheric pressure. A 3-point calibration curve was constructed for the SRI 9300 GC using standard CH_4-CO_2 gas mixtures at 5%, 25%, and 50% concentration.

Two sets of batch experiments were conducted. The first set of batch experiments were conducted with each media at five different moisture conditions contacted with synthetic LFG containing 50% CH_4 and 50% CO_2 by volume for a total duration of 24 hours. In the second series of batch tests, only BOF slag samples at a single moisture content of 40% were exposed to different gas compositions for extended periods up to 1,850 hours: 50% CH_4 and 50% CO_2 mixture, 99% CH_4 and 1% nitrogen mixture, and 50% CO_2 and 50% nitrogen mixture. These gas mixtures were selected to assess if there was any synergistic effects or interference on the

removal of CH_4 and CO_2 when both were present. The gas samples were analyzed from these vials until no further CO_2 removal by BOF slag was detected.

3.2.3 Column Experiments

Column experiments were conducted to determine the CO_2 removal capacity of the BOF slag using the experimental setup shown in **Figure 3-2.**

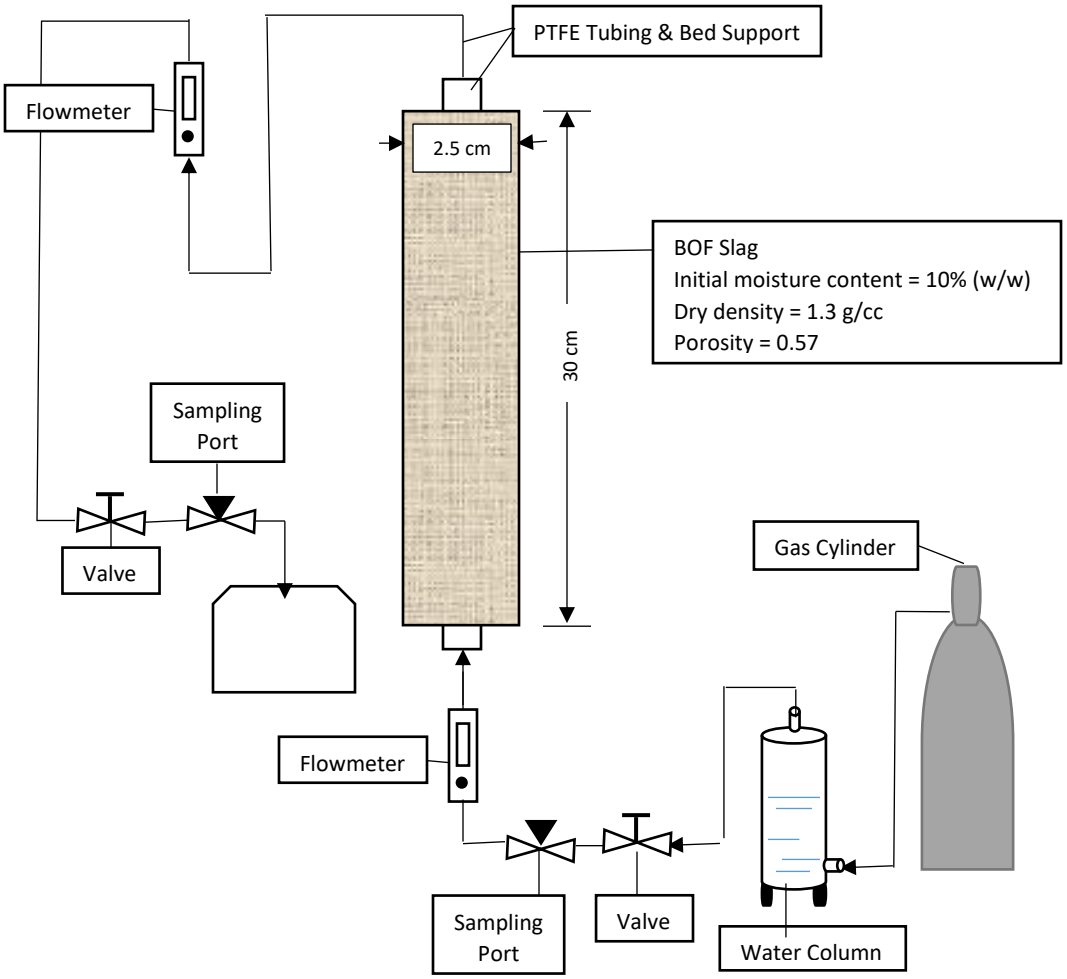

(a)

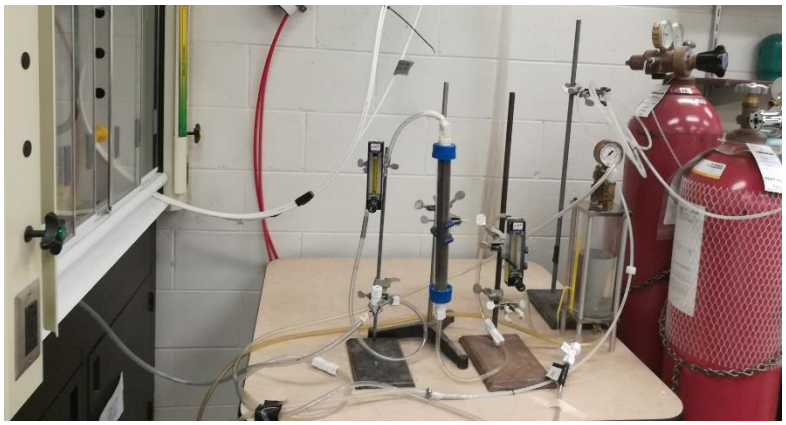

(b)

Figure 3-2: Column experimental setup (with humid gas): (a) Schematic; and (b) Photograph.

An acrylic glass column of 30 cm height and 2.5 cm inner diameter was filled with BOF slag with 10% moisture content up to its full length in 2 layers of 15 cm each with light tamping. It was secured with bed support mesh screen, end connections, and screw caps at both ends. PTFE tubing was used to connect all components in the setup. Flow meters were installed at both ends of the column to control the influent/effluent gas flow rates. Gas samples were collected from each port at different time intervals until CO_2 breakthrough ($C_{OUT}/C_{IN} = 1$). 1 ml of gas sample was collected from each sampling port at different time intervals, reduced to 0.5 ml and analyzed using SRI 9300 GC equipped with a thermal conductivity detector (TCD) and CTR-1 column for simultaneous analysis of CO_2, CH_4, O_2 and N_2. Three column tests were conducted as follows and summarized in **Table 3-2**:

- Column DC was tested under the dry continuous inflow gas (50% CH_4 and 50% CO_2) conditions at 12 psi inlet pressure and inlet flowrate 5-9 ml/min at normal atmospheric temperature (23°C).
- Column HC was tested for humid continuous inflow gas (50% CH_4 and 50% CO_2) conditions at an inlet pressure less than 6 psi and initial inlet flowrate 10-12 ml/min at

atmospheric temperature. The synthetic LFG was passed through a water cylinder to humidify the inlet gas to the Column (**Figure 3-2**).

- Column DI was conducted with dry intermittent gas (50% CH_4 and 50% CO_2) at 12 psi inlet pressure and inlet flowrate 7-11 ml/min at atmospheric temperature.

Humid inflow gas conditions (HC) were tested to simulate the humid LFG conditions and role of moisture on CO_2 removal, if any. The DC and DI tests were included to evaluate the effects of pulsed flow on CO_2 removal.

Table 3-2: Summary of column experimental conditions

Parameters	**DC**	**HC**	**DI**
Inlet gas:			
Moisture condition	Dry	Humid	Dry
Mode of injection	Continuous	Continuous	Intermittent
Carbon dioxide (%)	50	50	50
Methane (%)	50	50	50
***Column*:**			
Diameter (cm)	2.5	2.5	2.5
Length (cm)	30	30	30
BOF slag mass (g)	189.5	190.8	199.5
BOF slag particle size (mm)	< 4.75	< 4.75	< 4.75
Moisture content (%)	10	10	10
Dry density (g/cm^3)	1.3	1.3	1.38
Porosity (v/v)	0.57	0.57	0.55
Pore volume (ml)	82	82	80
***Flow*:**			
Inlet flow rate (ml/min)	5-9	10-12	7-11
Inlet pressure (psi)	12	< 6	12
Outlet flow rate (ml/min)	1-7	2-12	2-9
Total test duration (min)	17,159	11,167	17,678
Total pore volumes (#)	1553	1556	1882

3.3 RESULTS AND DISCUSSION

3.3.1 Slag Characteristics

Table 3-3 shows the mineralogy of the BOF slag based on XRD results**.**

Table 3-3: Mineralogy and bulk chemistry (oxide basis) of BOF slag

Minerals and Oxides	Mineral Formula	Percent Weight
Minerals		
Lime	CaO	2.0-2.2
Portlandite	$Ca(OH)_2$	9.4-9.5
Larnite	Ca_2SiO_4	9.5-11.4
Srebrodolskite	$Ca_2Fe_2O_5$	6.6-7.8
Akermanite	$Ca_2MgSi_2O_7$	0.0-6.4
Magnesioferrite	$MgFe_2O_4$	3.3-3.8
Katoite	$Ca_3Al_2(OH)_{12}$	3.8-4.3
Calcite	$CaCO_3$	2.8-2.9
Vaterite	$CaCO_3$	1.8-2.7
Wuestite	FeO	2.5-2.7
Mayenite	$Ca_{12}Al_{14}O_{33}$	2.7-2.9
Iron magnesium oxide	$FeO.76MgO.24O$	1.4-1.7
Merwinite	$Ca_3Mg(SiO_4)_2$	0.9-0.9
Periclase	MgO	0.4-0.6
Quartz	SiO_2	0.3-0.4
Brucite	$Mg(OH)_2$	0.3-0.6
Iron	Fe	0.0-0.1
Amorphous material		41.7-50.1
Oxide Basis		
CaO		33.6-33.8
SiO_2		13.3-13.4
Al_2O_3		3.6-3.6
Fe_2O_3		15.4-15.4
MgO		4.6-4.6
SO_3		0.3-0.3
Loss of Ignition (LOI)		8.6-8.6

Note: Analyzed by PMET, Inc., PA

The oxides composition is within the range reported in the published literature (Yildrim and Prezzi 2011; Grubb et al. 2011, 2014; Chiang and Pan 2017). These oxides are present in the form of minerals in BOF slag**.** Most reactive minerals in the order of decreasing reactivity commonly present in BOF slag are CaO, $Ca(OH)_2$ and Ca_2SiO_4 (Huijgen et al. 2005; Sarperi et al. 2014). The CaO and $Ca(OH)_2$ together form the effective "residual lime" immediately available for reaction with CO_2. In the BOF slag used in this study, ~2% CaO, ~9.5% $Ca(OH)_2$ are present, summing to 11.4-11.7 % residual lime content, along with ~11% Ca_2SiO_4. In addition, ~5% $CaCO_3$ in the form of calcite and vaterite was also measured, and reflects the influence of air/water cooling during processing at the steel mill.

The total, TCLP, and SPLP concentrations and leaching tests results of the BOF slag along with the RCRA limits as per 40 CFR 261 are summarized in **Table 3-4** for comparison purposes. The results show that all TCLP regulated concentrations are within the RCRA limits, thus the BOF slag is classified as non-hazardous. This observation is consistent with Proctor et al. (2000) in which slags [BOF, blast furnace (BF) and electric arc furnace (EAF)] from 58 active steel mills across North America (that contribute to more than 47% of the steel production in North America) were characterized to assess their impact on human and environmental health. None of the TCLP results from the slags exceeded the US EPA leaching thresholds, and therefore were characterized as non-hazardous. Steel slags included tightly bound metals that are not released even under acidic conditions. This is also an important consideration with the landfill cover amendment as the addition of BOF slag would not contribute/add to deterioration of landfill leachate quality.

Table 3-4: Total, TCLP and SPLP metal concentrations in BOF slag. (Data courtesy: Phoenix Services LLC)

Constituent	Symbol	Total (mg/kg)	TCLP (mg/L)	SPLP (mg/L)	RCRA Limit (mg/L)
Aluminum	Al	7,600	0.62	0.16	
Antimony	Sb	<0.76	<0.00031	<0.00016	
Arsenic	As	1.3	0.00087	0.00029	5
Barium	Ba	36	0.3-14	0.12	100
Beryllium	Be	<0.76	<0.00025	<0.00013	
Boron	B	330	0.12	0.027	
Cadmium	Cd	2.5	<0.00028	<0.00015	1
Calcium	Ca	290,000	2,300	800	
Chromium	Cr	1,600	0.011	0.002	5
Cobalt	Co	1.2	0.0034	0.0013	
Copper	Cu	7.4	<0.005	<0.0025	
Iron	Fe	210,000	0.031	0.011	
Lead	Pb	<0.76	<0.00041	<0.00020	5
Magnesium	Mg	65,000	0.077	<0.050	
Manganese	Mn	24,000	0.005	0.00072	
Mercury	Hg	<0.01	<0.00005	<0.00005	0.2
Nickel	Ni	8.2	0.036	0.013	
Potassium	K	<1,500	0.76	0.66	
Selenium	Se	<1.2	0.0047	0.0019	1
Silver	Ag	<0.76	<0.00025	<0.00013	5
Sodium	Na	<1,900	6.4	4.8	
Thallium	Tl	<0.23	<0.00025	<0.00013	
Vanadium	V	1,000	0.0058	0.00078	
Zinc	Zn	59	0.035	0.024	

Note: Analyzed by CH2M Hill, Inc.

Key features of BOF slag compared to other landfill cover materials tested such as soil and biochar are its high material density and high alkalinity. The high density of the BOF slag is attributed to the iron content (**Table 3-4**). However, the specific gravity of the BOF slag used (3.04) was much less than that reported for typical BOF slag (~3.5) in literature (Chesner et al. 1998; Grubb et al. 2011). According to Pan et al. (2013) and Morone et al. (2014) steel slags exhibited reducing specific gravity and particle density, respectively upon carbonation (aging).

Ko et al. (2015) also mentioned reduction in density from 3.35g/cm^3 to 2.21 g/cm^3 upon CaO hydration to $Ca(OH)_2$ and its carbonation. The presence of calcium carbonate polymorphs (calcite and vaterite) as shown in **Table 3-3** confirms the aging of BOF slag leading to the reduction in material density. The alkalinity associated with BOF slag resulting from its residual lime content and basic silicates were viewed as a major challenge with respect to the viability of bacteria (methanotrophs) to convert CH_4 to CO_2.

3.3.2 Batch Experiments

3.3.2.1 Effect of Moisture Content on Gas Removal

The 24-hour batch experiments were conducted with soil, BOF slag, and biochar at five different moisture contents by weight: 0%, 10%, 20%, 30% and 40% such that the values were within their WHC for typical unsaturated conditions in landfill covers (normal atmospheric temperature (23°C) and pressure). The CH_4 and CO_2 removal was calculated based on the differences in their initial concentrations and the quantities of each gas in the microcosm bottles for each testing intervals as reported by the GC, summarized in **Figure 3-3**. The CO_2 removal capacity of BOF slag was in the range of 53-68 mg/g, versus 10 mg/g and 24 mg/g for soil and biochar, respectively (**Figure 3-3a**). The CO_2 removal by BOF slag was substantially higher than that of soil and biochar, and moreover appeared to be independent of initial moisture content above 0%. The carbonation under dry conditions was only 5 mg/g (negligibly small) indicating that moisture is pre-requisite for carbonation. The CH_4 removal in all media was insignificant (<6 mg/g) as implied by **Figure 3-3b**.

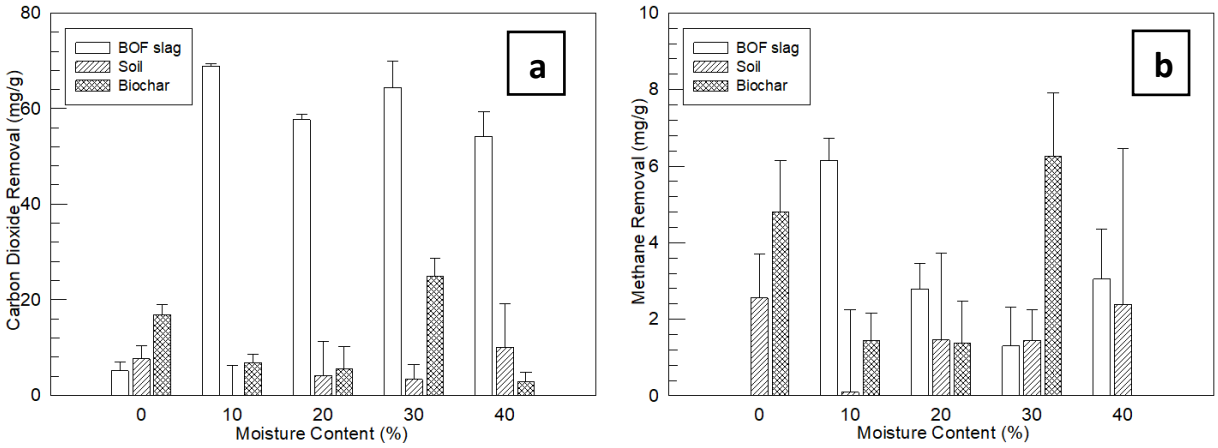

Figure 3-3: Cumulative (a) CO_2 and (b) CH_4 removal in 24 hours by BOF slag, soil and biochar at different moisture conditions (n = 3).

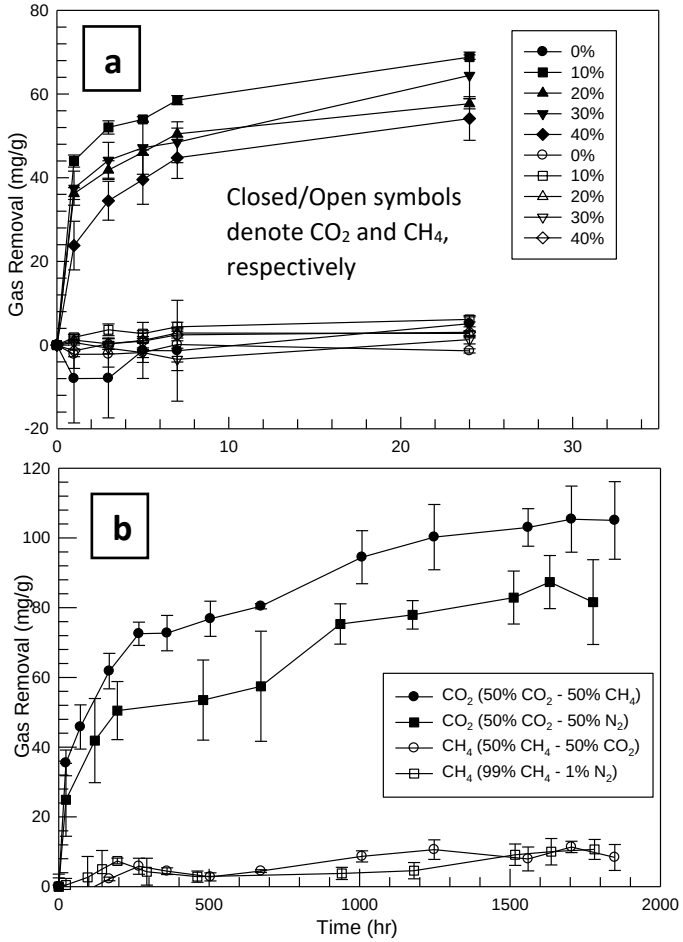

Figure 3-4: Cumulative CO_2 and CH_4 removal by BOF slag with time: (a) short-term batch experiments with different initial solid moisture contents; and, (b) long-term batch experiments with different gas mixtures at initial solid moisture content of 40%.

Figure 3-4a shows the CO_2 and CH_4 removal trends for the BOF slag during the 24-hour batch experiments. The CH_4 removal was negligible and there was no meaningful change with time. Likewise, CO_2 removal at 0% moisture was insignificant. Batch experiments demonstrated the significance of moisture in BOF slag carbonation by the sudden shift of CO_2 removal from 5 mg/g under dry conditions to 61 mg/g (average for all moisture contents tested) under moist conditions. It is suggestive of the initiation of the leaching of Ca^{2+} ion to the surface of slag particles facilitated by the presence of moisture, which forms the rate determining step of the carbonation reaction (Huijgen et al. 2005). The initial hydration of free lime and reaction of CO_2 with portlandite forms the initial carbonates. Further, the Ca^{2+} from the Ca-silicates sequentially leach out of the slag particles to react with CO_2 during which it leaves behind a shell of unreactive, Ca-exhausted SiO_2 rim. The Ca leaching even in the presence of moisture, could be limited by (1) formation of exhausted SiO_2 particle on the slag particle surface, hindering the Ca^{2+} from reaching surface, (2) precipitation layer of $CaCO_3$ on the surface of slag particles; and (3) stirring rate; a continuous stirring enhances the carbonation as it would make more Ca^{2+} available on the surface to react. Accordingly, as reported by Sarperi et al. (2014), an oven-dried slag (L/S = 0) did not exhibit CO_2 removal (0 g/kg_{BOF}) whereas the intrinsic water in the as-received slag initiated carbonation (24 g/kg_{BOF}), hence highlighting role of water in accelerated carbonation.

However, a direct carbonation-moisture content relationship could not be established from the 24-hour batch experiments in this study. Among the various moisture contents tested, the optimum MC for carbonation was found to be 10%, removing maximum of 68 mg/g CO_2. Thereafter, lower CO_2 removal was observed at both 20% and 40% moisture content, with a slight increased CO_2 removal of 63 mg/g at 30% moisture content. The CO_2 removal trends

observed in the present study (**Figure 3-4a)** affirms that while moisture is a necessary medium for accelerated carbonation of BOF slag, it alone cannot alter the extent of carbonation. Other factors such as BOF slag particle size, ambient temperature, and initial CO_2 pressure that usually control carbonation rates (Berryman et al. 2015; Su et al. 2016; Ukwattage et al. 2017) are viewed as the cause of this varying trend. Since the slag sample was taken as-received for the batch experiments, the particle sizes present in the samples varied which could have led to lesser carbonation in samples with higher coarser-to-finer particle ratio.

Previous studies were analyzed and summarized in **Table 3-5**.

Table 3-5: Comparison of batch experiments in previous and present study on CO_2 sequestration by steel slag

Reference	Experimental Conditions	Notes
Huijgen et al. (2005)	**Slag:** Linz Donawitz (LD) steel slag **Moisture:** 2-20 L/kg (L/S ratio) **Reactor:** AISI316 Autoclave Reactor **Stirring rate:** 500 rpm **Grain size:** < 0.106 mm **Temperature:** 100 °C **Pressure:** 20 bar (continuous CO_2 replenishment) **Reaction time:** 30 min **Analysis method:** Thermogravimetric Analysis (TGA) and acidification	▪ Optimum L/S: 2 L/kg ▪ Calcium conversion and carbonate content decreased from 60 to 50% and 12.5 to 10.5 (wt%), respectively with increasing L/S from 2 to 20 L/kg, explained by higher ionic strength and higher Ca solubility.
Su et al. (2016)	**Slag:** BOF slag **Moisture:** 0 -10 L/kg (L/S) **Reactor:** 20 ml capped (with 7 holes) cell within 500 ml autoclave **Stirring rate:** None **Grain size:** 3.5-2 (mm) **Temperature:** 100 °C **Pressure:** 250 kg/cm^2 **Reaction time:** 0.5-96 hours **Analysis method:** TGA	▪ Optimum L/S: 2-5 L/kg ▪ Carbonate content (wt%) and carbonation degree increased from 0 to 5 (L/S) and decreased from 5 to 10 (L/S).
Sarperi et al. (2014)	**Slag:** BOF slag **Moisture:** 0 - 0.5 L/kg **Reactor:** Atmospheric reactor **Stirring rate:** 300 rpm	▪ Optimum L/S: between 0.05 to 0.2 L/kg (with 65 g/kg$_{BOF}$ CO_2 removal at 0.1 L/kg) ▪ Oven-dried slag (L/S = 0) did not result in any CO_2 removal while the intrinsic water

	Grain size: 0-6 mm **Temperature:** 20°C(thermo-regulated room) **Pressure:** ND (CH_4/CO_2 gas mixture passed for 5 min at 10 ml/min) **Reaction time:** 6 hours **Analysis method:** Gas chromatography	in the as-received slag initiated carbonation, hence highlighting importance of water in accelerated carbonation.
Present study	**Slag:** BOF slag **Moisture:** 0 – 0.4 L/kg **Reactor:** 125 ml microcosm bottles **Stirring rate:** Only occassional shaking **Grain size:** <10 mm **Temperature:** Room temperature (~23°C, non-regulated) **Pressure:** ND (50% CH_4/50% CO_2 gas mixture purged in vial) **Reaction time:** Test 1: 24 hours; and Test 2: 1850 hours **Analysis method:** Gas Chromatography	▪ Optimum MC: 0.1 L/kg (68 mg CO_2 /g $_{BOF}$ removed) ▪ Oven-dried slag did not remove any CO_2

They also recommend optimum moisture ranges and did not establish a perfect correlation with its effect on CO_2 sequestration capacity of BOF slag. Both Huijgen et al. (2005) and Su et al. (2016) conducted experiments with BOF slag at more ideal conditions conducive for accelerated carbonation such as high temperature (100°C), high pressure and finer particle size exposed only to CO_2 to optimize parameters for industrial CCS. As per Su et al. (2016), carbonation increased from 6.19% to 17% in 24 hours upon increasing L/S from 0 to 2 (L/kg), while further increase of L/S to 5 L/kg decreased carbonation degree to 15%, followed again by increased carbonation (18%) at L/S = 10 (L/kg). Su et al. (2016) terms water as only a required medium, but advocates particle size as the major controlling factor on carbonation. The composition of water was also analyzed after the carbonation experiment where increased L/S ratio did not directly correspond to increased Ca^{2+} concentration. Huijgen et al. (2005) observed decrease in carbonation with

increasing moisture content owing to limitations of mixing in reactor and suggested higher ionic strength of Ca at lower L/S as the reason for better carbonation.

The study by Sarperi et al. (2014) was conducted at operating conditions closer to the landfill conditions maintained in the present study (**Table 3-5**). BOF slag (<6 mm) was experimented to analyze its capacity to sequester CO_2 from raw biogas at regulated temperature (20°C) and exposed to CO_2/CH_4 gas mixture initially supplied to the BOF slag at various moisture contents ranging from 0 to 0.5 L/kg. The CO_2 removal was monitored by gas chromatography and optimum L/S ratio was identified as 0.1 L/kg with carbonation decreasing on either side of 0.1 L/kg.

In contrast, this study shows CO_2 removal had two portions with distinct slopes in the presence of moisture (**Figure 3-4a**). Rapid carbonation occurred in the first 8 hours, followed by more gradual removal thereafter. A similar shift in the Ca leaching kinetics was also observed by Stolaroff et al. (2005). The authors described the Ca dissolution curve with a rapid initial kinetics in the first hour followed by a slower rate. The similarity between these observations show that the change in carbonation rate is a result of the Ca dissolution kinetics.

Hence, BOF slag sample (<10 mm) with 61±7 mg/g CO_2 removal capacity over 10-40% (0.1-0.4 L/kg) moisture content with the available mineral composition of the sample was successful in establishing the feasibility of BOF slag usage in normal landfill conditions for CO_2 removal. The optimum moisture content for CH_4 oxidation in landfill cover is within 10-20% (Visvanathan et al. 1999; Huber-Humer et al. 2008), which further confirms that the carbonation of BOF slag can be incorporated while maintaining a nominal moisture content for methanotrophic activity.

3.3.2.2 Maximum Gas Removal and Synergistic Effects of Gas Composition

Long-term batch experiments with different gas mixtures were conducted on BOF slag following the same procedure as that of the 24-hour batch experiments, except the initial solid BOF slag at an initial moisture content of 40% (0.4 L/kg) was exposed to four synthetic LFG mixtures to analyze the potential synergistic effects of CO_2 and CH_4 removal (**Figure 3-4**). **Figure 3-4b** follows a similar CO_2 removal trend as that observed in the 24-hour batch tests. The carbonation is initially rapid, followed by a continuous lower rate of CO_2 removal. A maximum of ~100 mg/g CO_2 was removed by BOF slag after ~1,850 hours exposure to 50-50 CO_2/CH_4 gas mixture. For the 50-50 CO_2/N_2 mixture, only ~84 mg/g of CO_2 was removed in ~1,630 hours. The partial pressure of CO_2 in the CO_2/CH_4 mixture (P_{CO_2}= 109,546 Pa) is slightly greater than its partial pressure in the CO_2/N_2 mixture (P_{CO_2}= 109,439 Pa). This may have favored more carbonation in the CO_2/CH_4 mixture. With respect to CH_4, about 10-11 mg of CH_4 was taken up by the BOF slag sample at 40% moisture content regardless of the gas mixture composition. The CH_4 removal fluctuates between 4-10 mg/g.

3.3.3 Column Experiments

Three column experiments were conducted at three inflow gas conditions as summarized in **Table 3-6** and discussed below.

Table 3-6: Cumulative CO_2 removed by BOF slag in column experiments with different flow conditions.

Column	1 PV (ml)	Breakthrough		Termination	
		PV (#)	CO_2 removed (mg/g)	PV (#)	CO_2 removed (mg/g)
DC: Dry & Continuous	82	100	42	1,553	155
HC: Humid & Continuous	82	100	42	1,556	315
DI: Dry & Intermittent	80	100	42	1,882	200

3.3.3.1 Dry Versus Humid Gas Injection

The DC column was run continuously with the inlet and outlet gas sampled and analyzed regularly for CO_2 and CH_4 concentrations. The CO_2 and CH_4 ratio of outlet concentration to inlet concentration (C_{OUT}/C_{IN}) as a function of pore volume (PV) injected are shown in **Figure 3-5**. Column HC was conducted similarly. The corresponding cumulative CO_2 and CH_4 removal versus PV are plotted in **Figure 3-6.**

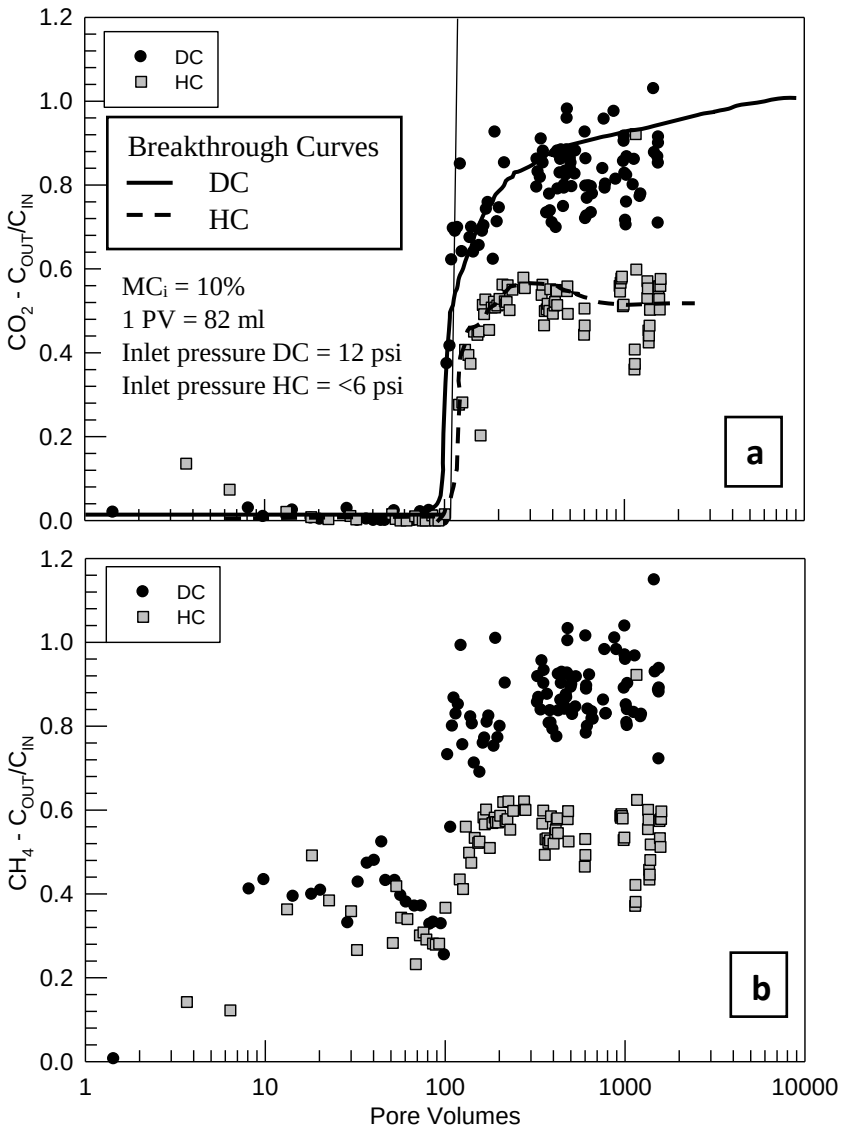

Figure 3-5: Outlet to inlet concentration ratio of CO_2 (a) and CH_4 (b) under dry (DC) and humid (HC) flow conditions on BOF slag column pore volume basis.

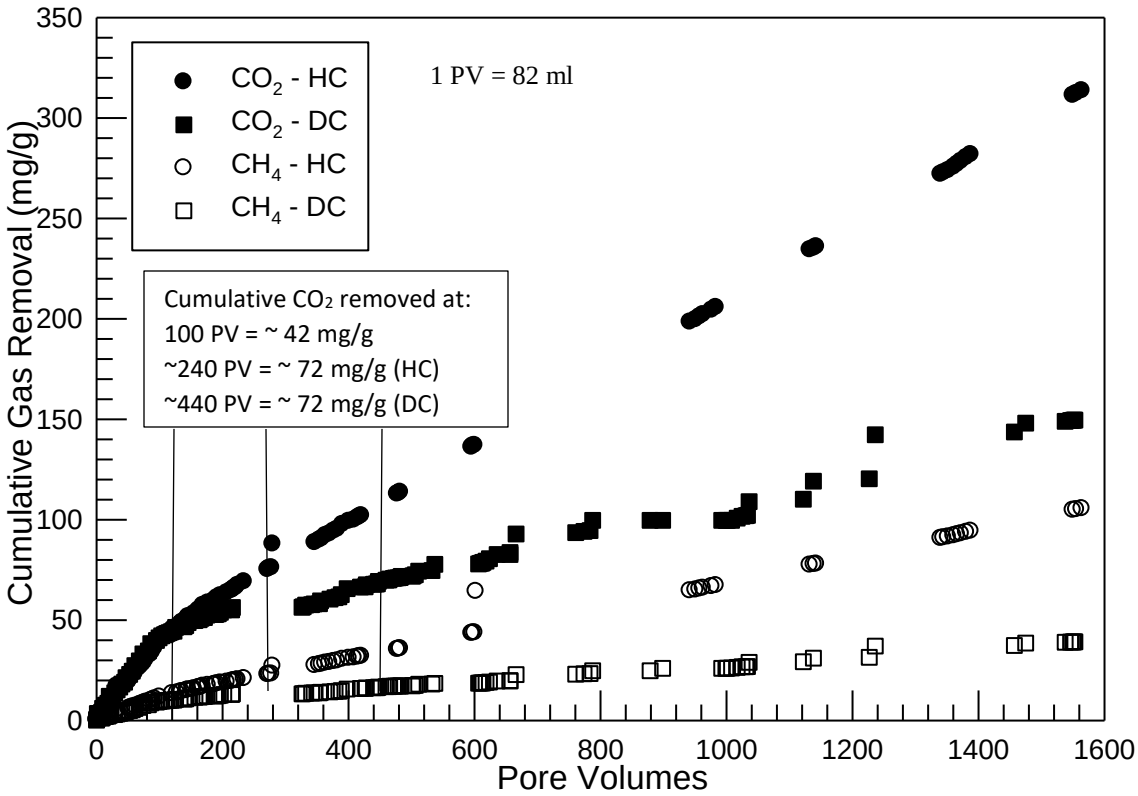

Figure 3-6: CO_2 and CH_4 removal under humid (HC) and dry (DC) flow conditions on BOF slag column pore volume basis.

Figure 3-5a shows that under DC conditions, the C_{OUT}/C_{IN} for CO_2 is ~ 0 implying 100% removal of CO_2 until 100 PV (42 mg/g CO_2). After 100 PV, C_{OUT}/C_{IN} increased rapidly to 0.7 at 150 PV. The ratio then gradually increased to ~1 around 1,553 PV, for a total of ~155 mg/g of CO_2 removed at test termination. For DC conditions, CH_4 was almost always present in the effluent. Up to 100 PV, the C_{OUT}/C_{IN} ratio of CH_4 fluctuated around 0.4, then rapidly increased to ~ 1 after the CO_2 breakthrough resulting in a 40 mg/g of total CH_4 removal.

For HC conditions, C_{OUT}/C_{IN} remained close to 0 for CO_2 until 100 PV, corresponding to ~ 42 mg/g CO_2 removal. Also, until 100 PV, C_{OUT}/C_{IN} for CH_4 remained ~0.4 (60% CH_4 removal). After 100 PV, the CO_2 C_{OUT}/C_{IN} increased rapidly to 0.6 at 200 PV (~ 58 mg/g) and

remained at this level until about 1,556 PV as shown in **Figure 3-5.** The test results of HC at same pore volumes as DC termination was used to compare the cumulative gas removal capacity of BOF slag. In the case of CH_4, the C_{OUT}/C_{IN} increased from 0.4 to 0.6 after breakthrough and followed the same trend as CO_2, removing about 100 mg/g CH_4, much greater compared to the cumulative CH_4 removal under DC conditions (**Figure 3-6**).

The slope of cumulative CO_2 removal curve under DC column conditions decreases from 0.4 to 0.07 at 100 PV (breakthrough) as shown in **Figure 3-6b**. Cumulative CH_4 removal also follows a similar trend changing from 0.11 to 0.02 after breakthrough. **Figure 3-6** shows cumulative CO_2 removal curve by BOF slag under HC conditions reduces from 0.4 to 0.2 before and after the breakthrough, respectively. A similar slope change in the cumulative CH_4 removal curve was observed from 0.13 to 0.06 before and after breakthrough, respectively.

3.3.3.2 Intermittent versus Continuous Gas Injection

Column DI was conducted such that the dry inlet gas was injected intermittently (9-10 hours ON/14-15 hours OFF). Each time the gas supply was reinstated, a C_{OUT}/C_{IN} similar to the previous cycle was re-established in approximately 45 minutes.

Figure 3-7a shows that the DI column exhibited essentially the same behavior as the DC column through 100 PV. Thereafter, the DI results were clustered slightly lower than the DC column data. The total CO_2 removal by the DI column system with BOF slag was 185 mg/g. **Figure 3-7b** shows more overlapping performance of the two columns for CH_4 removal, ultimately the DI column removing 50 mg/g slightly higher than DC conditions.

The slope of cumulative CO_2 removal curve by BOF slag changed from 0.4 to 0.11 at 100 PV, whereas the slope of the cumulative removal curve of CH_4 changed from 0.17 to 0.03 after the breakthrough (**Figure 3-8**).

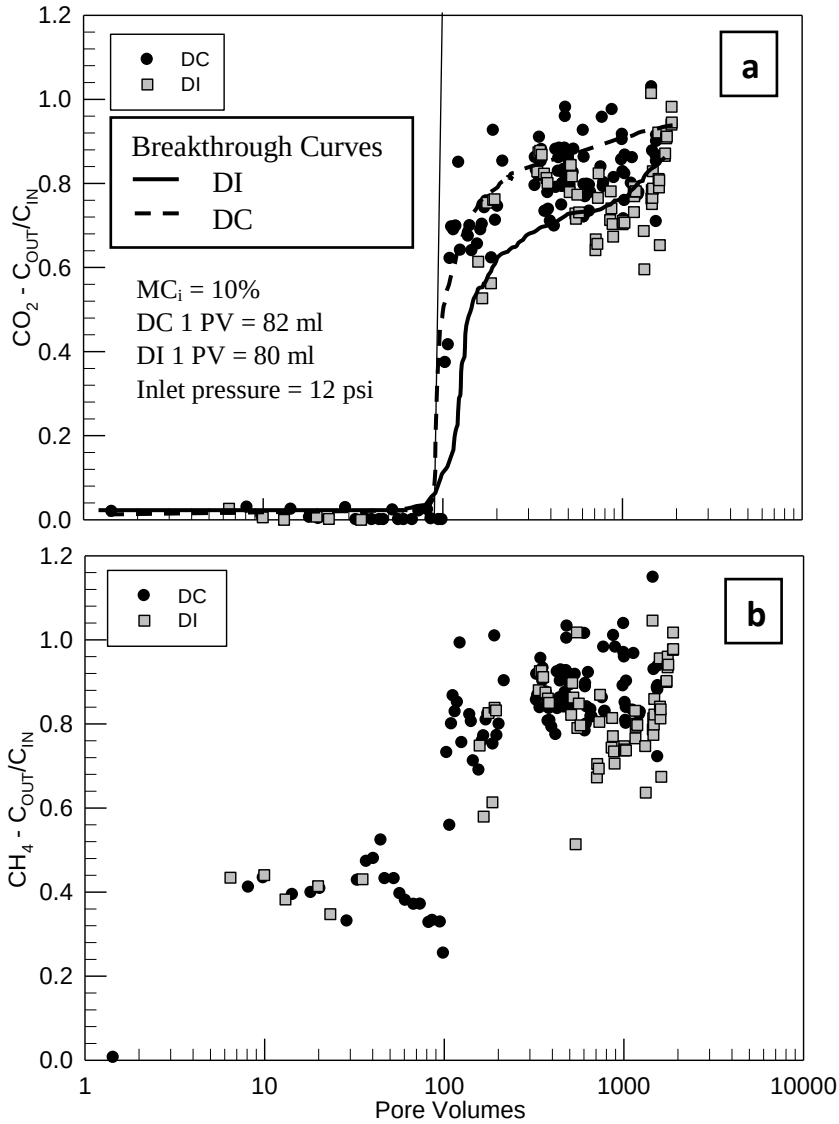

Figure 3-7: Outlet to inlet concentration ratio of CO_2 (a) and CH_4 (b) under dry continuous (DC) and dry intermittent (DI) flow conditions on BOF slag column pore volume basis.

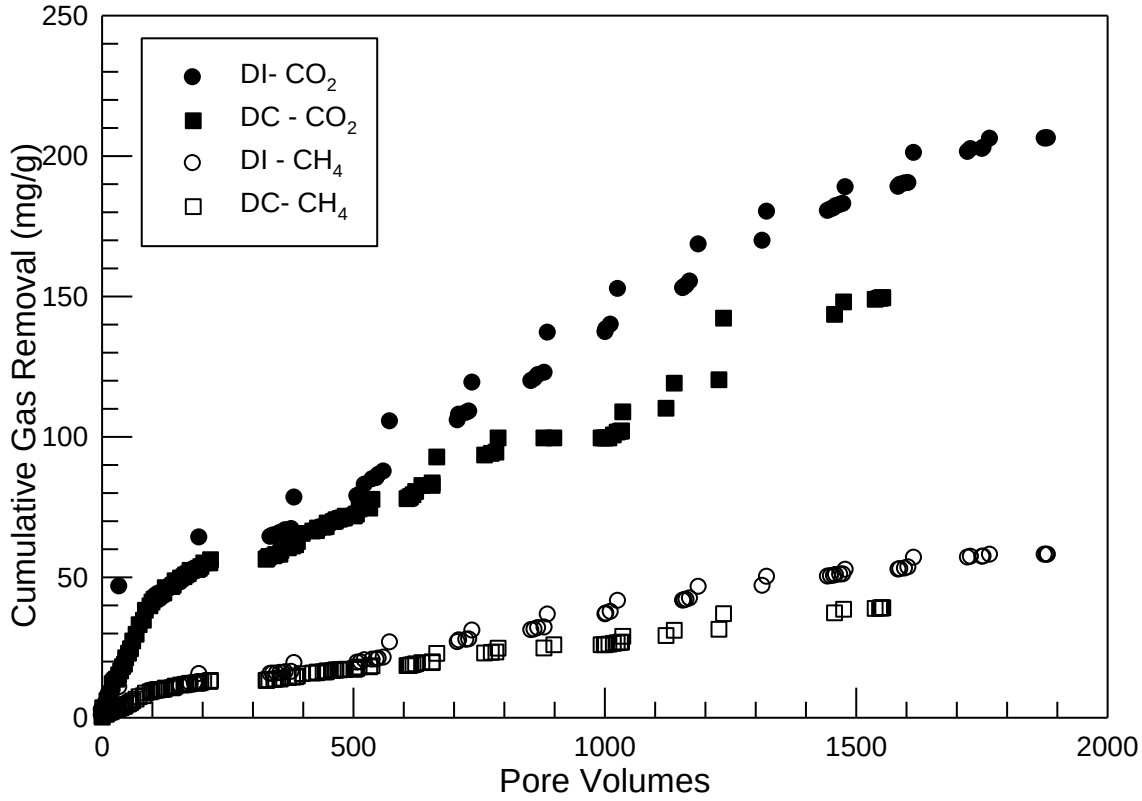

Figure 3-8: Comparison of cumulative CO_2 and CH_4 gas removal under dry continuous (DC) and dry intermittent (DI) flow conditions on BOF slag column pore volume basis.

3.3.3.3 Mechanisms of CO_2 Removal

Breakthrough point of CO_2 occurred at 100 PV = 8,000-8,260 ml or an approximate liquid to solid ratio of gas (50% CH_4 and 50% CO_2) of 40 L/kg for the BOF slag under all three conditions – DC, HC and DI. However, carbonation persisted for longer periods under HC conditions compared to DC/DI conditions. The similarity in the performance of DC and DI columns suggest that moist conditions (HC) are critical for sustained CO_2 removal. However, initial breakthrough appears independent of BOF slag moisture content and gas conditions suggesting availability of residual lime/portlandite on slag surface, is decisive.

Huijgen et al. (2005) observed $Ca(OH)_2$ was responsible for instantaneous carbonation of steel making slags, while Sarperi et al. (2014) suggested surface lime (CaO) as equally

responsible for instantaneous reactions upon its hydration to form $Ca(OH)_2$. Hence, the instantaneous CO_2 removal of BOF slag until 100 PV is assumed to be the reaction with available CaO and $Ca(OH)_2$ in the as-received BOF slag (11.4 – 11.7 wt%). The leaching of Ca^{2+} is thought to be the rate determining reaction step in the surficial carbonation mechanism according to Chiang and Pan (2017) and Huijgen et al. (2005), suggesting moisture accelerates the interstitial Ca availability required for sustained CO_2 sequestration by slag.

Until 100 PV, CO_2 supplied to the system is observed to be completely removed by the BOF slag (CO_2 supplied: CO_2 removed = 1:1). At 100 PV, 8,260 ml gas = 4,130 ml (8.113 g) CO_2 is injected into the BOF slag system, which if completely sequestered by BOF slag present in column (189.5 g) would amount to ~ 43 mg/g CO_2 removed which is comparable to the cumulative CO_2 removal at 100 PV obtained experimentally (**Figure 3-6a)**. Thereafter, CO_2 supplied to the system is not completely removed (CO_2 supplied: CO_2 removed ≠ 1:1) as can be seen from **Figure 3-6a**. Stoichiometric CO_2 sequestration capacity of residual lime (11.4-11.7 wt%) amounts to 72 mg/g CO_2. However, only 42 mg/g CO_2 (60% of 72 mg/g) was removed at breakthrough, 72 mg/g of CO_2 was removed around 250-300 PV under HC and 440-450 PV under DC conditions (**Figure 3-5 and 3-6)**. This suggests only 60% of the lime was surface accessible for instantaneous carbonation until breakthrough. The remaining residual lime was leaching dependent due to which the total CO_2 removal capacity of the residual lime was achieved earlier under HC conditions compared to DC.

The change in the slope of cumulative CO_2 removal graph after breakthrough depict shift from rapid to slower carbonation rate dependent on Ca leaching kinetics (Stolaroff et al. 2005). Carbonation by Ca^{2+} leaching from minerals in the slag matrix dependent on the mobility of ions and moisture is much slower than the reaction of CO_2 with the readily reactive surficial CaO and

$Ca(OH)_2$. The steeper slope of cumulative CO_2 removal after 100 PV under HC conditions compared to DC is indicative of increased Ca^{2+} ion leachability facilitated by moist gas flow in the HC column. Continuous reaction of CO_2 with the BOF slag after breakthrough until C_{OUT}/C_{IN} =1 is assumed to be due to continuous and slow leaching of Ca^{2+} from reactive silicates such as larnite present in BOF slag matrix. Other minerals that contain Ca such as Ca-Fe-O and Ca-Mg-silicates have also been reported to participate in CO_2 removal under variable conditions such as higher moisture availability, lower particle sizes and longer carbonation periods (Huijgen et al. 2005; Kasina et al. 2015).

Gradual white patchy formation of precipitates was observed in columns during the experiments. The precipitate formation was sporadic until the breakthrough, thereafter progressed uniformly from bottom to top in layers until C_{OUT}/C_{IN} = 1 when BOF slag particles were completely covered with white precipitates from carbonation and cemented together more tightly. The scattered formation of precipitates throughout the column in the beginning could be depictive of the consumption of surficial residual lime that must be spread across the mass. Thereafter, the uniform carbonation from bottom to top could suggest carbonation with more Ca^{2+} ions leaching out earlier at the bottom (entrance) where BOF slag gets exposed most to moist gas and then slowly progresses upward. This carbonation technique is often used in the construction of slag marine blocks where such uniform cementation and carbonate formation progresses through the slag filled mold when treated with CO_2 (Takahashi and Yabuta 2002).

The BOF slag compositions are mostly typical and contain CaO content within 10-12% by weight (Yildrim and Prezzi 2011; Grubeša et al. 2016). The variations in available residual lime content, reactive Ca-silicate minerals, factors like particle size (surface area) and moisture

are viewed as factors that could affect breakthrough point and cumulative CO_2 removal capacity of BOF slag.

3.3.3.4 Mechanisms of CH_4 Removal

For all the three conditions tested, complete removal of CH_4 was never obtained. However, from **Figures 3-5** and 3-**6**, it was observed that the breakthrough and cumulative removal curves of CH_4 followed a similar pattern to that of CO_2. In the breakthrough plot, the C_{OUT}/C_{IN} ratio of CH_4 remained around 0.4 until 100 PV and then rapidly increased to a higher constant value around 0.9, occasionally reaching to 1. This phenomenon leads to the assumption that removal of CH_4 occurred in the BOF slag system. The cumulative removal of CH_4 was about one-fourth of CO_2 removal in DC and DI system, while it was one-third of the CO_2 removal in the HC system. Further, the slope of the cumulative CH_4 removal gas followed a similar trend in DC, HC and DI systems, changing from ~0.13 to 0.03 at breakthrough (100 PV).

To understand the CH_4 removal, further in-depth study of chemical reaction mechanisms occurring within the BOF slag matrix is required. It is known from the published literature on steel slag carbonation as well as the XRD results that BOF slag is a complex system that consists of numerous minerals. The basic and amphoteric oxides in the BOF slag form several minerals that have different solubility, reactivity, bonding and other chemical characteristics. It is also a highly porous material with high alkalinity making suitable for environmental remediation that includes metals immobilization, arsenite removal, and acid mine drainage remediation (Grubb et al. 2011; Grubb and Wazne 2011; Ziemkiewicz and Skousen 1999). Earlier studies discussed about influence of oxygen vacancies in iron oxides to adsorb CH_4 and methyl radicals (Cheng et al. 2016) and CH_4 interaction with MgO and alumina (Li et al. 1994a, 1994b). These metal

oxides (FeO, MgO, Al_2O_3) are constituents of BOF slag matrix suggesting the possibility of CH_4 removal by BOF slag along those routes. Steel slags have been studied by Navarro et al. (2010) to consist of both mesopores and macropores with high specific surface area of 11 m^2g^{-1} providing more adsorptive and reactive area. These properties of steel slag along with slight acidic nature of CH_4 gas and roughness provides a conducive environment for CH_4 adsorption (Chiang et al. 2016).

The literature reviews and several observations made during both batch and column studies on CH_4 response to BOF slag leads to the assumption that BOF slag has the capacity for CH_4 removal in smaller amounts. However, it requires further dedicated analysis and study to confirm and delineate the reaction mechanisms of CH_4 with BOF slag.

3.3.4 SEM-EDS Analysis

The SEM images and the SEM-EDS results for as-received and carbonated BOF slag samples are shown in **Figure 3-9** and the respective quantitative elemental results are given in **Table 3-7**. The EDS result in terms of percentage weight can only be considered as a qualitative method for comparison of steel slag that exhibits surficial and interstitial heterogeneous distribution of elements as it mostly gives the surficial information of very tiny quantity of the crushed sample (<0.5 g) that is considered representative of the larger system.

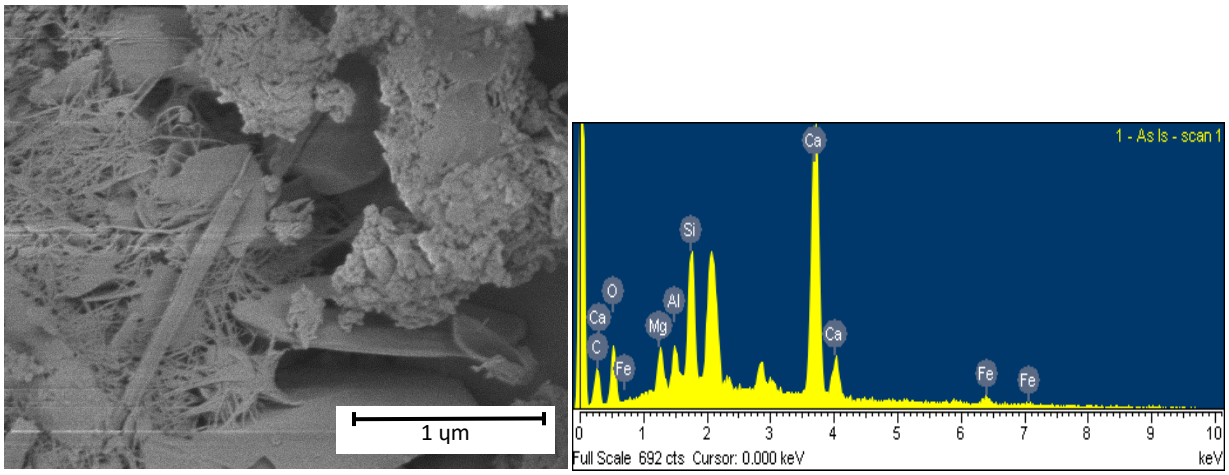

18000x magnification

(a)

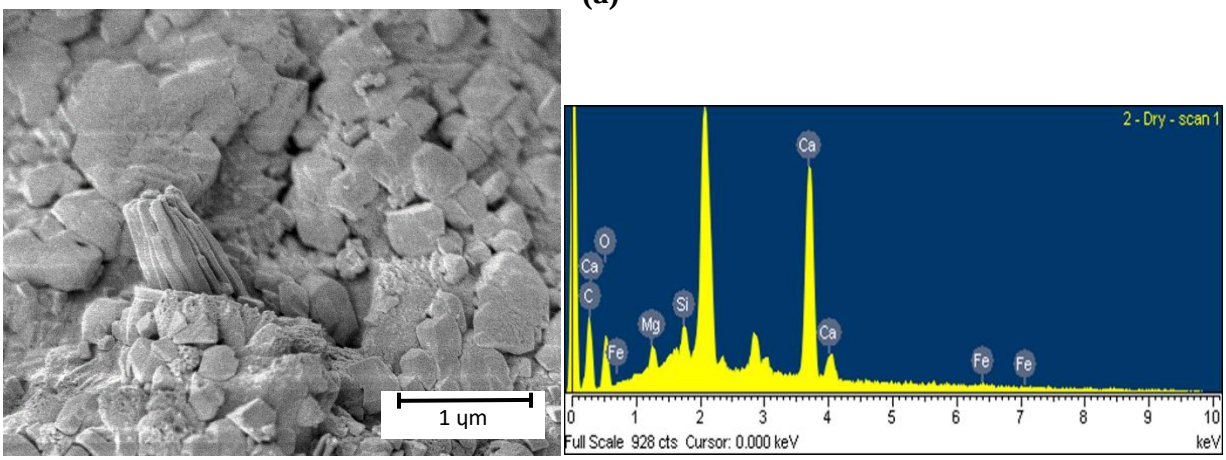

13000x magnification

(b)

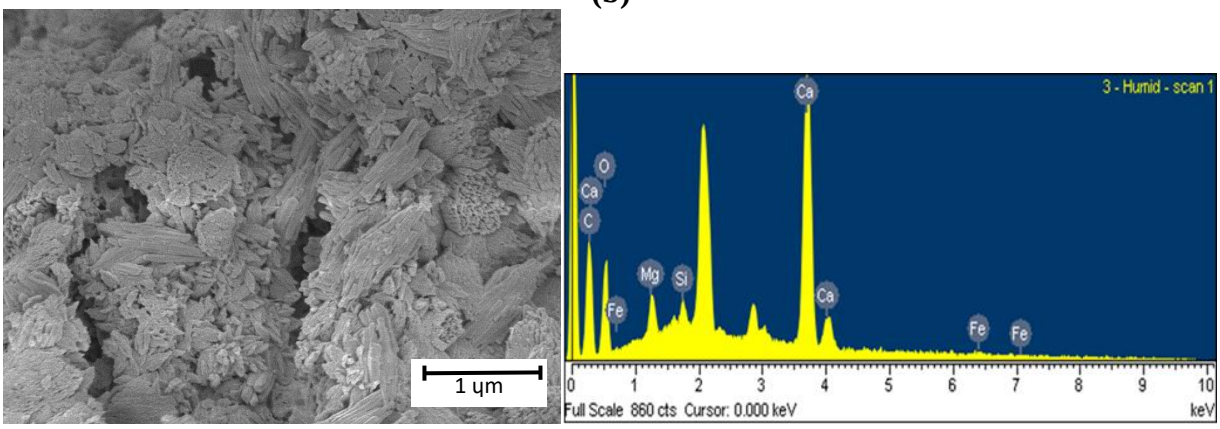

11000x magnification

(c)

Figure 3-9: Scanning Electron Microscopy- Energy Dispersive X-Ray Spectroscopy (SEM-EDS) images of BOF slag (a) As-received, (b) DC-Carbonated; and (c) HC-Carbonated (DC-dry gas conditions; HC-Humid gas conditions

Table 3-7: SEM-EDS elemental quantitative results for as-received and carbonated slag from DC and HC column experiments.

Element	Weight (%)		
	As-received	**DC**	**HC**
Ca	55.34	61.57	57.08
Si	9.70	3.92	2.22
Fe	9.69	ND	ND
Mg	2.26	1.87	2.43
Al	1.79	ND	ND
C	5.47	10.73	11.97
O	15.75	21.91	26.29

ND=non-detected

The image of as-received BOF slag shows the presence of large number of internal pores with a network of needle-like formations observed on the surfaces infringing on the pores. This network bares close resemblance to the $CaCO_3$ formations as described by Chiang and Pan (2017). The needle-like formations, rhombohedrals and orthorhombic structures that are visible in the SEM image are different polymorphic formations of $CaCO_3$. In addition, the SEM-EDS spectrum and the quantitative results in **Table 3-7** confirmed that the original sample tested for the experiments had already started undergoing carbonation during cooling and processing with the presence of carbon (C), oxygen (O) along with calcium (Ca) peaks suggestive of $CaCO_3$. The possibility of slow steel slag carbonation under normal atmospheric conditions in the presence of atmospheric CO_2 have been discussed in Gupta et al. (1994) while discussing stockpiling of steel slag for pavement construction.

The BOF slag collected from the DC and HC columns at the end of testing were subjected to SEM-EDS analysis to compare the surface and compositional changes due to carbonation. The sample from DI was not analyzed separately due to the similarity in its response to that of DC conditions. Increasing C and O peaks were detected with increasing degrees of carbonation (As-is → DC → HC). The increase in terms of percentage weight of

elements C and O are given in **Table 3-7.** Both the samples from DC and HC exhibited reduction in pores as well as formation of more needle-like and rhombohedral structures in the BOF slag matrix as compared to the as-received sample. The precipitate formed at the end of the column tests was observed to be the carbonates under SEM analysis due to the formations that resulted in Ca, C and O peaks.

3.4 CONCLUSIONS

The properties of BOF slag were explored in this study for its suitability and applicability in the landfill environment for mitigation of landfill gas emissions. Based on the series of batch and column experiments conducted in this study, the following conclusions can be drawn:

- BOF slag is shown to possess high capacity to sequester CO_2. In batch tests, the BOF slag was found to sequester an average of 61 mg/g of CO_2 at all moisture contents tested in 24 hours. In a system with continuous injection of humid synthetic landfill gas, ~ 315 mg/g of CO_2 was sequestered by 3/8 inches (minus) BOF slag. This capacity of CO_2 removal is divided into (i) instantaneous, and (ii) long-term capacity. The instantaneous reaction is attributed to the residual lime content in the BOF slag. Upon completion of the instantaneous reaction, a breakthrough occurs. Thereafter, Ca^{2+} ions must be leached from other reactive silicates, and thus depends on aqueous reactions. This is aided with the help of moisture in the system as seen from column HC. A further mineralogical analysis of the carbonated BOF slag from such column experiments based on XRD and TGA is recommended to better understand the carbonation mechanism. The analysis of samples collected before and after breakthrough will be helpful in determining the carbonate formation and the changes from

original mineralogy. A direct measurement of change in mass of the BOF sample at test-end would also be helpful in stoichiometric calculations.

- CO_2 removal at breakthrough being only 60% of the residual lime capacity (72 mg/g), suggested the distribution of only 60% of the total residual lime content as surface lime for immediate carbonation. Hence, breakthrough is assumed as function of mineral composition of BOF slag and surficial residual lime content. While breakthrough at 100 PV is true for the 3/8" (or 10 mm) minus BOF used in this study, it could differ with particle size (surface area variation) and mineral composition. Finer particles possess higher specific surface area, porosity and hence better interaction between the reactants. In the case of steel slag carbonation in specific, it also reduces the Ca^{2+} leaching pathway to the particle surface increasing the reaction rate. With regards to this hypothesis, Reddy et al. (2018a) and (2018b) discusses the effect of BOF slag particle size and BOF slag types, respectively on CO_2 sequestration.
- After 100 PV, the capacity of total residual lime content in BOF slag (72 mg/g CO_2 removal) achieved by the steel slag under HC conditions compared to DC conditions, affirm that Ca leaching supported in the presence of moisture determines the rate of reaction after breakthrough. Further, moisture also aids in increasing the total CO_2 removal capacity of the BOF slag by initiating and sustaining leaching of ions from reactive minerals.
- A smaller CH_4 removal capacity was also exhibited by BOF slag during the batch and column experiments (~ 30 mg/g) indicating its potential to mitigate both CH_4 and CO_2 from landfill gas.

3.5 CITED REFERENCES

Berryman, E. J., Williams-Jones, A. E., & Migdisov, A. A. (2015). "Steel slag carbonation in a flow-through reactor system: The role of fluid-flux." *J. Environ. Sci.*, 27, 266-275.

Cheng, Z., Qin, L., Guo, M., Fan, J. A., Xu, D., & Fan, L. S. (2016). "Methane adsorption and dissociation on iron oxide oxygen carriers: the role of oxygen vacancies." *Phys. Chem. Chem. Phys.*, 18(24), 16423-16435.

Chesner, W. H., Collins, R. J., & MacKay, M. H. (1998). *User Guidelines for Waste and By-product Materials in Pavement Construction*, Federal Highway Administration (FHWA), FHWA-RD-97-148.

Chiang, W. S., Fratini, E., Baglioni, P., Chen, J. H., & Liu, Y. (2016). "Pore size effect on methane adsorption in mesoporous silica materials studied by small-angle neutron scattering." *Langmuir*, 32(35), 8849-8857.

Chiang, P. C., & Pan, S. Y. (2017). *Carbon Dioxide Mineralization and Utilization*, Springer, Singapore.

Grubb, D. G., Wazne, M., Jagupilla, S. C., & Malasavage, N. E. (2011). "Beneficial use of steel slag fines to immobilize arsenite and arsenate: slag characterization and metal thresholding studies." *J. Hazard. Toxic Radioact. Waste*, 15(3), 130-150.

Grubb, D. G., and Wazne, M. (2011). *Metal Immobilization Using Slag Fines*, U.S. Patent Application No. 12/874,079.

Grubeša, I. N., Barisic, I., Fucic, A., & Bansode, S. S. (2016). *Characteristics and Uses of Steel Slag in Building Construction*, 1st Ed., Woodhead Publishing.

Gupta, J. D., Kneller, W. A., Tamirisa, R., and Skrzypczak-Jankun, E. (1994). "Characterization of base and subbase iron and steel slag aggregates causing deposition of calcareous tufa in drains". *Transportation Research Record*, (1434).

Holtz, R. D., & Kovacs, W. D. (1981). *An Introduction to Geotechnical Engineering*, 2nd Ed., Prentice-Hall, New Jersey.

Huber-Humer, M., Gebert, J., & Hilger, H. (2008). "Biotic systems to mitigate landfill methane emissions." *Waste Manag. Res.*, 26(1), 33-46.

Huijgen, W. J., Witkamp, G. J., & Comans, R. N. (2005). "Mineral CO_2 sequestration by steel slag carbonation." *Environ. Sci. Technol.*, 39(24), 9676-9682.

Ko, M. S., Chen, Y. L., & Jiang, J. H. (2015). "Accelerated carbonation of basic oxygen furnace slag and the effects on its mechanical properties." *Constr. Build. Mater.*, 98, 286-293.

Li, C., Yan, W., & Xin, Q. (1994a). "Interaction of methane with surface of alumina studied by FT-IR spectroscopy." *Catal. Lett.*, 24(3-4), 249-256.

Li, C., Li, G., & Xin, Q. (1994b). "FT-IR spectroscopic studies of methane adsorption on magnesium oxide." *J. Phys. Chem.*, 98(7), 1933-1938.

Morone, M., Costa, G., Polettini, A., Pomi, R., & Baciocchi, R. (2014). "Valorization of steel slag by a combined carbonation and granulation treatment." *Miner. Eng.*, 59, 82-90.

Navarro, C., Díaz, M., & Villa-García, M. A. (2010). "Physico-chemical characterization of steel slag. Study of its behavior under simulated environmental conditions." *Environ. Sci. Technol.*, 44(14), 5383-5388.

Ng, C. W. W., Ng, M., & Leung, A. K. (2017). "Removal of Hydrogen Sulfide Using Soil Amended with Ground Granulated Blast-Furnace Slag." *J. Environ. Eng.*, 143(7).

Pan, S. Y., Chiang, P. C., Chen, Y. H., Tan, C. S., & Chang, E. E. (2013). "Ex situ CO_2 capture by carbonation of steelmaking slag coupled with metalworking wastewater in a rotating packed bed." *Environ. Sci. Technol.*, 47(7), 3308-3315.

Proctor, D. M., Fehling, K. A., Shay, E. C., Wittenborn, J. L., Green, J. J., Avent, C., Bigham, R.D., Connolly, M., Lee, B., Shepker, T.O., & Zak, M. A. (2000). "Physical and chemical characteristics of blast furnace, basic oxygen furnace, and electric arc furnace steel industry slags." *Environ. Sci. Technol.*, 34(8), 1576-1582.

Reddy, K.R., Yargicoglu, E.N., Yue, D., & Yaghoubi, P. (2014). "Enhanced microbial methane oxidation in landfill cover soil amended with biochar." *J. Geotech. Geoenviron. Eng.*, ASCE, 140(9).

Sadasivam, B.Y., & Reddy, K.R. (2014). "Landfill methane oxidation in soil and bio-based cover systems." *Reviews in Environ. Sci. Bio/Technol.*, 13(1), 79-107.

Sarperi, L., Surbrenat, A., Kerihuel, A., & Chazarenc, F. (2014). "The use of an industrial by-product as a sorbent to remove CO_2 and H_2S from biogas." *J. Environ. Chem. Eng.*, 2(2), 1207-1213.

Spokas, K., Bogner, J., Chanton, J. P., Morcet, M., Aran, C., Graff, C., Moreau-Le Golvan, L., & Hebe, I. (2006). "Methane mass balance at three landfill sites: What is the efficiency of capture by gas collection systems?." *Waste Manage.*, 26(5), 516-525.

Stolaroff, J. K., Lowry, G. V., & Keith, D. W. (2005). "Using CaO-and MgO-rich industrial waste streams for carbon sequestration." *Energy Convers. Manag.*, 46(5), 687-699.

Su, T. H., Yang, H. J., Shau, Y. H., Takazawa, E., & Lee, Y. C. (2016). "CO_2 sequestration utilizing basic-oxygen furnace slag: Controlling factors, reaction mechanisms and V–Cr concerns." *J. Environ. Sci.*, 41, 99-111.

Takahashi, T., & Yabuta, K. (2002). *New Application of Iron and Steelmaking Slag*, NKK Technical Report-Japanese Edition, 87, 43-48.

Ukwattage, N. L., Ranjith, P. G., & Li, X. (2017). "Steel-making slag for mineral sequestration of carbon dioxide by accelerated carbonation." *Measurement*, 97, 15-22.

US Environmental Protection Agency (US EPA). "Landfill Methane Outreach Program (LMOP)." <https://www.epa.gov/lmop/benefits-landfill-gas-energy-projects> (June 4, 2018).

US EPA. "Greenhouse Gas Reporting Program (GHGRP)." <https://www.epa.gov/ghgreporting/ghgrp-waste> (June 4, 2018).

US EPA. (2015). "Understanding global warming potentials." <https://www.epa.gov/ghgemissions/understanding-global-warming-potentials> (June 4, 2018).

Visvanathan, C., Pokhrel, D., Cheimchaisri, W., Hettiaratchi, J. P. A., & Wu, J. S. (1999). "Methanotrophic activities in tropical landfill cover soils: effects of temperature, moisture content and methane concentration." *Waste Manag. Res.*, 17(4), 313-323.

Yargicoglu, E., Sadasivam, B.Y., Reddy, K.R. & Spokas, K. (2015). "Physical and chemical characterization of waste wood derived biochars." *Waste Manage.*, 36(2), 256-268.

Yargicoglu, E. N., & Reddy, K. R. (2015). "Characterization and surface analysis of commercially available biochars for geoenvironmental applications." *IFCEE 2015*, 2637-2646.

Yargicoglu, E. N., & Reddy, K. R. (2017). "Effects of biochar and wood pellets amendments added to landfill cover soil on microbial methane oxidation: A laboratory column study." *J. Environ. Manag.*, 193, 19-31.

Yildirim, I. Z., and Prezzi, M. (2011). “Chemical, mineralogical, and morphological properties of steel slag.” *Adv. Civil Eng.,* 2011.

Ziemkiewicz, P., & Skousen, J. (1999). “Steel Slag in Acid Mine Drainage Treatment and Control'.” *Proc., Annual National Meeting of the Society for Surface Mining and Reclamation*, 16, 651-656.

CHAPTER 4 - EFFECT OF BASIC OXYGEN FURNACE SLAG PARTICLE SIZE ON SEQUESTRATION OF CARBON DIOXIDE FROM LANDFILL GAS

ABSTRACT: Sequestration of carbon dioxide (CO_2) from landfill gas (LFG) emissions appears feasible with the use of basic oxygen furnace (BOF) slag in landfill cover system. The minerals alkaline and Ca-rich minerals present in the BOF slag have the potential to react with the CO_2 to form carbonate precipitate. In a previous study, CO_2 and CH_4 removal from the landfill gas was investigated by batch and column experiments with BOF slag under different moisture and synthetic LFG gas exposure conditions. The initial CO_2 removal (~56 mg/g) was assumed to be dependent on the characteristics and mineralogy of the BOF slag. The long-term CO_2 sequestration was found to be dependent on the slow release of Ca^{2+} from minerals (Ca-silicates) present in BOF slag which resulted in a maximum CO_2 removal of 155 mg/g. This study investigates the effect of BOF slag particle size of on CO_2 sequestration by batch and column experiments using three particle size ranges: (1) coarse (D_{50} = 3.05 mm), (2) original (D_{50} = 0.47 mm) and (3) fine (D_{50} = 0.094 mm). The coarse, original and fine, sequestered 66 mg/g, 155 mg/g and 255 mg/g of CO_2. The breakthrough of CO_2 corresponded with 6 mg/g CO_2, 42 mg/g CO_2, 120 mg/g CO_2 removal with increasing fineness. Though none of the particle sizes exhibited significantly high CH_4 removal, the coarse, original and fine BOF slag removed ~10 mg/g, ~20 mg/g and ~30 mg/g of CH_4, respectively.

4.1 INTRODUCTION

Landfill gas (LFG) that contains both methane (CH_4) and carbon dioxide (CO_2) is one of the most common sources of greenhouse gas emissions. The landfill gas is produced upon anaerobic biodegradation of the municipal solid waste in landfills. At present, the landfill gas emissions are controlled by the simultaneous use of landfill covers and the LFG recovery system at municipal solid waste landfills. The LFG collection systems are not 100% efficient. Landfill gases cannot be completely collected with these systems. There have also been increased research and promotion on reducing methane emissions by methane-oxidizing biocovers that utilize the organic materials such as compost and even biochar to create a conducive environment for aiding the growth and proliferation of methanotrophs and enhanced CH_4 oxidation with the landfill cover. CH_4 which is a 28 times more potent greenhouse gas than CO_2 has been the focus in the design of biocover systems until now, but CO_2 is an equally important and more common emission that contribute to the global warming. A cover system including CO_2 sequestration would result in substantial decrease of LFG emission, potentially leading way to "zero-emissions" landfill. Accordingly, the alkaline and Ca-rich BOF slag was analyzed for CO_2 sequestration from the LFG by batch and column experiments (Reddy et al. 2018).

The readily reactive chemical species within the BOF slag matrix are free CaO, portlandite [$Ca(OH)_2$] and larnite (Ca_2SiO_4) (Huijgen et al. 2005; Yilmaz et al. 2013; Sarperi et al. 2014). The BOF slag mineral reactions with CO_2 are similar to the weathering process in nature (Kasina et al. 2015) , while in the presence of moisture, the reaction is accelerated to occur within a time-scale conducive for engineering applications. The main mechanisms that occur within BOF slag that are responsible for its weathering rely on transformation of the above

mentioned three reactive components in BOF slag by water and CO_2 (Yilmaz et al. 2013) as given below:

$$CaO_{(s)} + H_2O \leftrightarrow Ca^{2+} + 2OH^-$$

$$Ca_2SiO_4 \leftrightarrow CaSiO_{3(s)} + SiO_2 + H_2O \leftrightarrow Ca^{2+} + SiO_2 + 2OH^-$$

$$Ca(OH)_{2(s)} \leftrightarrow Ca^{2+} + 2OH^-$$

$$CO_2 + H_2O \leftrightarrow CO_3^{2-} + 2H^+$$

$$Ca^{2+} + CO_3^{2-} \rightarrow CaCO_{3(s)}$$

The results from Reddy et al. (2018) demonstrated a two-stage carbonation mechanism in BOF slag. The first phase of instantaneous complete removal as a function of surficial residual lime content [CaO and $Ca(OH)_2$] in the slag followed by a continuous sustained removal of CO_2 by leachable metal ions from slag matrix. The breakthrough was found to be independent of moisture availability and inlet gas pressure. The study concluded that CO_2 sequestration potential of BOF slag was a function of slag characteristics like particle size and mineralogy.

Smaller particle size increases the reactivity of the available minerals within the same BOF slag and shorten leaching pathway, making the ions reach easily to the slag surface. The higher porosity and specific surface area increase interaction between reactants leading to complete and efficient reaction. According to Huijgen et al. (2005), the leaching of ions from the slag matrix to the surface is the rate-determining step in carbonation. Hence, the smaller particle sizes are conducive to increase carbonation capacity of BOF slag by increasing the availability of reactive ions. On the contrary, the larger particle sizes are considered to reduce the capacity of carbonation.

This study is aimed at investigating the effect of BOF slag particle size on carbonation capacity. A BOF slag sample as received from a steel plant consisted of a mixture of particles of

different sizes. The original slag sample was sieved to form two different particle size fractions which were chosen to evaluate the effect of particle size. A detailed characterization of the original BOF slag and its carbonation potential was given in Reddy et al. 2018. Several batch and column experiments were conducted on coarse and fine particle size BOF slag and then compared with the results of original slag to discern the effects of particle size on CO_2 sequestration.

4.2 MATERIALS AND METHODS

4.2.1 Materials

The crushed and screened BOF slag with a top size of 10 mm (3/8 inches) was obtained from Indiana Harbor East Steel Mill and supplied by the Phoenix Services, LLC (Reddy et al. 2018). The as-received BOF slag is denoted as the 'original' slag in this study and it consisted of different particle sizes. In order to obtain the coarse and fine fractions, the original slag was sieved with material passing through #4 sieve and retained on #10 sieve designated as the 'coarse' slag and the material passing through #140 and retained on #200 designated as the 'fine' slag. The grain size distributions of the coarse, original and fine BOF slags were determined in accordance with ASTM D422.

The minerals present in as-received BOF slag were determined by X-ray powder diffraction (XRD) and Rietveld quantification analysis. 3 g BOF slag sample was ground and spiked with corundum (Al_2O_3) on a 90:10 weight basis in a mixer for 10 min. Standard spike intensity reference was used to determine the amorphous content. Step-scanned XRD data were collected by Siemens D500 computer-automated diffractometer using Bragg-Brentano geometry

with reference databases as the International Center for Diffraction Data database (ICDD, 2001) and the Inorganic Crystal Structure Database (ICSD, 2010, v.2).

Crushed and air-dried coarse, original and fine of as-received and carbonated BOF slag were used for Scanning Electron Microscopy (SEM) imaging and analysis. Images and compositional information were captured using a JEOL JSM-6320F High Resolution Scanning Microscope operated at 2.5 kV accelerating voltage and Oxford X-Ray Energy Dispersive Spectrometer (XEDS) fitted with a Hitachi S-3000N Variable Pressure Electron Microscope, respectively. The specimens were sputter coated with 20 nm Pt/Pd using Cressington HR208 sputter coater to minimize sample charging.

4.2.2 Batch Experiments

24 hour batch experiments were conducted for coarse, original and fine BOF slags. The samples were oven-dried at 100-110°C overnight before they were used in batch experiments. 1 g dry material was taken in a 125 ml microcosm bottle and mixed with 10%, 20%, 30% and 40% water under normal atmospheric temperature (23°C) and pressure. Each bottle was then purged completely with synthetic landfill gas consisting of 50% CH_4 and 50% CO_2 by volume, closed with rubber septa, and secured tightly with a metal crimp cap. For each of the water contents evaluated, the experiments were conducted in triplicates. Gas was sampled from their headspace at different time periods and analyzed using SRI 9300 GC equipped with a thermal conductivity detector (TCD) and CTR-1 column. For each replicate, 1 ml gas sample was withdrawn from the headspace and 0.5 ml was wasted before injection into the GC. This ensured the sample volume was within the acceptable limit for GC and in equilibrium with the atmospheric pressure. A 3-

point calibration curve was constructed for the SRI 9300 GC using standard CH_4-CO_2 gas mixtures at 5%, 25%, and 50% concentrations.

4.2.3 Column Experiments

Column experiments were conducted using continuous dry synthetic LFG flow conditions on coarse, original, and fine BOF slags, separately to determine CO_2 removal capacity with BOF slag particle size variation following the same column experimental setup as shown in **Figure 3-2.** An acrylic glass column of 30 cm height and 2.5 cm inner diameter was filled with the selected BOF slag mixed with 10% moisture to its full length in 2 layers of 15 cm each with light tamping. The column was secured with bed support mesh, end connections, and screw caps at both ends. PTFE tubing was used to connect all components and flow meters were installed at both ends of the column to control the influent/effluent gas flow rates. 1 ml gas samples were collected from influent/effluent sampling ports and analyzed for CO_2 and CH_4 using the SRI 9300 GC at different time intervals until CO_2 breakthrough (C_{OUT}/C_{IN} =1). The column experimental conditions are summarized in **Table 4-1**.

Table 4-1: Summary of column experiments conditions

Parameters	**Column CS (Coarse Slag)**	**Column OS (Original Slag)**	**Column FS (Fine Slag)**
***Column*:**			
Diameter (cm)	2.5	2.5	2.5
Length (cm)	30	30	30
BOF slag mass (g)	220	189.5	152
BOF slag type	Coarse	Field	Fine
BOF slag particle size range (mm)	~ 2 - 4.75	< 4.75	~ 0.075 - 0.106
BOF slag mean particle size (mm)	3.05	0.47	0.094
Moisture content (%)	10	10	10
Dry density (g/cm^3)	1.5	1.3	1.05
Porosity (v/v)	0.49	0.57	0.65
Pore volume (ml)	72	82	94

***Inlet gas*:**			
Methane (%)	50	50	50
Carbon dioxide (%)	50	50	50
Moisture condition	Dry	Dry	Dry
Inlet flow rate (ml/min)	11-15	5-9	8-13
Inlet pressure (psi)	12	12	12
Outlet flow rate (ml/min)	3-14	1-7	1-12
Total test duration (min)	11,575	17,159	14,599
Total pore volumes (#)	2,022	1,553	1,736

4.3 RESULTS AND DISCUSSION

4.3.1 Composition of BOF Slags

Figure 4-1 shows the grain size distribution of the three BOF slags particles. Average particle size (D_{50}) of coarse, original and fine slags were 3.05 mm, 0.47 mm, and 0.094 mm, respectively.

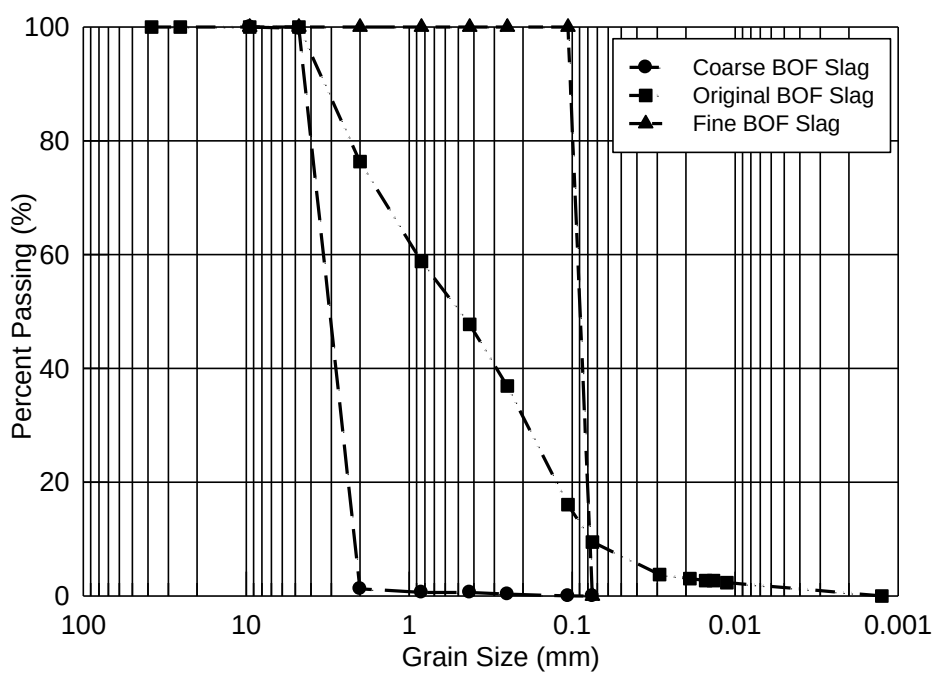

Figure 4-1: Grain size distribution of coarse, original and fine BOF slag samples

The mineralogical composition of the original BOF slag as per the XRD results is as summarized in the previous chapter and given in **Table 4-2**.

Table 4-2: Mineralogy and bulk chemistry (oxide basis) of BOF slag

Minerals and Oxides	Mineral Formula	Percent Weight
Minerals		
Lime	CaO	2.0-2.2
Portlandite	$Ca(OH)_2$	9.4-9.5
Larnite	Ca_2SiO_4	9.5-11.4
Srebrodolskite	$Ca_2Fe_2O_5$	6.6-7.8
Akermanite	$Ca_2MgSi_2O_7$	0.0-6.4
Magnesioferrite	$MgFe_2O_4$	3.3-3.8
Katoite	$Ca_3Al_2(OH)_{12}$	3.8-4.3
Calcite	$CaCO_3$	2.8-2.9
Vaterite	$CaCO_3$	1.8-2.7
Wuestite	FeO	2.5-2.7
Mayenite	$Ca_{12}Al_{14}O_{33}$	2.7-2.9
Iron magnesium oxide	$FeO.76MgO.24O$	1.4-1.7
Merwinite	$Ca_3Mg(SiO_4)_2$	0.9-0.9
Periclase	MgO	0.4-0.6
Quartz	SiO_2	0.3-0.4
Brucite	$Mg(OH)_2$	0.3-0.6
Iron	Fe	0.0-0.1
Amorphous material		41.7-50.1
Oxide Basis		
CaO		33.6-33.8
SiO_2		13.3-13.4
Al_2O_3		3.6-3.6
Fe_2O_3		15.4-15.4
MgO		4.6-4.6
SO_3		0.3-0.3
Loss of Ignition (LOI)		8.6-8.6

Note: Analyzed by PMET, Inc., PA

The BOF slag consists of highly reactive Ca^{2+} ions in the form of free CaO (~2.2 wt%) and $Ca(OH)_2$ (~9.5 wt%), and 9-11% Larnite (Ca_2SiO_4). The presence of 4-6% $CaCO_3$ in the form of calcite and vaterite is suggestive of aging (carbonation) in progress from cooling and processing

of BOF slag. The calcite and vaterite are polymorphs of $CaCO_3$ usually found in aged steel slag (Chiang and Pan 2017; Grubb et al. 2014). The quantitative elemental composition from SEM-EDS results also show that presence of 5-6% wt% of C, 15-16 wt% O and 55-64 wt% Ca in as-received BOF slag depicting initial $CaCO_3$ levels. Aging of steel slag can be found even in the absence of excess moisture or CO_2 pressure in its surrounding atmosphere that leads to a disappearance or decrease in minerals such as Larnite and Portlandite from the slag matrix. In a study by Grubb et al. (2013), a 365-day old sample of 100% steel slag fines (SSF) was found to exhibit decrease of about 8% Larnite and an increased amorphous content.

4.3.2 Batch Experiments

The batch experiments were conducted on the three BOF slags at 10%, 20%, 30% and 40% water content. The maximum water content of 40% was chosen in these experiments as this value is close to the water holding capacity of the BOF slag tested (Chapter 3). Dry slags were not tested as carbonation at 0% moisture was found to be insignificant from the previous study (Chapter 3) and Sarperi et al. (2014).

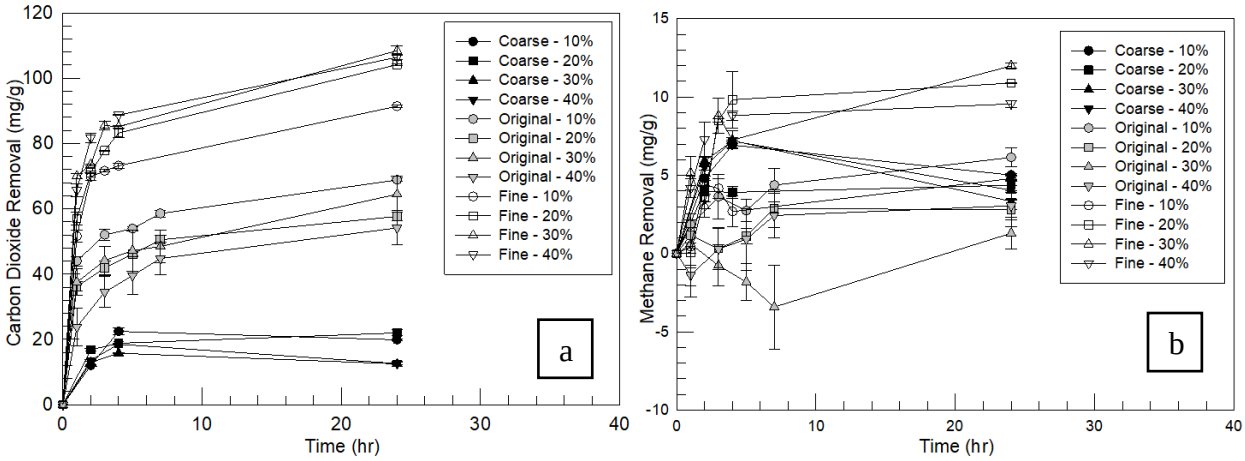

Figure 4-2: Removal of (a) CO_2 and (b) CH_4 by coarse, original and fine BOF slags versus time.

Fine slag exhibited significantly higher CO_2 removal capacity compared to original and coarse slags (**Figure 4-2)**. Particle size was the dominant factor in CO_2 removal creating clustered datasaets, within which, moisture content then became the controlling factor. The CO_2 removal capacity of fine BOF slag was in the range of 92-112 mg/g with varying moisture content, while the maximum CO_2 removal by original and coarse slag was only 68 mg/g and 20 mg/g, respectively. The CO_2 removal plots of the three slag samples (coarse, original and fine) suggest an initial phase (~1-2 hr) of rapid carbonation, followed by a slower reaction phase.

The coarse and fine BOF slag exhibited minimum and maximum CO_2 removal capacity, respectively, while original BOF slag (fine and coarse particle mix) exhibited CO_2 sequestration capacity influenced by both particle sizes. The fine and coarse particles oppose each other by increasing and decreasing carbonation, respectively, limiting the original BOF slag from reaching full potential. In addition, the non-homogenous distribution of the coarser to finer particles in the original slag suggest the irregular trend of carbonation with moisture content. According to the studies by Huijgen et al. (2005) and Zhang et al. (2011), a relation was drawn between the increased availability of CaO with decrease in BOF slag particle size leading to increased CO_2 sequestration. The higher mineral availability and better interaction within the slag-water-gas system facilitated by the smaller particle sizes confers the fine BOF slag its higher CO_2 removal capacity. **Figure 4-2** shows that the fine BOF slag had the highest removal capacity for CH_4 (~14 mg/g), though a specific trend was not established with time or moisture content.

The two-step reaction mechanism as observed from **Figure 4-2** is similar to the observation from previous studies (Reddy et al. 2018; Stolaroff et al. 2005; Lekakh et al. 2008), associated with Ca^{2+} dissolution kinetics of the slag. Further, it was observed that the ultimate carbonation facilitated by the original slag in 24 hours was achieved by the fine slag within the

initial 1 hour itself. The fine slag favored better Ca^{2+} dissolution in the system leading to higher carbonation during the rapid carbonation phase. According to Lekakh et al. (2008), approximately 33% of the calcium leached from the 45 – 75 µm fraction in the first hour, while less than 5% of the calcium was leached from the 2300 – 3300 µm fraction after 24 hours. Similarly, about 6 times more CO_2 was sequestered by the fine slag (D_{50} = 0.094 mm) compared to the coarse slag (D_{50} = 3.05 mm) during 24 hours depicting that with smaller particle size, better Ca^{2+} leaching is favored that leads to higher carbonation capacity within the same BOF slag.

In addition, the carbonation capacity of the coarse and original BOF slag sample did not exhibit a specific trend with the change in moisture content, while the carbonation capacity of fine slag increased with increasing moisture until 30% and reduced slightly at 40% (**Figure 4-3**). The fine slag responded best to both CO_2 and CH_4 at 20%-30% moisture content while original slag reacted showed a better carbonation at 10% moisture content. The reactivity of coarse slag with both CO_2 and CH_4 was observed to be much lower and nearly the same at all moisture contents compared to the original and fine slag samples (**Figure 4-3)**.

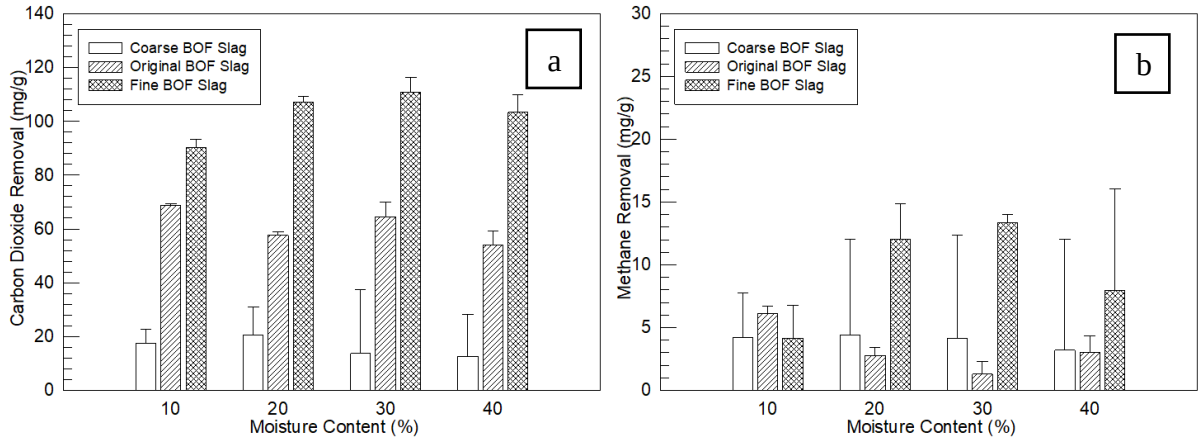

Figure 4-3: Cumulative removal of (a) CO_2 and (b) CH_4 by coarse, original and fine BOF slags at 24 hours in batch experiments.

Another factor that influences the carbonation of BOF slag is the interplay of several metal oxides present in BOF slag that confers certain characteristics like reactivity and hydraulic activity to the slag. Iron content in BOF slag limit its use in cement industry as it minimizes hydraulic activity in cement blends (Chiang and Pan 2017). The coarse BOF slag have higher iron content (Zhang et al. 2011) that could limit the slag-water interaction necessary for efficient slag carbonation. Zhang et al. (2011) also observed BOF slag divided into five size fractions and found that the CaO and SiO_2 content increased and iron oxide content increased with finer and coarser fractions, respectively, suggesting better Ca oxide availability and carbonation potential of the fine slag.

4.3.3 Column Experiments

The column experiments were conducted under continuous dry simulated landfill gas inflow conditions at 12 psi inlet pressure into BOF slags containing 10% initial moisture content. The initial moisture content was maintained as 10% for the three selected slags as it was the moisture content at which coarse, original and fine exhibited significant carbonation in the batch experiments. One pore volume (PV) of the column for the coarse, original and fine BOF slags were calculated to be 72 ml, 82 ml, and 94 ml, respectively. The CO_2 and CH_4 elution with number of PV of gas injected is shown in **Figure 4-4**. The cumulative CO_2 and CH_4 removal by the slags are plotted in **Figure 4-5** with respect to the PV of inlet gas. **Table 4-3** summarizes the results from column experiments.

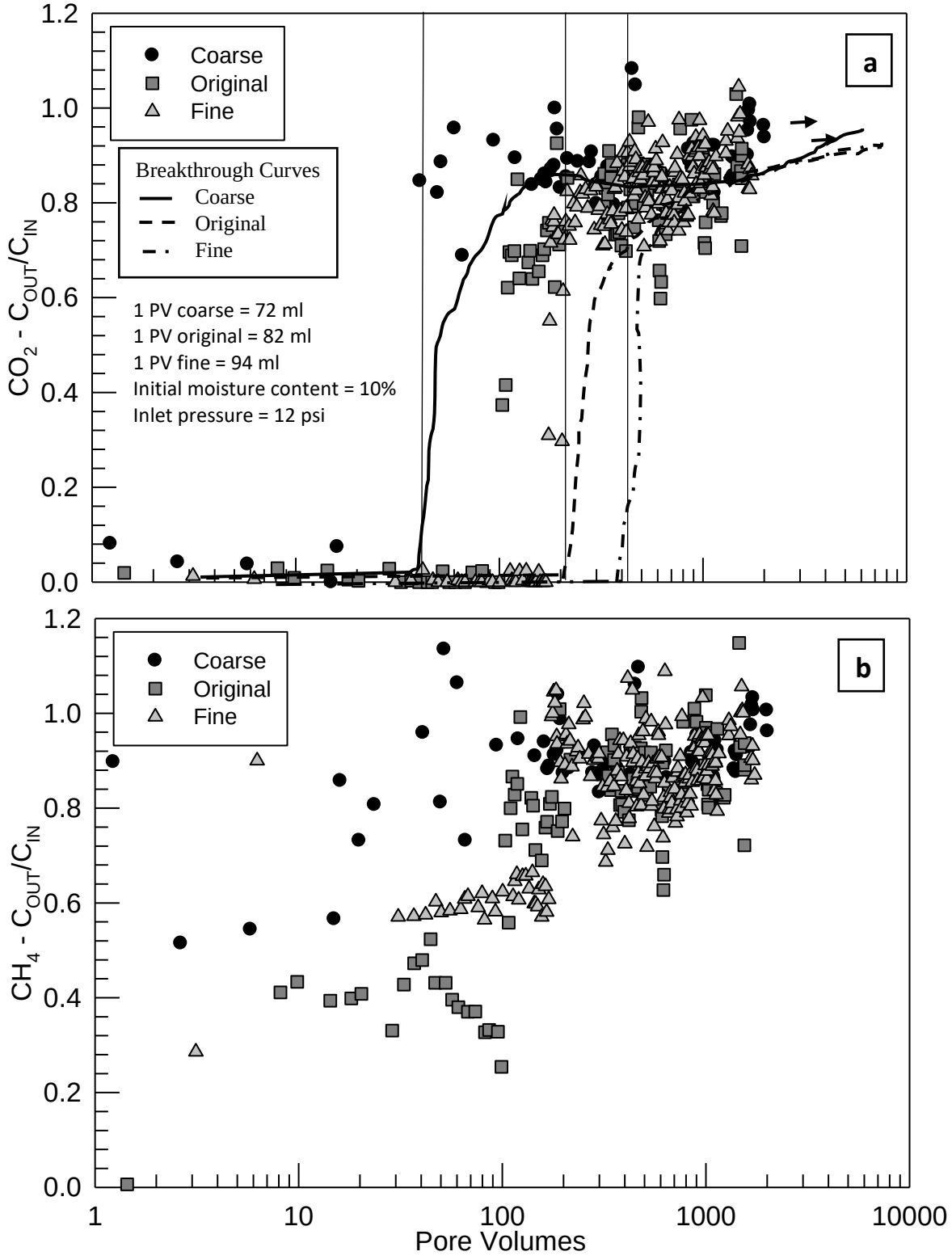

Figure 4-4: Outlet to inlet concentration ratio of CO_2 (a) and CH_4 (b) by coarse, original and fine BOF slags at 10% moisture on a pore volume basis.

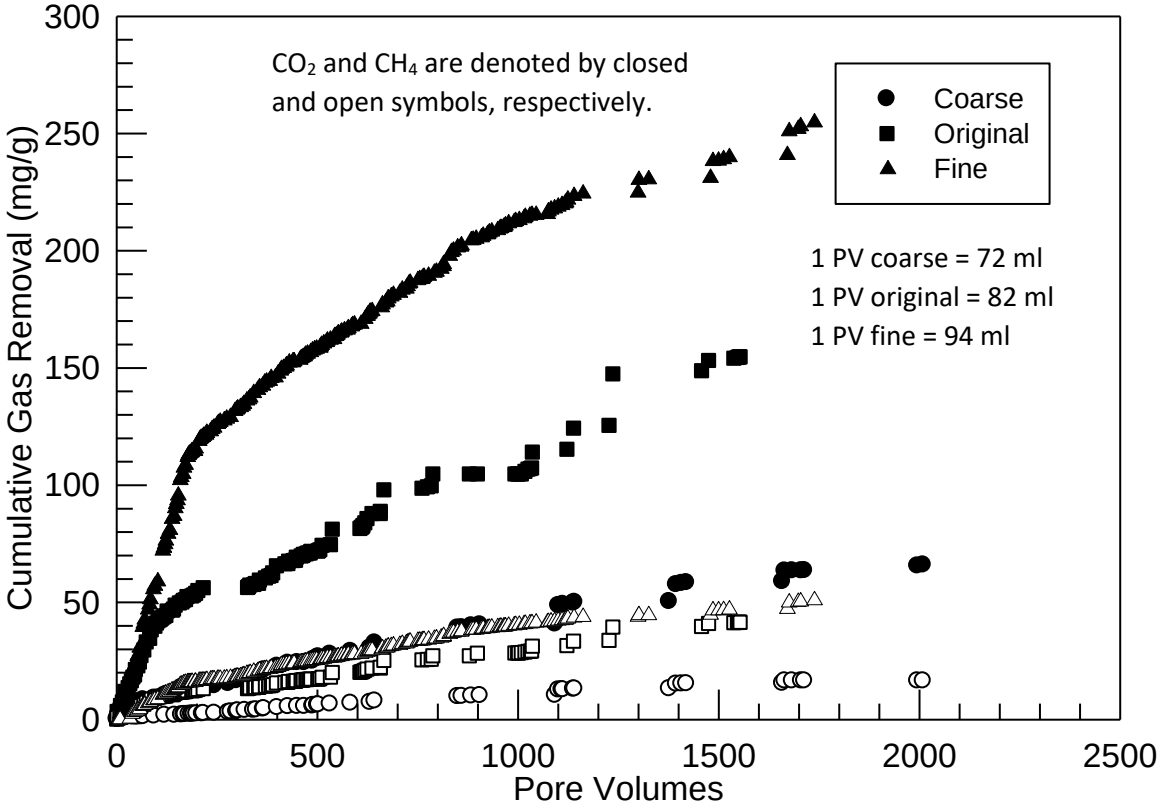

Figure 4-5: Comparison of cumulative gas removal of gas in coarse, original and fine BOF slags on a pore volume basis.

Table 4-3: Cumulative CO_2 removed from column experiments with coarse, original and fine BOF slags

Column	1 PV (ml)	Breakthrough		Termination		Cumulative CO_2 removal slope	
		PV (#)	CO_2 removed (mg/g)	PV (#)	CO_2 removed (mg/g)	Before breakthrough	After breakthrough
CS	72	15	6	2022	66	0.4	0.04
OS	82	100	42	1553	155	0.4	0.07
FS	94	190	118	1736	255	0.6	0.12

In the coarse slag, CO_2 breakthrough was established faster than fine and original slag samples (**Figure 4-4**). The breakthrough was observed at ~15 PV of inflow gas corresponding to cumulative 6 mg/g CO_2 removal (**Figure 4-5**). Thereafter, C_{OUT}/C_{IN} increased to 0.9 at 60 PV.

CO_2 removal by the coarse BOF slag at test termination was ~ 66 mg/g (at ~ 2000 PV) and cumulative CH_4 removed was only ~15 mg/g. The cumulative CO_2 removal slope dropped from 0.4 to 0.04 at breakthrough (**Figure 4-5**). The CO_2 breakthrough point of original BOF slag was 100 PV (**Figure 4-4**) removing much higher CO_2 (~ 42 mg/g) compared to coarse BOF slag (**Figure 4-5**). Before breakthrough, the CO_2 was completely removed ($C_{OUT}/C_{IN} = 0$) from the system due to its reaction with BOF slag. The cumulative CO_2 removal by original slag was ~155 mg/g and exhibited drop in its slope from 0.4 to 0.07 at breakthrough indicating slower carbonation rate after breakthrough. The breakthrough curve and cumulative removal curves were also established for CH_4 gas. The C_{OUT}/C_{IN} ratio changed from 0.4 before breakthrough to 1 after breakthrough, resulting in 28 mg/g cumulative CH_4 removal by original BOF slag. Slope of CH_4 cumulative removal also decreased from 0.11 to 0.02 at 100 PV (Reddy et al. 2018). Fine BOF slag removed CO_2 completely ($C_{OUT}/C_{IN} = 0$) until ~190 PV (**Figure 4-4**) resulting in 118 mg/g CO_2 sequestration (**Figure 4-5**) before the breakthrough. CO_2 removal still continued after breakthrough in fine BOF slag indicated by the C_{OUT}/C_{IN} ratio that remained constant at 0.9 around 300 PV eventually reaching 1 around 1736 PV, resulting in ~ 250 mg/g ultimate CO_2 removal. The slope of cumulative CO_2 removal shifted from 0.6 to 0.12 at the breakthrough. The CH_4 C_{OUT}/C_{IN} remained 0.6 before breakthrough which rapidly rose to 1 after the breakthrough, with corresponding drop in slope of cumulative CH_4 removal from 0.07 to 0.04. The ultimate CH_4 removal capacity of the fine BOF slag was calculated as 40 mg/g.

From column experiments on coarse, original and fine particles of BOF slag, the amount of CO_2 that was completely sequestered before breakthrough increased in the order: coarse (6 mg/g) → original (42 mg/g) → fines (118 mg/g) (**Figure 4-5**). CO_2 sequestration by coarse slag before breakthrough was significantly low, though it ultimately removed ~ 66 mg/g of CO_2.

Further, ultimate CO_2 sequestration by original BOF slag (~155 mg/g) was achieved almost entirely by the fine BOF slag by the end of the breakthrough. Fine slag sequestered maximum CO_2 with cumulative removal of ~250 mg/g at termination. Earlier studies (Huijgen et al. 2005; Stolaroff et al. 2005; Lekakh et al. 2008) also analyzed leaching of Ca^{2+} ions from slag and carbonation separately along with the dominant influence of particle size (i.e., surface area) on the amount of Ca^{2+} leached suggesting inverse relation of particle size with calcium leaching which is in line with the observations from the current study. Ca^{2+} availability was observed to be higher for finer particles within the breakthrough period as it resulted in higher CO_2 sequestration. The cumulative gas removal curves also show that the carbonation reaction in all three slag fractions followed the similar trend of a fast reaction before breakthrough which then sets to slower reaction rate. Close examination of the slopes of cumulative CO_2 removal curves show that the reaction rate remains the same until breakthrough for coarse and original slags, with higher carbonation rate in fine slag (**Table 4-3)** while after the breakthrough, reaction rate is slowest for coarse slag followed by original slag and fastest in fine slag. This is also in conjunction with the faster and higher leaching of Ca^{2+} in fine slag compared to coarse slag by Lekakh et al. (2008). Comparing slopes of coarse and fine BOF slag CO_2 removal (0.4) against that of fine BOF slag (0.6) before breakthrough suggests that the coarser particles dominated over the fine particle effect by lowering the carbonation rate of original slag.

According to the XRD test results, the original BOF slag consists of 2.2 wt% CaO, 9.5 wt% $Ca(OH)_2$ and 11 wt% Ca_2SiO_4. Upon stoichiometric calculations based on the following reactions,

$$CaO + H_2O \rightarrow Ca(OH)_2$$

$$Ca(OH)_2 + CO_2 \rightarrow CaCO_3 + H_2O$$

$$Ca_2SiO_4 + 2CO_2 \rightarrow 2CaCO_3 + SiO_2$$

CaO, $Ca(OH)_2$ and Ca_2SiO_4 present in the BOF slag can sequester 56 mg/g, 17 mg/g and 57 mg/g CO_2 respectively for a total of 130 mg/g. Accordingly, it can be inferred that the rapid reaction in original sample is due to the immediate reaction of $Ca(OH)_2$ with the CO_2 from the inflow gas that amounted to ~ 56 mg/g (**Figure 4-5**) by the time the C_{OUT}/C_{IN} ratio reached a constant 0.9. Complete removal capacity of the original sample was achieved upon exhaustion of CaO, $Ca(OH)_2$ and Ca_2SiO_4 (17+56+57 = 130 mg/g < 166 mg/g). In the case of fine BOF slag, CaO, $Ca(OH)_2$ and Ca_2SiO_4 minerals could have been exhausted by the time the slower reaction phase kicked in as the cumulative removal of CO_2 at that point is ~130 mg/g (**Figure 4-5**).

The carbonation of BOF slag particles are suggestive of the key role played by Ca^{2+} leaching in BOF slag carbonation. Cumulative CO_2 removal by coarse sample was even lesser than the total capacity of residual lime content (72-73 mg/g) in the BOF slag (Reddy et al. 2018). Some of the water was observed dripping out of the column with coarse BOF slag during the experiment, limiting hydration of free CaO and Ca^{2+} ions leaching that extend carbonation. The inability of coarse BOF slag particles to hold moisture further confirms the water repelling nature of the coarser BOF slag particles as discussed earlier. Higher CO_2 removal capacity and utilization of CaO/$Ca(OH)_2$ capacity in original slag suggests better CaO dissolution and leaching of Ca^{2+} ions with lowering of mean particle size. Further, fine BOF slag particles enhanced slag-moisture-gas interaction and shortened leaching pathway that led to complete utilization of the mineral's carbonation capacity. Carbonation in fine BOF slag beyond the capacity of CaO, $Ca(OH)_2$ and Ca_2SiO_4 (130 mg/g) must have been promoted by leaching of reactive metal ions from other minerals present in slag. Cumulative gas removal in column experiments also exhibited two-step carbonation indicated by change (decrease) in its slope for

three particle sizes. This result further confirms the two-step Ca^{2+} dissolution kinetics prevalent in the slag carbonation.

The methane removal mechanism is not completely explored. Nevertheless, CH_4 removal capacity was lowest for coarse slag (~15 mg/g) and highest for the fine slag (~ 40 mg/g), within a range of 30 ± 10 mg/g. The removal capacity does not differ significantly with change in particle size. In the previous study (Reddy et al. 2018), significant difference in ultimate CH_4 removal was observed upon introducing humid gas to the original BOF slag column. Further, from cumulative removal graphs, it was found that though the slag-CH_4 interaction did not lead to a substantial CH_4 sequestration, a similar interaction curve was followed such as the slag-CO_2 interaction wherein a shift from fast to slow reaction after the breakthrough (change in slope) was observed in all three slag (Chapter 3).

4.3.4 SEM-EDS Analysis

The SEM-XEDS images and spectra of the fresh coarse, original and fine slags are shown in **Figure 4-6** and quantitative elemental composition summarized in **Table 4-4**.

Table 4-4: SEM-EDS elemental quantitative results for non-carbonated and carbonated slag samples (

Element	Weight (%)					
	CS Column		OS Column		FS Column	
	NC	C	NC	C	NC	C
Ca	59.15	57.09	55.34	61.57	64.24	51.12
Si	11.15	9.65	9.70	3.92	7.43	1.70
Fe	6.96	8.73	9.69	ND	4.39	ND
Mg	0.53	0.71	2.26	1.87	0.49	0.72
Al	0.00	0.38	1.79	0.00	0.56	6.72
C	5.56	5.12	5.47	10.73	6.30	10.50
O	16.64	18.31	15.75	21.91	16.59	29.24

As-received | Carbonated

CS

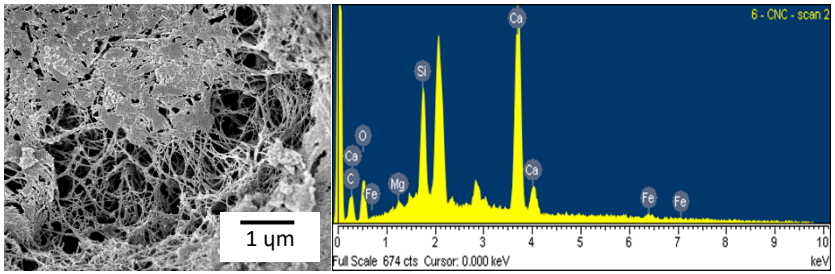

13000 x

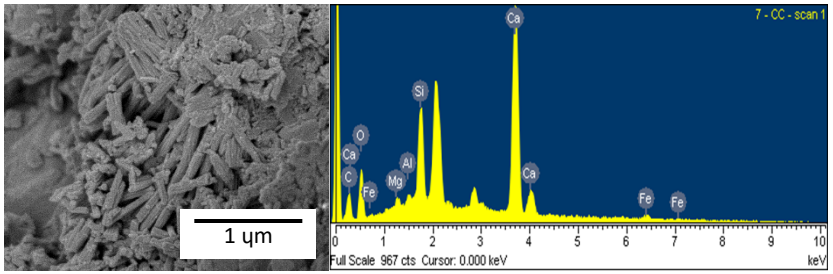

27000 x

OS

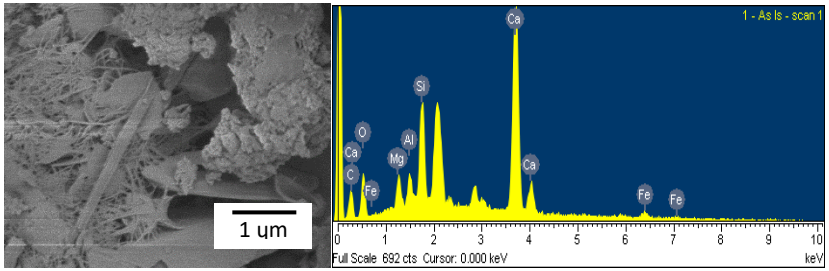

18000 x

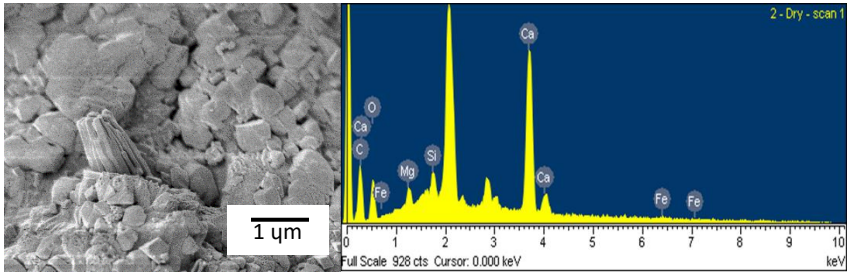

13000 x

FS

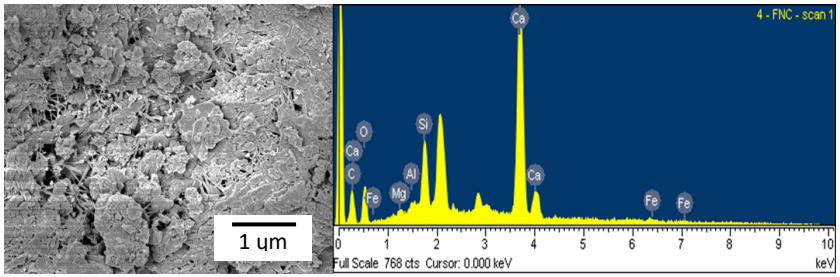

16000 x

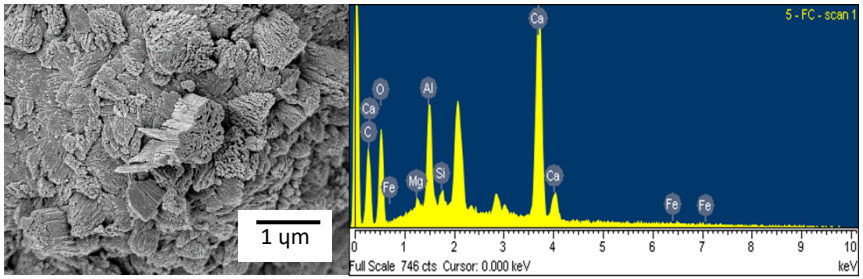

20000 x

Notes: CS=Coarse Slag; OS=Original Slag; FS=Fine Slag

Figure 4-6: SEM-EDS images of as-received and carbonated coarse, original and fine slags.

The SEM images of as-received samples of coarse, original and fine slag show the presence of both pores and network of needle-like structures on slag surface before carbonation. The needle-like structures across the porous openings indicate the beginning of pore-closure. These formations are characteristic of CaCO3, confirmed through the SEM-XEDS spectra that contains carbon (C), oxygen (O) and calcium (Ca) peaks, also detected by XRD as calcite and vaterite in the as-received slag sample. In general, the Fe content in BOF slag from SEM-EDS report is 4-9%, much lower than that expected in the as-received BOF slag which usually contains 20-25 wt% Fe (Yildrim and Prezzi 2011). The lower detection of Fe content in SEM-EDS can be explained by the predominant surface composition detection that is possible with SEM, heterogeneous surface distribution of elements on slag surface and possibility of larger Fe deposition within the slag core. Further, the lower Fe detection also affirms the lowering of Fe content with decrease in particle size (Zhang et al. 2011) as the samples were crushed before SEM analysis.

The carbonated samples of the original and fine slag samples showed significant increase in C, O and Ca peaks and a drop in the Si peak as compared to their non-carbonated counterparts, depicting increased calcium carbonate density on the carbonated slag surface. However, C, O and Ca peak variation was not significant in coarse sample tested. From the batch and column experiments, it was evident that the coarse slag was not as efficient as the original and fine slags in terms of carbonation. The calcium depleted Si rim is coated by the thicker calcium carbonate layer on the surface decreasing the Si detection in SEM-EDS. The drop in Si peak was also observed upon carbonation in several previous studies (Kasina et al. 2015) due to dissolution of the silicates that take part in carbonation.

The SEM images of carbonated coarse, original and fine slags exhibit needle-like formations characteristic of carbonates abundantly. The large pores that were found in as-received samples decreased substantially with carbonation of the samples. The network of needle-like formations formed thicker and denser formations (bush-like) that covered slag surface and infringed pores, decreasing general pore size in slag (Yilmaz et al. 2013). The highest and lowest C peak increase from as-received to carbonated sample in fine and coarse BOF slag, respectively confirms the results from column experiments.

4.4 CONCLUSIONS

Based on batch and column experiments conducted on coarse, original, and fine BOF slags, the following conclusions can be drawn:

- Particle size variation of BOF slag affected the carbonation capacity of the BOF slag mainly due to reactive mineral availability. The reactive minerals were easily available in fine slag leading to more exposure of CO_2 thereby leading to increased CO_2 removal and shift to higher breakthrough PV compared to original BOF slag.
- The particle size was also found to affect the extent of reaction. In coarser slag, even the full carbonation capacity of residual lime could not be achieved due to insufficient interaction between Ca^{2+} and carbonate ions, complete carbonation capacity of the three highly reactive species (CaO, $Ca(OH)_2$ and Ca_2SiO_4) was achieved by fine slag, followed by reaction due to dissolution of more reactive metal ions. In the original BOF slag, carbonation capacity equivalent to that of available $Ca(OH)_2$, CaO and Ca_2SiO_4 (130 mg/g) was achieved by test termination. Hence, the particle size variation has an inverse relationship to the mineral participation in carbonation.

- Change in cumulative CO_2 removal slope signifies a shift to lower carbonation rate that was dominated by the coarse particles.
- Though a significant variation of CO_2 sequestration was observed with change in particle size, the CH_4 removal efficiency only slightly increased with decrease in particle size of BOF slag. Variation of CH_4 removal capacity was within 30±10 mg/g, lower removal capacity being that of the coarser particles suggesting the significance of higher surface area of BOF slag particles in promoting better CH_4 and CO_2 removal efficiency.

4.5 CITED REFERENCES

Chiang, P. C., & Pan, S. Y. (2017). *Carbon Dioxide Mineralization and Utilization*, Springer, Singapore.

Grubb, D. G., Wazne, M., Jagupilla, S., Malasavage, N. E., & Bradfield, W. B. (2013). "Aging effects in field-compacted dredged material: steel slag fines blends." *J. Hazard. Toxic Radioact. Waste*, 17(2), 107-119.

Grubb, D. G., Jagupilla, S. C., Cummings, R., & Wazne, M. (2014). "Immobilization of lead, tungsten, and phosphate by steel slag fines: Metals thresholding and rate studies." *J. Hazard. Toxic Radioact. Waste*, 18(3).

Huijgen, W. J., Witkamp, G. J., & Comans, R. N. (2005). "Mineral CO_2 sequestration by steel slag carbonation." *Environ. Sci. Technol.*, 39(24), 9676-9682.

Kasina, M., Kowalski, P. R., & Michalik, M. (2015). "Mineral carbonation of metallurgical slags." *Mineralogia*, 45(1-2), 27-45.

Lekakh, S. N., Rawlins, C. H., Robertson, D. G. C., Richards, V. L., & Peaslee, K. D. (2008). "Kinetics of aqueous leaching and carbonization of steelmaking slag." *Metall. Mater. Trans. B,* 39(1), 125-134.

Sarperi, L., Surbrenat, A., Kerihuel, A., & Chazarenc, F. (2014). "The use of an industrial by-product as a sorbent to remove CO_2 and H_2S from biogas." *J. Environ. Chem. Eng.,* 2(2), 1207-1213.

Stolaroff, J. K., Lowry, G. V., & Keith, D. W. (2005). "Using CaO-and MgO-rich industrial waste streams for carbon sequestration." *Energy Convers. Manag.,* 46(5), 687-699.

Yildirim, I. Z., and Prezzi, M. (2011). "Chemical, mineralogical, and morphological properties of steel slag." *Adv. Civil Eng.,* 2011.

Yilmaz, D., Lassabatere, L., Deneele, D., Angulo-Jaramillo, R., & Legret, M. (2013). "Influence of carbonation on the microstructure and hydraulic properties of a basic oxygen furnace slag." *Vadose Zone J.,* 12(2).

Zhang, T., Yu, Q., Wei, J., Li, J., Zhang, P. (2011). "Preparation of high performance blended cements and reclamation of iron concentrate from basic oxygen furnace steel slag". *Resour. Conserv. Recycl.,* 56(1), 48-55.

CHAPTER 5 - OVERALL SUMMARY AND CONCLUSIONS

This Masters' thesis investigated the use of BOF slag in CO_2 sequestration from LFG emissions as a part of an ongoing project funded by the U.S. National Science Foundation that aims at achieving a “zero-emission” landfill cover by complementing CH_4 oxidizing biocovers with CO_2 sequestration. The alkalinity and abundant Ca^{2+} content were viewed as the BOF slag properties responsible for its CO_2 capture capacity. As against previous studies on BOF slag carbon sequstration capacity aimed at CO_2 scrubbing from industrial flue gas conducted at elevated temperatures and pressures at saturated conditions, the present study was conducted to study the BOF slag CO_2 sequestration capacity under normal atmospheric and unsaturated conditions prevalent at landfills. The CO_2 sequestration capacity of BOF slag and the effect of two parameters: moisture content; and particle size, on the BOF slag CO_2 sequestration capacity were also studied as a part of this work.

24-hour batch experiments, column experiments and SEM-EDS analysis were adopted as the experimental methods to analyze the above mentioned mechanisms and parameters affecting BOF slag carbonation. Batch experiments resulted in the studies on moisture dependency of carbonation in BOF slag. Column experiments were conducted for long periods on BOF slag at an initial moisture content of 10% (0.1 L/kg) subjected to continuous gas (50-50 CO_2/CH_4) flow until breakthrough ($C_{OUT}/C_{IN} = 1$) to monitor the CO_2 removal behavior and mechanisms. Thereafter, SEM-EDS analysis of non-carbonated and carbonated slag samples were also used to observe changes in morphology and to obtain a rough quantitative analysis.

Overall, CO_2 sequestration by BOF slag was found employable under normal atmospheric conditions pertinent to landfill sites. Even under unsaturated static conditions with as-received

gradation (<10 mm), BOF slag exhibited appreciable CO_2 removal capacity though CO_2 removal capacity was enhanced with humid gas and use of finer BOF slag particles. Carbonation mechanism in BOF slag was consistently observed to consist of two stages: initial rapid reaction thought to be a function of surficial accessible CaO and $Ca(OH)_2$, followed by Ca^{2+} leaching dependent gradual CO_2 removal. The two-stage reaction mechanism further emphasizes the important role of moisture and fine BOF slag in enhancing CO_2 capture capacity of BOF slag as they increase leachability and shorten leaching pathway, respetively. During the column experiments with BOF slag, small levels of CH_4 removal was also observed which was viewed as an effect of high alkalinity, porosity and mineral availability in BOF slag, though it requires detailed study.

CO_2 removal capacity and carbon sequestration mechanisms in BOF slag under landfill conditions was successfully established by the present study based on batch and column experiments as well as inferences from historical studies. However, more detailed studies involving TGA and XRD analysis of as-received and carbonated samples at different carbonation stages could throw light on mineral reactions within slag matrix. Raman spectroscopy and Fourier Transform Infrared Spectroscopy (FT-IR) could also be performed on slag samples exposed to LFG to assess the CH_4-slag reactions. The effect of the high alkalinity of BOF slag on methanotrophs, the effect of BOF slag cementation upon carbonation in landfill cover and particle size optimization for CO_2 sequestration should also be considered before the “zero-emission” landfill cover with BOF slag-amended biocover could be implemented.

VITA

NAME:	Archana Gopakumar
EDUCATION:	B.Tech, College of Engineering Trivandrum, Kerala, India, 2015
	MS, University of Illinois at Chicago, Illinois, USA, 2018
PROFESSIONAL EXPERIENCE:	Graduate Research Assistant, University of Illinois at Chicago
	Graduate Teaching Assistant, University of Illinois at Chicago
	Civil Engineer, Keerthi and Bhavana Architects, Kerala, India
	Site Engineer, Delta Projects, Kerala, India
AWARDS:	ASCE IL Section Geo-Institute Scholarship, 2017
PROFESSIONAL MEMBERSHIPS:	American Society of Civil Engineers (ASCE)
	ASCE – Geo Institute
	Solid Waste Association of North America (SWANA)